COMPUTATIONAL NETWORK MODELLING OF EXCITATORY AND INHIBITORY RESPONSES IN HIPPOCAMPAL CA3 NEURONS

M SANJAY

Department of Bioengineering

Christian Medical College Vellore

Ph. D THESIS

2017

CHRISTIAN MEDICAL COLLEGE

VELLORE

COMPUTATIONAL NETWORK MODELLING OF EXCITATORY AND INHIBITORY RESPONSES IN HIPPOCAMPAL CA3 NEURONS

A THESIS PRESENTED BY

M SANJAY

DEPARTMENT OF BIOENGINEERING

CHRISTIAN MEDICAL COLLEGE VELLORE

TO

SREE CHITRA TIRUNAL INSTITUTE FOR MEDICAL SCIENCES AND TECHNOLOGY, TRIVANDRUM

THIRUVANANTHAPURAM

IN PARTIAL FULFILLMENT OF THE REQUIREMENTS

FOR THE AWARD OF

DOCTOR OF PHILOSOPHY

2017

CERTIFICATE

I hereby certify that I had personally carried out the work depicted in the thesis entitled "Computational Network Modelling of Excitatory and Inhibitory Responses in Hippocampal CA3 Neurons".

No part of this thesis has been submitted for the award of any other degree or diploma prior to this date.

Date: 09-02-2017.

M SANJAY

CERTIFICATE BY GUIDE

Dr. K. Srinivasa Babu
Neurophysiology Unit
Department of Neurological Sciences
Christian Medical College, Vellore

This is to certify that **M. Sanjay** in the Department of Bioengineering, Christian Medical College, Vellore has fulfilled the requirements prescribed for the Ph.D. degree of Sree Chitra Tirunal Institute for Medical Sciences and Technology, Trivandrum.

The thesis entitled, "Computational Network Modelling of Excitatory and Inhibitory Responses in Hippocampal CA3 Neurons" was carried out under my direct supervision. No part of this thesis has been submitted for the award of any other degree or diploma prior to this date.

Signature:

Date: 9/2/17

THESIS EVALUATION FORM

The thesis entitled

COMPUTATIONAL NETWORK MODELLING OF EXCITATORY AND INHIBITORY RESPONSES IN HIPPOCAMPAL CA3 NEURONS

Submitted by

M. SANJAY

for the degree of

Doctor of Philosophy

of

SREE CHITRA TIRUNAL INSTITUTE

FOR

MEDICAL SCIENCES AND TECHNOLOGY, TRIVANDRUM

THIRUVANANTHAPURAM

is evaluated and approved by

Dr. K. Srinivasa Babu

(Guide)

Dr. .....

(External Examiner)

ACKNOWLEDGEMENTS

It is indeed a privilege and pleasure to acknowledge the guidance and support of various people and sources that has made this work possible.

To begin with, I sincerely thank my guide **Dr. K. Srinivasa Babu**, Senior Scientist, Neurophysiology Unit, Department of Neurological Sciences at Christian Medical College (CMC) Vellore for his continuous support, suggestions, criticisms, provision of facilities and conducive working environment, all of which have helped immensely in realization of this thesis.

I thank **Dr. Suresh Roland Devasahayam**, Professor and Head, Department of Bioengineering, CMC Vellore for permitting and encouraging me to pursue this interesting area of research and all the valuable help and support as a Doctoral Advisory Committee (DAC) member.

I acknowledge the valuable suggestions and guidance of **Dr. Sanjeev V Thomas**, Professor of Neurology, Sree Chitra Tirunal Institute for Medical Sciences and Technology (SCTIMST), Trivandrum and **Dr. Niranjan D. Khambete**, former Engineer (Instrumentation), SCTIMST, Trivandrum as members of the DAC.

The realization of most of this work has been possible due to my selection to attend the **Okinawa Computational Neuroscience Course (OCNC) 2013** held by the Okinawa Institute of Science and Technology (OIST), Okinawa, Japan in their campus in June-July 2013. I sincerely thank **Dr. Erik De Schutter**, Head of Computational Neuroscience Unit, OIST and the other co-ordinators of OCNC 2013, **Drs. Kenji Doya** and **Jeff Wickens** at OIST for the excellent conduct of the course, provision of every help, guidance and support for travel and stay for this highly valued programme and making this first international visit of mine very memorable.

Next, I most sincerely acknowledge the immense help and excellent companionship provided by **Dr. Samuel A Neymotin**, Research Assistant Professor, jointly with State University of New York and Yale University, USA. His guidance as tutor at OCNC 2013 in understanding the software and programmimg and insightful suggestions have been very crucial in leading this work in proper direction. I also acknowledge his continued guidance for the thesis related work and our publications. I also thank **Dr. Selvakumar Maran,** former Post Doctoral Fellow

at Emory University, USA and tutor at OCNC 2013 for all his guidance and support.

I acknowledge the various **sources of financial support** during the Ph.D work - Christian Medical College Vellore, The National Hub for Health Care Instrumentation Development Project, Department of Science and Technology, Govt. of India and The Dr. Marcus Devanandan Memorial Fund, CMC Vellore. I thank the **Institutional Review Board** of CMC Vellore for the approval of the study.

The members of Neurophysiology Lab at CMC Vellore require special mention for making my work place interesting by their lively involvement and help in all my academic and personal pursuits. My respectful thanks to **Ms. K. Deepa, Dr. K. V. Parthiban, Mr. S. Deepak, Ms. Arathi Radhakrishnan, Ms. Meena S S** and **Ms. Deborah Daphne** for all their support and encouragement.

My heartfelt thanks to each and everyone in the home department, the Department of Bioengineering, CMC Vellore for all the help and support, especially **Dr. Syrpailyne Wankhar, Dr. Rajdeep Ojha, Mr. Akhil Mohan** and **Mr. Vinil.**

I acknowledge all the help rendered for administative work by **Ms. Lalitha** and **Ms. Devi**, Department of Bioengg and **Mr. Vasudevan** and **Ms. Vijayalakshmi**, Department of Neurological Sciences at CMC Vellore.

My sincere thanks to all my friends in CMC Vellore for making my long stay memorable and creating a homely atmosphere away from home. Among so many of them, I would like to specially mention **Dr. Ranjith P** and **Dr. Ajith Sivadasan.**

All of this would not have been possible without the tremendous support from the family. I thank my parents **C Sasidharan** and **M Sreedevi** and every one in the family including the extended family for their immense patience and valuable help in various aspects of my academic and personal life. My heartfelt thanks to my second-half **Anjitha** and my dearest little one **Niranjan** whom I have really missed to be with.

And finally, **The Almighty,** for His choicest blessings that have helped me achieve whatever I could.

SANJAY

TABLE OF CONTENTS

LIST OF FIGURES

LIST OF TABLES

LIST OF ABBREVIATIONS

aCSF	Artificial Cerebrospinal Fluid
AED	Antiepileptic Drug
AMPA	α-amino-3-hydroxy-5-methyl-4-isoxazolepropionic acid
BAS	Basket Cell
CA	Cornu Ammunis
DB	Depolarization Block
DG	Dentate Gyrus
DI	Dendritic Inhibition
FR	Firing Rates
GABA	Gamma Amino Butyric Acid
g(Ih)	HCN Channel Conductance
HCN	Hyperpolarization-activated Cyclic Nucleotide-gated
LFP	Local Field Potential
MS	Medial Septum
NMDA	N-Methyl D-Aspartate
OLM	Oriens Lacunosum Moleculare
PYR	Pyramidal Cell
REM	Rapid Eye Movement
VFO	Very Fast Oscillations

SYNOPSIS

Hippocampus is a structure in the temporal lobe of the brain playing a major role in learning, memory, spatial navigation etc. It is a part of the limbic system along with other structures like dentate gyrus, subiculum, entorhinal cortex and amygdala.The network interactions involving various neuron types of the hippocampus generates its functions. Derangements in these interactions lead to a spectrum of disorders like alzheimers, stress, schizophrenia, epilepsy etc. In this work, epileptic activity is studied as a condition caused due to imbalances in excitatory and inhibitory interactions between the neurons in the hippocampus.

The aim of this study is to understand how a network of neurons in hippocampal CA3 subfield becomes hyperexcitable leading to epileptic activity due to - impaired dendritic inhibition (structural change) and high extracellular potassium (change in chemical environment), using computational modelling. Experimentally, loss of dendritic inhibition has been observed in pilocarpine treated rats as evident from histological studies. This is also reported to lead to dendritic sprouting in pyramidal cells and increased reception of excitatory external input by pyramidal cells. The network hyperexcitability is known to increase extracellular potassium levels. The experimental models become important since abnormal patterns of neuronal activity observed are comparable to those observed in human epilepsy patients. The objectives of this study were:

(1) To characterize a normal CA3 neuron network

(2) To understand what changes in the network lead to epileptic activity generation due to impaired dendritic inhibition caused by dysfunction of OLM interneurons (changes in network connectivity, characteristic of hippocampal sclerosis)

(3) To understand how in addition to (2) above, elevated extracellular potassium levels (changes in chemical environment) lead to epileptic activity in the network.
(4) To understand how drugs like gabapentin bring about elimination of epileptic activity in this network, enhancing the conductance of hyperpolarization-activated cyclic-neucleotide-gated (HCN) channel, g(Ih).

In this study, a computer model of CA3 network consisting 800 pyramidal cells, 200 basket cells and 200 OLM interneurons was used from the Model Database of the software NEURON (www.neuron.yale.edu). The simulations were performed using a Linux-based 2.66 GHz quad-core laptop computer. The pyramidal cells excited OLM and basket cells while the latter two inhibited pyramidal cells. Pyramidal and basket cells were recurrently connected. The basket cells connected to OLM cells. External excitatory and inhibitory inputs along with inputs from medial septum to the interneurons were simulated. The excitatory connections were through AMPA and NMDA synapses and inhibitory connections through GABA-A synapses. The baseline activity of the network - theta modulated gamma oscillations, was characterized first. To simulate impaired dendritic inhibition, the weight of connectivity between O-LM interneurons and pyramidal cells was reduced from baseline 100% to 0%. Correspondingly , the effect of increased external excitatory inputs received by pyramidal cells was simulated by changing the weights of these inputs at the distal dendritic compartments of pyramidal cells. Finally, overall network changes occuring at the connections between all the neuron types was simulated.

In the next part of the study, along with decreased connectivity from OLM to pyramidal cells (from baseline 100% to 70%, since epileptic activity could be

simulated at this level) and other simultaneous network changes, extracellular potassium levels were increased from the baseline 5 mM to 7.1 mM. As an associated change, the reversal potential of inhibitory synapses, E_{GABA} was changed from -80 to -75 mV.

In the final part of the study the effect of increased conductance of HCN channels (g(Ih)) on the epileptic network was tested , similar to the effect of antiepileptic drugs like gabapentin. For this, g(Ih) was incorporated in the basket cells also (based on literature) since the original model had this activated in pyramidal and OLM cells alone. First, the g(Ih) was increased systematically in steps in individual cell types separately and then in the all cells simultaneously in a normal network. This was done to understand the contribution of this conductance to the activity of that particular cell type. Thereafter, g(Ih) was increased in similar steps in all neurons simultaneously in the epileptic network. It was also tested whether enhanced g(Ih) is effective in control of epileptic activity at increased levels of impaired dendritic inhibition.

The obtained data were analysed using the software pClamp v.10 (Molecular Devices Inc, USA). Various parameters like firing rates of neurons, frequency of theta and gamma components in the simulated output, synchrony of activity between the neuron types and theta- and gamma- power were analysed. About 1000 simulations were run for the entire study. The results of the studies were compared with published experimental results for validation.

The following were the observations of the study:

1) Baseline Network: Consistent with experimental observations, the baseline network generated theta-modulated gamma oscillations with theta component of 6.7

Hz and gamma component of 33.3 Hz.

The firing rates (**FR**) of cells were 2.36+/-0.02 Hz for pyramidal cells, 16.05+/-0.15 Hz for basket cells and 0.96+/-0.03 Hz for OLM interneurons. The powers of theta and gamma components were 5.35 mV^2/Hz and 2.55 mV^2/Hz respectively. The cell types showed synchronous activity between each other.

2) Reduced dendritic inhibition and generation of epileptic activity:

(A) When strength of connection from OLM interneurons to pyramidal cells was reduced from baseline 100% to 0%, the FR of all three cell types increased. It was 4.19+/-0.04 Hz for pyramidal cells, 30.98+/-0.07 Hz for basket cells and 2.7+/-0.03 Hz for O-LM interneurons. The baseline activity changed from the normal theta-modulated gamma pattern to a predominantly gamma pattern with a frequency of 33 Hz. The power of gamma oscillations increased from baseline 2.55 to 8.7 mV^2/Hz.

(B) With decrement in dendritic inhibition and simultaneous increments in external excitatory inputs received by pyramidal cells was simulated considering sprouting in pyramidal cell dendrites. When the OLM-Pyramidal cell connection was reduced from 100% to 0% and external inputs to pyramidal cells increased from baseline 100% to 200% proportionately, the pyramidal cell firing frequency increased from 2.36+/-0.02 to 6.14+/-0.05 Hz, basket cell frequency from 16.05+/-0.15 to 24.26+/-0.44 Hz and OLM frequency from 0.96+/-0.03 to 4.98+/-0.04 Hz. The theta and gamma frequencies remained constant at 6.7 and 33 Hz till the connectivity was lowered to 10%. At total impairment of dendritic inhibition, the theta component was 0 Hz while gamma component rose to about 38 Hz.

The baseline activity was found to be very much altered when OLM to pyramidal cell connectivity was reduced to 10% (90% impairment) of baseline. A

special condition was tested here - a simultaneous large increase in the external excitatory inputs received by pyramidal cells, about 15 times the baseline was simulated. The basket cells entered a state of depolarization block (**DB**), causing the network to generate a typical ictal activity pattern which occured at 1.5 seconds from the start of the simulation. This ictal-tonic pattern was comparable to experimentally published results (Cymerblit-Sabba and Schiller, 2012 and Isaev et al., 2007)

(C) Finally, with impaired dendritic inhibition and changes simultaneously made in synaptic connectivity between all neurons in the network, the basket cells were again entered DB and the network output showed ictal activity. In this case, impairment of dendritic inhibition required to generate an ictal activity pattern was 70% (30% connectivity between OLM and pyramidal cells), which is lesser than the two previous cases. Moreover, the ictal like activity began earlier, at 1.2 seconds from the start of the simulation. These observations suggest that greater synaptic plasticity occurring in the whole network due to increase in reception of external excitatory inputs (due to impaired dendritic inhibition) makes the network more susceptible to generation of epileptic activity.

3) Reduced dendritic inhibition and simultaneous increment in extracellular potassium: After setting the baseline, dendritic inhibition was reduced first to 80% and then to 70% of the baseline values (20 and 30% impairment respectively) and corresponding extracellular potassium levels incremented to 6 and 7.1 mM respectively. Changes in connectivity between all neuron types in the network and increment of external excitatory inputs were also simulated. As in the first part of the study, an ictal tonic activity was observed in the local field potential when the extracellular potassium levels were 7.1 mM and dendritic inhibiton only 70% of

baseline (30% impairment).

4) The effect of enhanced (g(Ih)) in all neurons of the normal and epileptic network was tested to study the effect of antiepileptic drugs like gabapentin that increase this conductance in neurons. When g(Ih) was increased by two, four and six times the baseline values in one type of cell in a normal network, the FR of that cell type increased. Particularly, the dendritie-inhibiting OLM interneurons showed the maximum increase in FR. When g(Ih) was similarly increased uniformly across all cell types in the normal network, the overall network activity was suppressed. When g(Ih) was similarly increased uniformly across all cell types in the epileptic network (the network with 30% impaired dendritic inhibition), DB of basket cells was eliminated and overall network activity suppressed. This control of network hyperexcitability was not effective at severe impairments of dendritic inhibition.

In this study, the network connectivity and cell specific parameters had to be assumed since the exact mechanisms of epilepsy generation is still unknown. Only three major cell types in hippocampus have been considered though many other cell types are available in the biological network. The study outcomes can be used to plan further research studies having clinical impact. Studies can be designed to relate the onset of the disorder to the extent of neurodegeneration in the temporal lobe. Understanding the mechanism of epileptic activity generation could help to study the effect of drugs as well as decide on the dosage required. Mutual correlation between the electroencephalographic recordings and underlying network activity may be established to help better diagnosis of the disorder.

CHAPTER 1

INTRODUCTION

1.1 OVERVIEW

Hippocampus, situated in the temporal lobe of the brain forms a part of the limbic system. This temporal lobe structure plays significant role in short-term and long-term memory, spatial navigation, memory consolidation etc. The various functions of hippocampus are realized due to the balanced excitatory and inhibitory network interactions of various types of neurons. The pyramidal neurons are the major excitatory neurons of the hippocampus while inhibitory responses are mediated by a variety of interneurons. These interneurons synapse onto the pyramidal neurons at different segments in different layers of hippocampus. For example, the basket cells provide inhibition in the perisomatic regions of pyramidal cells in the stratum pyramidale layer while the Oriens-Lacunosum Moleculare **(OLM)** interneurons synapse at the apical dendrites of pyramidal cells in the stratum moleculare layer. Bistratified cells synapse on both apical and basal dendrites of pyramidal neurons while axo-axonic cells synapse onto the axon initial segments of a pyramidal cell. Hippocampus receives external excitatory inputs from adjoining areas like entorhinal cortex and the contralateral hippocampus and inhibitory inputs from areas like medial septum.

Varieties of disorders are attributed to derangements in these network interactions. eg., Alzheimer's, stress, schizophrenia, epilepsy etc. An imbalance in excitatory - inhibitory interactions can lead to these disorders. For example, stress reduces the neuronal excitability in hippocampus, causes atrophy of dendrites in CA3

subfield of hippocampus and leads to impaired neurogenesis in the dentate gyrus. In schizophrenia, a psychiatric disorder, changes in synaptic organization, connectivity, and aberrant oscillatory activities are observed in the hippocampus. The familiarly known Alzheimer's disease is also caused due to hippocampal disruption and affects short-term memory due to biochemical changes. Epilepsy is also caused due to a variety of reasons as mentioned above. Besides these, external factors like stroke and brain injuries can also lead to epilepsy. Interestingly, the clinical outcome seen in epilepsy is a combination of what is seen in other disorders – impaired memory, disturbed thoughts etc. Hence, in this thesis, the focus is on epilepsy and the excitatory-inhibitory interactions in hippocampus that lead to epileptic activity.

1.2 TEMPORAL LOBE EPILEPSY

Epilepsy is a neurodegenerative disease caused by imbalances in excitatory and inhibitory neuronal responses in a network, characterized by recurrent seizures which are abnormal electrical activities of the brain. The symptoms of epilepsy occur as seizures in a subject; however not everyone who has seizures have epilepsy. The seizures are manifested clinically in the form of transient abnormal phenomena like altered consciousness, motor convulsions, and other sensory events experienced by a subject. When seizures occur repeatedly in a subject, it is termed as epilepsy.

Temporal Lobe Epilepsy is a common type observed in human subjects with hippocampus as the usual site of origin. Different situations can lead to generation of epileptic activity in human brain, which include cerebrovascular accidents, brain injuries, tumours and unidentified etiology (cryptogenic epilepsy). The hippocampus, specifically its CA3 subfield, and entorhinal cortex are two areas reported to generate

independent epileptiform activity (Lytton et. al, 2005). The exact mechanisms involved in the generation of this epileptic activity are not yet properly understood.

Degeneration of neurons as a consequence of brain injuries, stroke, anoxia etc could lead to modifications in neuronal networks leading to pathological states including epilepsy. In the temporal lobe and specifically hippocampus, the structural manifestation of this pathological condition is called hippocampal sclerosis which refers to the loss or impaired function of different types of neurons in an otherwise balanced normal network. Both excitatory and inhibitory neurons are vulnerable to damage, some earlier and some later. Certain types of inhibitory interneurons are known to be damaged earlier than excitatory pyramidal neurons (Cossart et. al, 2001; Dinocourt et. al, 2003). Within the hippocampal formation, sclerosis has been observed in different areas like dentate gyrus, CA3 and CA1 regions of hippocampus proper in patients with epilepsy (Dinocourt et. al, 2003). This leads to an imbalance between excitation and inhibition, with increase in excitatory responses leading to hyperactivity in the network. Disinhibition of pyramidal cells due to impaired inhibitory mechanisms also results in 'sprouting' on their distal dendritic arbors. This further enhances the capability of pyramidal cells to receive external excitatory inputs (McAllister, 2000). This enhances excitatory activity in a feedback manner leading to pathological conditions like epileptic activity.

An intact hippocampus generates theta-modulated gamma oscillations which can be recorded experimentally as local field potentials **(LFP)**. This oscillatory behaviour could be significantly altered due to dysfunction of the contributing neurons. eg., dysfunction of the pyramidal cell dendrite-inhibiting OLM interneurons leads to reduced theta-component that they contribute. Dysfunctions of interneurons

along with changes in network connectivity and chemical environment could trigger abnormal network functions, leading to epilepsy (Karlocai et. al, 2014; Liu et. al, 2014).

1.3 RECOVERY FROM EPILEPSY

The clinical management of patients with epilepsy could be pharmacological, using antiepileptic drugs or surgical, by resecting the epileptic focus. About 30% of the patients who undergo surgical interventions to cure epilepsy do not get relief. In these patients, epilepsy recurs, presumably due to the shift of epileptic focus over time to another otherwise normal area of the brain. Various drugs like gabapentin, lamotrigine, carbamazepine, valproate etc. are prescribed to patients, starting with a low dose and increasing it further in a phased manner as felt necessary. The dosage of drug required to contain the disorder is widely variable across the patient group and depends on the severity of the disorder. An exact method to evaluate the severity of the disease (extent of sclerosis) and decide a titrated dosage of the drug is yet to be discovered. Developing such a method for treatment will greatly help in earliest effective management of the disease and if found ineffective, will help to suggest other modalities like surgery.

1.4 COMPUTATIONAL MODELLING

Computational models are developed to study brain function in health and disease at various hierarchial levels - channel, cellular, micronetwork, larger network and systems level. Computational modelling complements experimental studies, clinical observations and helps to understand the mechanisms of generation of experimentally observed results in sufficient detail. Modelling studies begin with

simulation of normal baseline activity of a neuron or a network or a system. The details of anatomy, biophysics, connectivities, functions etc. are decided by modellers as felt necessary. The required parameters or input conditions are changed to study the response of the system, eg., changing the strength of connectivity between a particular pair of neurons to study its effect on network behaviour. Once the conditions leading to a pathological state are understood, then these parameters and their combinations can be altered systematically to simulate the control of the disorder. These could be in a way to mimic current treatment modalities such as pharmacological methods, application of external electrical stimulus etc. For example, antiepileptic drugs act on specific channels to alter their conductivities to control epileptic activity. Pharmacokinetic models may be further developed to explore and predict the mechanisms of absorption, distribution, metabolism and excretion of drugs etc.

1.5 THE COMPUTATIONAL MODEL OF HIPPOCAMPAL CA3 SUBFIELD

In this thesis, two major approaches were made to study the changes in excitatory and inhibitory interactions in hippocampal CA3 subfield, leading to epileptic activity generation, using computational modelling. The freely downloadable software NEURON (www.neuron.yale.edu) with Python interpreter is used in this study. The first part describes how changes in network connectivity (structural change - impaired dendritic inhibition) alone make the CA3 network hyperexcitable leading to epileptic activity. The second part describes how in addition to first, changes in chemical environment, specifically increase in extracellular potassium, lead to generation of epileptic activity. Thereafter, the effect

of enhancing the conductance of hyperpolarization-activated cyclic-nucleotide-gated **(HCN)** channel, g(Ih), on control of epileptic activity is studied. The increase of this conductance is a realistic effect of anticonvulsive drugs like gabapentin and lamotrigine (Poolos et.al, 2002, Surges et.al, 2003).

Experimentally, impaired dendritic inhibition has been observed in pilocarpine treated rats as evident from histological studies (Dinocourt et. al, 2003; Cymerblit-Sabba & Schiller, 2012). This is also reported to lead to dendritic sprouting in pyramidal cells and increased reception of excitatory external input by pyramidal cells (McAllister, 2000; Ren et al, 2014). The network hyperexcitability is known to increase extracellular potassium levels. The experimental models become important since abnormal patterns of neuronal activity observed are comparable to those observed in human epilepsy patients (Mora et. al, 2009; Furman, 2013). The specific goals of this study are:

(1) To characterize a normal CA3 neuron network

(2) To study what changes in the network lead to epileptic activity generation due to impaired dendritic inhibition caused by dysfunction of OLM interneurons (changes in network connectivity, characteristic of hippocampal sclerosis)

(3) To understand how in addition to above objective (2), elevated extracellular potassium levels (changes in chemical environment) lead to epileptic activity in the network, and

(4) To understand how drugs like gabapentin control epileptic activity in this network, enhancing the conductance of HCN channels, g(Ih).

1.5.1 Modelling impaired dendritic inhibition and its network effects

A computer model of the CA3 network (Neymotin et al, 2011) consisting of 800 pyramidal cells (each having a single-compartment soma, single-compartment basal dendrite and three-compartment apical dendrite), 200 single-compartment OLM interneurons and 200 single-compartment basket cells has been adopted from the ModelDB of NEURON software (Accession No. 139421). Sufficient anatomical, biophysical and connectional details have been incorporated in the model to generate theta-modulated gamma oscillations as baseline activity of the network. While theta oscillations play a significant role in spatial navigation and motor behaviour, gamma oscillations are important in learning and memory, encoding and retrieval (Colgin & Moser, 2010). In the course of leading to the generation of epileptiform activity, the changes occurring in the baseline oscillatory behavior are also studied.

After establishing the baseline network activity, the impaired function of somatostatin expressing, pyramidal cell dendrite-inhibiting OLM interneurons in the CA3 subfield was modelled systematically. This impairment would increase the excitatory activity of pyramidal cells which are highly recurrently connected. In this part of the study, it was explored how:

1) impaired connectivity from OLM interneurons (inhibitory interneurons) to excitatory pyramidal cells alone influences the behaviour of other neurons and the network as a whole,

2) increased reception of external excitatory inputs by pyramidal neurons affect the network activity, and

3) how changes in strength of connection at synapses between all the neurons influence the overall network activity in the CA3 subfield.

1.5.2 Modelling changes in chemical environment and its network effects

Next, the gradual increase in extracellular potassium is modelled as a consequence of network hyperexcitability. Extracellular potassium levels have been observed to rise with increased firing activity of neurons in lab experiments as well as human subjects (Florence et.al, 2012). Enhanced extracellular potassium could further suppress the inhibitory responses by rise in GABA reversal potential (Korn et. al, 1987). Several other factors including enhanced recurrent excitation of CA3 pyramidal cells and enhanced reception of external excitatory inputs by pyramidal cells could lead to faster generation of epileptic activity at lesser impairment of interneuronal function. These conditions are individually considered to study how they generate experimentally observed epileptic activity.

1.5.3 Modelling the effect of anticonvulsive drugs

The next focus of the thesis is to understand the role of HCN channel conductance, g(Ih), in controlling epileptic activity. Drugs like gabapentin and lamotrigine are reported to increase this conductance in neurons thus leading to more efficient hyperpolarization and control neuronal hyperexcitability (Surges et. al, 2003). The effects of changing g(Ih) on the epileptic activity generated in the high extracellular potassium condition are studied step by step.

First, g(Ih) was increased specifically in the pyramidal cells alone in the baseline CA3 network. Similarly, g(Ih) was enhanced in basket cells alone and then in OLM interneurons alone to study changes in their intrinsic activity. Finally, g(Ih) was enhanced in all the three cell types - pyramidal cells, basket cells and OLM interneurons simultaneously. Thereafter, g(Ih) was increased in similar steps in all

neurons simultaneously in the epileptic network. Further, it is tested whether increased g(Ih) can effectively control the hyperexcitability caused due to increased neurodegeneration and whether it is possible to suggest titration of drug dosage at higher levels of network impairment than that which caused epilepsy in the model.

1.6 ORGANIZATION OF THE THESIS

This thesis consists of six chapters. Chapter 2 reviews the state of the art knowledge and information related to temporal lobe epilepsy, the available experimental and computational models, clinical management and successes, role of computer modelling in epilepsy etc.

Chapter 3 covers the development of the computer model and characterization of baseline activity, steps to simulate epileptic activity generation in hippocampal CA3 due to impairment in dendritic inhibition and enhancements in extracellular potassium levels and also the effect of anticonvulsive drugs.

Chapter 4 presents the results of the simulations along with their clinical implications.

Chapter 5 addresses the research findings and discusses the limitations related to the findings and concludes by providing possible solutions for future work.

Chapter 6 summarizes the overall research work done in this thesis .

CHAPTER 2

REVIEW OF LITERATURE

2.1 THE HIPPOCAMPUS - LAYERS AND SUBFIELDS

The hippocampus, named after its resemblance to seahorse, is a major component of human brain and other vertebrates. The features of hippocampus (Amaral, 1993; Witter, 2007) that have made it favourable for numerous studies are its neat organization of cells into different layers and unique function. The hippocampus has three sub-fields viz., CA3 (Cornu Ammunis 3), CA2 and CA1. The cells in these subfields are arranged in six layers. They are stratum (str.) oriens, str. pyramidale, str. radiatum, str. lucidum (present in CA3 alone), str. lacunosum and str. moleculare **(Figure 2.1)**

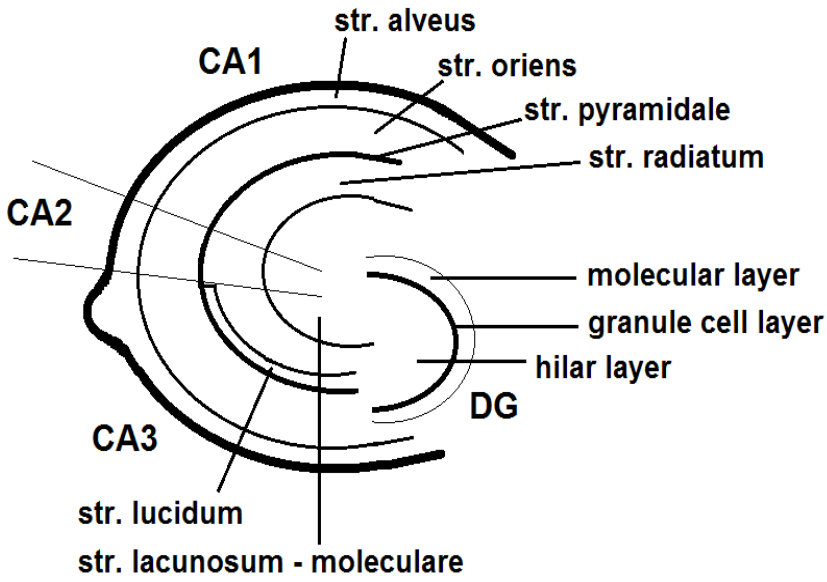

Figure 2.1 Schematic drawing of the subfields and layers of the hippocampus. CA - Cornu Ammunis (hippocampal subfield), DG - Dentate Gyrus

The main source of input signals to hippocampus is from the adjoining entorhinal cortex. The inputs from entorhinal cortex project to dentate gyrus and

CA3 subfield of hippocampus. The axons of the CA3 pyramidal cells called the Schaffer Collaterals synapse onto the CA1 pyramidal cells. The CA1 pyramidal cells thereafter project to entorhinal cortex through an area called subiculum. There is another set of neurons from entorhinal cortex that project directly onto the CA1 pyramidal neurons and this pathway is called temporo-ammonic pathway.

2.2 THE CA3 SUBFIELD

This subfield is located proximal to the dentate gyrus and receives inputs from entorhinal cortex and dentate gyrus. The pyramidal neurons form the large majority of neurons in this subfield, comprising about 88% of total neurons (Cutsuridis et.al, 2010). Various types of interneurons, including the pyramidal cell dendrite-inhibiting OLM interneurons and soma-inhibiting basket cells comprise the rest 12%. The CA3 pyramidal neurons receive inputs from entorhinal cortex and dentate gyrus at the stratum lucidum layer of CA3 subfield which comprises of dendritic spines in the pyramidal cells. The synaptic outputs of CA3 pyramidal neurons reach the CA1 pyramidal neurons.

One particular feature of CA3 subfield is its highly recurrent connections to its constituent neurons. This auto-associative network contributes to easier amplification of excitatory responses in the network (Amaral, 1993; Witter, 2007). The threshold of hyperexcitability is relatively low in this subfield for this reason and has been implicated in pathological conditions including epilepsy (Stoop & Pralong, 2000; Lytton, 2005). The pyramidal neurons of this subfield show frequent bursting behaviour compared to the neurons of other subfields.

2.3 PHYSIOLOGY OF HIPPOCAMPUS

The hippocampus is known to have functional roles in learning, short-term and long-term memory, spatial navigation, stress behaviour etc. All these are implicated through the electrical behaviour of its neurons and network activity patterns that it generates. The significant role of hippocampus in learning and memory was derived from surgical cases where hippocampal resection to alleviate temporal lobe epilepsies led to severe loss of memory. The most discussed such case in the history of neuroscience is that of a patient identified as H.M who lost the ability to learn new information after bilateral resection of hippocampus (Squire, 2009).

Theta and gamma oscillations are two main patterns generated by the hippocampus. The hippocampal *theta rhythms* or slow rhythmic activity is an oscillatory pattern generated by the hippocampus and measures between 4 - 10 Hz in frequency (Buzsaki, 2002; Wang, 2002). These rhythms are seen during experiments in rodents in spatial navigation (exploratory motor activity), rapid eye movement (REM) sleep, facilitating induction of synaptic plasticity (Buzsaki, 1989; Huerta & Lisman, 1993) etc. These oscillations have also been recorded from human subjects and studies are being conducted to understand how similar or different are they when compared to rodents and their functional implications (Jacobs, 2014; Zhang and Jacobs, 2015). In CA3 subfield of hippocampus, theta oscillations are produced by the network interactions between pyramidal and OLM interneurons (Neymotin et al, 2011).

The *gamma rhythms* of hippocampus are oscillatory patterns that have frequencies above 30 Hz (Colgin & Moser, 2010). These rhythms play a role in

higher brain functions like dynamic grouping, memory encoding, memory retrieval, feature binding etc (Bartos et. al, 2002; Colgin & Moser, 2010). The role of hippocampal gamma oscillations in human subjects have not been clearly known. Of late, studies have been published on their role in formation of memories in humans (Park et. al, 2014; Lega et. al, 2016).

Gamma oscillations are often found to be nested with theta-oscillations (theta-modulated gamma) though they are independently generated by cell assemblies (Colgin & Moser, 2010). The amplitude of nested gamma was found to be higher at the peak of theta-oscillations in various experimental studies during new episodic memories (Buzsaki et. al, 1983; Bragin et. al, 1995; Lega et. al, 2016). In CA3 subfield of hippocampus, the network interactions between basket and pyramidal cells is a main generator of gamma oscillations (Neymotin et al, 2011).

The oscillatory behaviour of neural networks undergoes notable changes in pathological conditions. In schizophrenia, a psychiatric disorder, the mechanisms generating theta oscillations in hippocampus are known to be suppressed, resulting in increased gamma frequency and power (Uhlhaas and Singer, 2006; Neymotin et. al, 2011). Change of oscillatory behaviour by way of abnormal neuronal synchronizations has been observed in basal ganglia disorders like Parkinson's disease (Balasubramani et. al, 2015). Epileptic activity has been characterized by abnormal oscillatory behaviour in many experimental studies. Absence seizures and Lennox-Gastaut seizures have been observed in experimental animals in the form of spike-wave complexes of about 2-3 Hz. Fast ripples have been linked to seizure initiation and epileptogenesis in the hippocampal–entorhinal cortex axis (Bragin et.al, 2002; Timofeev & Steriade, 2004). Fast and very fast oscillations **(VFO)** have

been associated with seizure activity. In hippocampal slice experiments, VFOs have been found to occur before, between and after epileptic bursts. VFOs have also been observed to superimpose on gamma oscillations induced by carbachol or high extracellular potassium in rat hippocampal slices (Traub et. al, 2001). High frequency electroencephalographic activities which are manifested from the underlying neuronal network behaviour have been observed in human subjects at the start of seizures (Fisher et. al, 1992).

2.4 EXPERIMENTAL MODELS OF EPILEPSY IN HIPPOCAMPUS

The sum total of various processes by which a part of the brain becomes epileptic is called epileptogenesis. Hippocampal formation is an area of temporal lobe which is found to be highly prone to epileptogenesis and hence has been a widely used model to study epileptic activity. The commonly followed experimental methods to induce epileptiform activity are application of convulsant chemicals like bicuculline, magnesium – free artificial cerebrospinal fluid **(aCSF)** perfusion, elevating extracellular potassium in aCSF, electrical stimulation, intraperitoneal administration of pilocarpine etc.

Bicuculline blocks fast GABAergic transmission and produces synchronized, intermittent bursts resembling human interictal-like activity mediated through AMPA/Kainate and NMDA receptors (Stoop & Pralong, 2000). Perfusing live rat brain slices with magnesium–free aCSF, dislodges the magnesium ions in the NMDA receptors. Glutamatergic synaptic events ensue, leading to hyperexcitability of neurons and epileptiform activity (Whittington et al, 1995; Barbarosie & Avoli, 1997). The elevation of extracellular potassium to about 6.5 mM and more

diminishes its driving force (difference between membrane potential and potassium Nernst potential), lowers outward potassium current and results in relative depolarization (Korn et. al, 1987; Dzhala and Staley, 2003; Id Bihi et al, 2005). Electrical stimulation (Berenyi et.al, 2012; Fisher & Velasco, 2014) in the form of continuous short stimuli, called kindling, can make the area of application generate continuous electrical discharges resembling epileptiform activity. Pilocarpine induction causes structural and connectional changes in neural networks. In rat hippocampus, the dendrite-inhibiting OLM interneurons have been found to be damaged due to pilocarpine administration (Cossart et. al, 2001; Dinocourt et. al, 2003). This leads to reduced inhibition in the neuronal network, causing hyperexcitability, characteristic of epilepsy. The hyperexcitability in neuronal networks could be so high in some pathological conditions that it could suppress inhibitory mechanisms contributed by interneurons due to their 'depolarization block', a state of inactivity due to high excitatory drive. All these experimental models induce epileptic activity by shifting the balance between excitatory and inhibitory neurons by different mechanisms.

This thesis focusses on modelling epileptic activity due to hippocampal sclerosis (structural changes) and elevating extracellular potassium (chemical changes).

2.5 LOSS OF DENDRITIC INHIBITION - THE PILOCARPINE MODEL.

Certain types of neurons especially interneurons are known to be destroyed or become dysfunctional as a consequence of factors like anoxia, stroke, brain injuries, ageing etc. This along with other associated network changes can lead to pathological conditions like epilepsy in animal models (Sloviter, 1987) and human

subjects (Laneroll et. al, 1989; Robbins et. al, 1991). The loss of somatostatin-expressing OLM interneurons in CA3 and CA1 subfields of hippocampus have been reported in pilocarpine models of experimental epilepsy (Cossart et. al, 2001; Dinocourt et. al, 2003). Due to this, the reception of excitatory inputs by pyramidal cells have been found to increase. But the exact further network mechanisms that lead to generation of epileptic activity were not understood. The pilocarpine animal model of temporal lobe epilepsy has been used since early 1980s and replicates the general progression of events leading to epileptic activity seen in humans (Mora et al., 2009). In this model, systemic injection of the convulsant pilocarpine induces *status epilepticus*, a condition where there are prolonged recurrent seizures, likely through activation of M1 muscarinic receptors, followed by a latent seizure-free period, followed by recurrent seizures during the rest of the animal's life (Furman, 2013). The computational model described in this thesis proposes a set of network changes that could trigger experimentally comparable epileptic activity in the CA3 subfield of hippocampus, given the condition of OLM interneuron dysfunction.

2.6 ELEVATION OF EXTRACELLULAR POTASSIUM IN EPILEPSIES

The potassium currents play a significant role in controlling the neuronal excitability. The rise of potassium in extracellular spaces in the neocortex during epilepsies have been reported by Robert Fischer and group as early as four decades ago (Fisher et. al, 1976). Since then, elevated potassium as a consequence of neuronal network hyperexcitability has been reported (Dzhala & Staley, 2003; Frohlich et. al, 2008). Increased extracellular potassium enhances the excitability of neurons in a feed-forward manner whereby with increasing excitability, more and

more potassium ions are expelled out of neurons and thus further raising the neuronal excitability. This observation named potassium accumulation hypothesis have been known and published decades back itself (Green et. al, 1964; Fertziger & Ranck, 1970). These 'runaway' dynamics stop when the neuronal depolarization reaches the maximum and further spiking stops due to sodium channel inactivation. Though originally rejected, results from later computational studies have prompted neuroscientists to further investigate this mechanism of seizure generation (Somjen, 2004; Frohlich et. al, 2007). Experimental animal models of epilepy show that increasing extracellular potassium in the aCSF to about 6 mM and more leads to seizure generation in hippocampal slices (McBain, 1994; Jensen & Yaari, 1997; Frohlich et. al, 2008).

Though a series of network and biochemical consequences may ensue, two main implications of increased extracellular potassium are considered in the second part of this study based on literature and reported as long ago as 1987 by Korn et.al. The reversal potential of potassium becomes more positive with excessive potassium reaching the extracellular fluid. This has a significant effect on the reversal potential of GABAergic inhibitory mechanisms, E_{GABA}. The E_{GABA} also becomes more positive, reducing the GABAergic inhibitory effect in the neuronal network leading to hyperexcitability, a characteristic feature of pathological states like epilepsy.

2.7 EPILEPSY TREATMENT AND CHALLENGES

The treatment of epilepsy could be a long-term process, first using pharmacological interventions (anti-epileptic drugs (**AEDs**)). The AED is decided based on evidence of its efficacy for a particular seizure type and tolerability.

A variety of AEDs are used these days - Gabapentin, Lamotrigine, Phenytoin, Sodium Valproate, Vigabatrin, Clonazepam etc. In some patients, a combination of some of these drugs might be necessary to effectively control the disorder.

Epilepsies in some patients are *intractable*, failing control with pharmacological treatment. Surgical resection of epileptic focus becomes a reasonable approach to treat such epilepsies. Various factors like the patient's overall general health, age, type of epilepsy, child-bearing potential, and other medical history are considered before the physician takes a decision. Various procedures are done for resurgical evaluation of these patients, including techniques like electrocorticography to locate the epileptic focus and decide the amount of tissue to be resected. Surgical treatment is individualized to the patient and can be *definitive*, if 80 - 90% cure is expected, or *palliative*, if the aim is to reduce seizure frequency.

Various challenges are faced by clinicians as well as patients in the treatment of epilepsy, the most prominent being pharmacoresistance. The available AEDs fail to control seizures in around 30% of epileptic patients worldwide (Regesta & Tanganelli, 1999; French, 2007). Pharmacoresistance is seen in about 75% of patients diagnosed with mesial temporal lobe epilepsy (Leppik, 1992; Spencer, 2002). This rate is more than 50% for patients with Lennox–Gastaut syndrome (Arts et. al, 2004) and could be as high as 90% in certain brain abnormalities, eg., hippocampal sclerosis combined with focal dysplasia or similar situations (Wahab et. al, 2010).

The AEDs give only symptomatic relief and do not stop epileptogenesis as such and their efficacy is further limited by the side effects they may have. Various drugs that are prescribed to patients have a variety of side effects. For example, gabapentin and vigabatrin treatments are known to cause weight gain (Biton, 2003;

Ben-Menachem, 2007); phenytoin, lamotrigine and carbamazepine treatment could cause skin rashes, ataxia, vertigo etc (Asconape, 2002; Wilby et. al, 2005; Zaccara et. al, 2007). Unfortunately, some of the AEDs can also aggravate seizures. Eg., myoclonic seizures may be aggravated by AEDs like gabapentin, phenytoin, vigabatrin and carbamazepine (Greenwood, 2000; Gayatri & Livingston, 2006).

Noncompliance in patients is another challenge in treating epilepsy (Leppik, 1988; Leppik, 2001). One main reason for this is side-effects themselves and another important factor being inconvenient dosage (Cramer et. al, 1995; Patsalos et. al, 2008). Noncompliance of even a short duration has been reported to lead to *breakthrough seizures*, even after months of successful treatment (Cramer et. al, 1995). It has also been observed that the compliance increases with less frequent dosing say, once or twice a day. Inconvenient dosage could also be related to incorrect dosage, presumably due to the unknown etiology or extent of alterations in brain circuitry. In ideality, if the extent of causative factor say, tissue damage could be quantified and dosage titrated accordingly, then the clinicians would be able to prescribe the correct dosage of drugs and thus ensure compliance.

2.8 HCN CHANNELS AND THE ROLE OF DRUGS

Hyperpolarization-activated cyclic nucleotide-gated (HCN) channels pass a mixed sodium and potassium current (called I_h) which is known to control the rhythmic activity in cardiac pacemaker cells and spontaneously firing neurons. I_h is also known to play roles in determining resting membrane potential, synaptic transmission etc. Research on development of drugs that act on HCN channels have been ongoing to control cardiac rhythm generation as well as neurological disorders.

Epilepsy and neuropathic pain are two neurodisorders in which HCN channels are reported to be involved (Poolos, 2004; Bender & Baram, 2008; Noam et. al, 2011) both characterized by enhanced and aberrant neuronal firing patterns. HCN channels are of four types HCN1-4, among which HCN1 and HCN2 are associated with epilepsies (Dyhrfjeld-Johnsen et. al, 2009). Though the exact role of HCN channels in epilepsy is not known, several mechanisms, including alterations in subunit compositions at different temporal and spatial scales are thought to be involved in human epilepsy (Postea & Beil, 2011).

Due to the complex and diverse mechanisms of HCN channels leading to epilepsy, it has been difficult to develop anticonvulsive drugs with a generally applicable rationale. Both activation and blocking of these channels have been observed to control epileptic activity. For example, ZD7288, an HCN channel inhibitor reduced hipppocampal epileptic discharges in rabbits (Kitayama et. al, 2003), while the anticonvulsant drugs gabapentin and lamotrigine upregulated the activity of HCN channels (Poolos et. al, 2002; Surges et. al, 2003). The most challenging aspect of drug development to target HCN channels is the design of subtype-specific ones. Drugs targeting HCN1 or HCN2 subtype could alleviate neurological disorders including epilepsy and neuropathic pain while those targeting HCN4 subtype could recover normal cardiac function (Postea & Beil, 2011).

2.9 ROLE OF COMPUTATIONAL MODELLING

The advances in the field of computational neuroscience have provided a strong platform to study the mechanisms of brain function in health and disease. Computer models could help to complement experimental studies, gain new insights

into the mechanisms of seizure generation and suggest therapy. Modelling studies may be designed at various levels - molecular, cellular, network and systems level to simulate the normal baseline function of a neuron or a network with necessary details of its anatomy, biophysics, connectivity etc. The technically challenging experiments can be more easily performed using computer models, eg., modelling lesions. The results obtained from computational studies can be further verified by designing appropriate experiments.

Various computational models have been developed to understand the mechanisms of epileptic seizures at cell and network levels (Bazhenov et. al, 2008), prediction of seizures (O'Sullivan-Green et. al, 2009) and therapeutic control of seizures (Iasemidis, 2003). Computational models of epilepsy are available from large-scale mean field models of dynamics (Gonzalez-Ramirez et. al, 2015) to detailed neural network models of network activity (Lytton et. al, 1998; Morgan & Soltesz, 2008) to hyperexcitable cell models (Migliore et. al, 1995; Lazarewicz et. al, 2002; Hemond et. al, 2008) to intricate ion channel models of epileptogenic ion channel mutations (Klassen et. al, 2011). As for therapeutic applications, Jobst et. al (2010) mentions the use of computer modeling to suggest implantable devices for seizure detection and their suppression using electrical signals. For example, AEDs act by changing various cellular and molecular mechanisms like channel conductivity among many other parameters to control epileptic activity. Pharmacokinetic models developed to explore and predict the absorption, distribution, metabolism and excretion mechanisms of drugs can be coupled to these neural models. A number of other computational models of epileptic activity have

been described in reviews by Lytton (2008), Case & Soltesz (2011) and Stefanescu et. al (2012).

2.10 THE NEURON SIMULATION ENVIRONMENT

The software used for the simulations in this work is NEURON with Python interpreter, developed by Ted Carnevale and Michael Hines at Yale University and freely downloadable from the website www.neuron.yale.edu (Carnevale & Hines, 2006; Hines et al, 2009).This software is particularly useful if larger biophysical details of neurons are to be included. Currently there are about 1700 research publications that actually used NEURON, which shows the wide acceptability of this software in research labs across the world.

CHAPTER 3

MATERIALS AND METHODS

3.1 THE MODEL

The insilico biophysical model of CA3 neuronal network described in this study was adopted from the ModelDB of NEURON software (Neymotin et. al, 2011, Accession No. 139421). Additional connectivities consistent with anatomical data were added as described in Sanjay et. al (2015). Initially normal baseline network activity was established, followed by network changes to systematically explore how: 1) reduction in connectivity from OLM to pyramidal cells alone influences overall network activity, 2) changes in reception of external inputs by pyramidal cells alter the network activity 3) changes in connectivity between all neuron types affect overall network activity, generating a characteristic epileptiform activity 4) how increased extracellular potassium along with network changes lead to epileptic activity and 5) how drugs acting on HCN channel conductance control epileptic activity. The part of the work showing the effect of network changes alone in the model (1, 2 and 3 mentioned above) is available in the ModelDB of NEURON (Sanjay et. al (2015), Accession No.186768).

The following sub-sections 3.2 and 3.3 describe the features of the normal baseline network model that generates theta-modulated gamma oscillations.

3.2 CELL TYPES AND CURRENTS

3.2.1 Pyramidal Cells

A pyramidal cell has pyramid-shaped cell body or soma and two distinct types of dendrites - apical and basal (Cutsuridis et. al, 2010; Neymotin et. al, 2011).

A single axon sends the signals along and transmits them to the connected neurons. The morphologies of pyramidal neurons of CA3 subfield of hippocampus vary within the subfield. The pyramidal cells of this subfield have high degree of recurrent connections. This is thought to significantly enhance the excitability of neurons and lead to pathological states like epilepsy.

The neuron network model used in this study has 800 pyramidal cells each with five compartments - one somatic, three apical and one basal dendritic compartment. To obtain stable baseline activity, a -50 pA current is injected in this cell model. This injected current substitutes external inputs that were not exclusively modelled. The pyramidal cells contained leak current, transient sodium current I_{Na}, delayed rectifier current $I_{K\text{-}DR}$, A-type potassium current $I_{K\text{-}A}$ and hyperpolarization-activated current I_h. The leak current, I_{Na} and $I_{K\text{-}DR}$ were for action potential generation and $I_{K\text{-}A}$ for rapid inactivation.

3.2.2 Basket Cells

A basket cell is named so since their dendrites form a basket-like shape around its cell body. These cells have inhibitory effect on the neurons they project . They are located near the somatic regions of pyramidal cells and connected to somatic and perisomatic regions of pyramidal cells. Their proximity to the pyramidal cells facilitates their easier excitation due to the drive from the pyramidal neurons. Their close proximity and projection to soma controls the excitability of pyramidal cells. The pyramidal - basket feedback interactions generate gamma frequency oscillations of about 35 Hz in the normally connected network. These oscillations are important in learning and memory, encoding and retrieval (Colgin and Moser, 2010).

In this model , there were 200 single-compartment basket cells in the network. The basket cells contained leak current, transient sodium current I_{Na} and delayed rectifier potassium current $I_{K\text{-}DR}$.

While studying the effect of enhanced extracellular potassium on the network and the effect of hyperpolarization-activated current (I_h) modulating drugs, Ih-currents were also incorporated in the basket cells and baseline activity again characterized.

3.2.3 OLM Interneurons

The Oriens-Lacunosum Moleculare (OLM) inhibitory interneurons have anatomical presentation from stratum oriens extending to stratum lacunosum-moleculare in the hippocampus and their axons synapse onto the distal apical dendrites of the pyramidal cells. The feedback interactions between pyramidal and OLM cells generated theta oscillations in the normally connected network. These 4-8 Hz oscillations play a significant role in spatial navigation and motor behaviour (Colgin & Moser, 2010). The model network contained 200 one-compartment OLM interneurons. Apart from leak current, I_{Na} and $I_{K\text{-}DR}$, the OLM interneurons contained calcium-activated potassium current $I_{K\text{-}Ca}$, high-threshold calcium current I_L, hyperpolarization-activated current Ih and intracellular calcium dynamics. $I_{K\text{-}Ca}$ allowed long-lasting inactivation after bursting, I_L augmented bursts and activated $I_{K\text{-}Ca}$ and I_h allowed bursting.

All the current types were based on the published work by Tort et. al (2007) and Gloveli et. al (2007). The selection of these currents and synaptic and connectivity parameters established the normal baseline activity of the CA3 network.

3.3 NEURONAL CONNECTIVITY AND SYNAPTIC MECHANISMS

This section describes the connectivity between different neurons and synaptic mechanisms in the model network **(Figure 3.1)**. The convergence for each neuron type (number of neurons synapsing on each type), synaptic mechanisms involved and external inputs received by these neurons are further discussed. The inputs from Medial Septum onto the inhibitory neurons are separately mentioned.

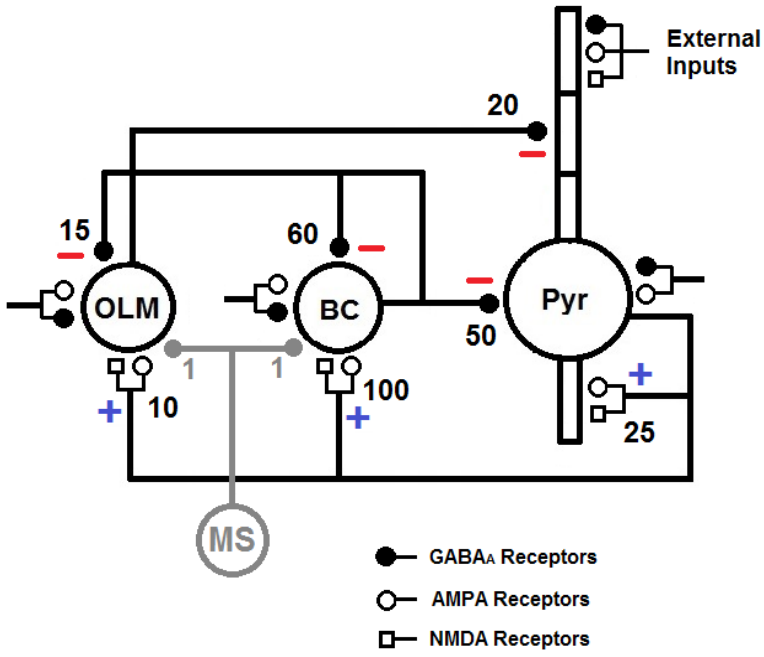

Figure 3.1: Schematic network with 800 Pyramidal cells (Pyr), 200 Basket cells (BC), 200 OLM interneurons. The number of inputs for an individual synapse (convergence) are shown near synapses. Synapses with truncated lines - External random inputs. MS - Medial Septum inputs. '+' and '-' shows excitatory and inhibitory connections respectively.

The pyramidal cells are recurrently connected similar to anatomical observation (Witter, 2007; Amaral, 1993). Each pyramidal cell receives AMPA and NMDA mediated excitatory inputs from 25 other pyramidal cells at their basal dendritic compartment. The pyramidal cells excite basket cells and OLM interneurons through AMPA and NMDA receptors. A pyramidal cell receives inhibitory inputs at their soma from 50 basket cells. The middle apical dendritic

compartment of each pyramidal cell receives inhibitory inputs from 20 OLM interneurons. Both basket and OLM inputs received by pyramidal cells are inhibitory, and $GABA_A$ receptor-mediated. The pyramidal cells also receive external random inputs at their somatic compartment through AMPA and $GABA_A$ receptors. Random inputs are received at the distal-most apical dendritic compartment through AMPA, NMDA and $GABA_A$ receptors. These mainly simulate the inputs from the entorhinal cortex.

The basket cells in the model are also recurrently connected, similar to pyramidal cells. Each basket cell receives inhibitory inputs from 60 other basket cells through $GABA_A$ receptors and excitatory inputs from 100 pyramidal cells through AMPA and NMDA receptors. The basket cells inhibit pyramidal cells at their soma through $GABA_A$ synapses. Based on published anatomical information, a new connection was added in the model from basket cells to OLM interneurons through $GABA_A$ synapses (Cobb et. al, 1997). The basket cells also receive external random inputs through AMPA and $GABA_A$ receptors.

The OLM interneurons inhibit the dendrites of pyramidal cells and synapse on the middle compartment of the apical dendrite through $GABA_A$ receptors. Excitatory inputs are received by each OLM interneuron from 10 pyramidal cells through AMPA and NMDA receptors and inhibitory inputs from 15 basket cells through $GABA_A$ receptors. External random inputs reach OLM interneurons through AMPA and $GABA_A$ receptors.

There are 155,000 synapses in the model. The basket cells and OLM interneurons receive inhibitory inputs from Medial Septum **(MS)** through $GABA_A$ receptors. The MS acts as a pacemaker (Stewart & Fox,1990; Dragoi et al., 1999;

Borhegyi et al, 2004) and is modelled as a rhythmic input received every 150 ms. Tables 3.1 and 3.2 list the parameters for modelling background activity and connectivity along with their values.

Table 3.1: Parameters for modelling background random activity

Cell Type	Section	Synapse	Type	τ_1(ms)	τ_2 (ms)	Conductance (nS)
PYR	Dendrite	AMPA	Excitatory	0.05	5.3	0.05
PYR	Dendrite	NMDA	Excitatory	15	150	6.5
PYR	Dendrite	$GABA_A$	Inhibitory	0.07	9.1	0.012
PYR	Soma	AMPA	Excitatory	0.05	5.3	0.05
PYR	Soma	$GABA_A$	Inhibitory	0.07	9.1	0.012
BC	Soma	AMPA	Excitatory	0.05	5.3	0.02
BC	Soma	$GABA_A$	Inhibitory	0.07	9.1	0.2
OLM	Soma	AMPA	Excitatory	0.05	5.3	0.0625
OLM	Soma	$GABA_A$	Inhibitory	0.07	9.1	0.2

PYR - Pyramidal Cell, BC - Basket Cell, OLM - Oriens Lacunocum Moleculare interneuron

These parameters are based on previous publications: Stewart & Fox, 1990; White et. al, 2000; Destexhe et. al, 2003; Gloveli et. al, 2005; Tort et. al, 2007; Hangya et al., 2009; Stacey et. al, 2009; Neymotin et. al., 2011.

Table 3.2: Synaptic parameters for neuronal connectivity in the model

Presynaptic	Post-synaptic	Receptor	Type	τ_1 (ms)	τ_2 (ms)	Conductance (nS)
PYR	PYR	AMPA	Excitatory	0.05	5.3	0.02
PYR	PYR	NMDA	Excitatory	15	150	0.004
PYR	BC	AMPA	Excitatory	0.05	5.3	0.36
PYR	BC	NMDA	Excitatory	15	150	1.38
PYR	OLM	AMPA	Excitatory	0.05	5.3	0.36
PYR	OLM	NMDA	Excitatory	15	150	0.7
BC	PYR	$GABA_A$	Inhibitory	0.07	9.1	0.72
BC	BC	$GABA_A$	Inhibitory	0.07	9.1	4.5
*BC	OLM	$GABA_A$	Inhibitory	0.07	9.1	0.0288
OLM	PYR	$GABA_A$	Inhibitory	0.2	20	72
MS	BC	$GABA_A$	Inhibitory	20	40	1.6
MS	OLM	$GABA_A$	Inhibitory	20	40	1.6

PYR - Pyramidal Cell, BC - Basket Cell, OLM - Oriens Lacunosum Moleculare interneuron, MS - Medial Septum inputs

These parameters are based on previous publications: Stewart & Fox, 1990; White et. al, 2000; Gloveli et. al, 2005; Tort et. al, 2007; Hangya et al., 2009; Stacey et. al, 2009; Neymotin et. al, 2011. *The connectivity from basket to OLM interneurons was additionally incorporated in the model (Sanjay et. al, 2015).

3.4 PROPOSED MECHANISM OF EPILEPTIC ACTIVITY GENERATION

To study how decreased dendritic inhibition of pyramidal cells led to epileptic activity, three scenarios were considered stepwise as follows:

1) reducing the strength of connection from OLM interneuron to pyramidal cell in steps, without other changes in the network.

2) along with 1) above, proportionately increasing the reception of external excitatory inputs by the pyramidal cells;

3) changes in synaptic strength simulated at all synapses in the network.

The network activity is considered to be epileptic when, the baseline theta-modulated gamma is totally disrupted, the firing rates **(FR)** of constituent cells become high with pyramidal cell FR reaching close to 5 Hz or more, as experimentally observed (Ziburkus et. al, 2006) and the local field potential (LFP) record shows a spiking pattern characteristic of an experimentally comparable ictal / epileptic condition (10 - 20 ictal spikes per second (Isaev et. al, 2007; Cymerblit-Sabba & Schiller, 2012)).

Scenario 1

In this scenario **(Figure 3.2)**, the strength of connectivity from OLM to pyramidal cells was reduced in steps from baseline 100% to 80%, 60%, 40%, 20%, 10%, 5% and 0% (total loss). This was simulated to study the influence of dendritic inhibition by OLM interneurons in the network and if this change alone could lead to network hyperexcitability.

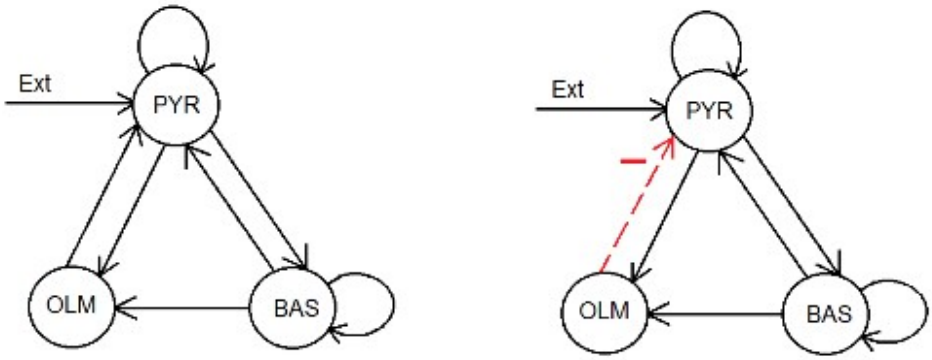

Figure 3.2: Reduced schematic diagram showing normal baseline connectivity (left) and reduction in OLM to pyramidal cell connectivity alone (right figure, red dashed arrow). PYR - Pyramidal cell, BAS - Basket Cell, OLM - Oriens-Lacunosum Moleculare interneuron.

Scenario 2

Along with reducing the dendritic inhibition of pyramidal cells provided by OLM interneurons, a proportionate increase in external excitatory inputs received by pyramidal cells at their distal apical dendritic compartment was simulated **(Figure 3.3)**. These simulated excitatory inputs are received mainly from the entorhinal cortex. The strength of connection from OLM interneuron to pyramidal cells is reduced in steps from the baseline 100% to 80%, 60%, 40% 20%, 10%, 5% and 0% (total loss of OLM connectivity onto pyramidal cells). Correspondingly, the reception of external excitatory inputs at the distal apical dendritic compartment of pyramidal cells was proportionately increased from baseline 100% to 120%, 140%, 160%, 180%, 190%, 195% and 200% respectively.

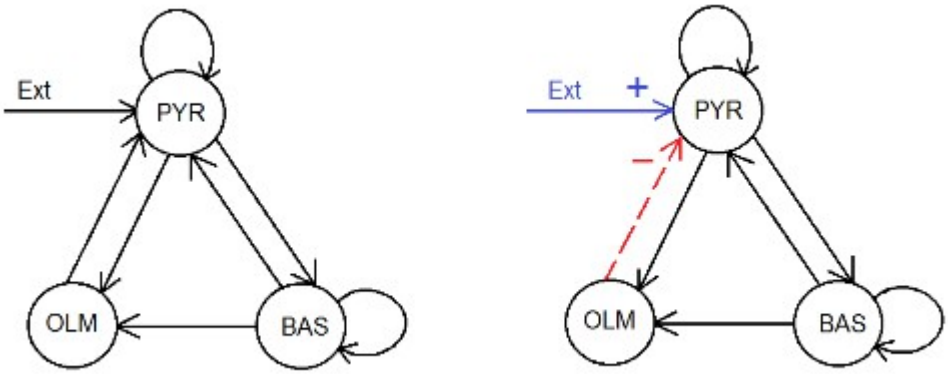

Figure 3.3: Reduced schematic diagram. Left shows normal baseline connectivity. Right shows reduction (red arrow) in OLM - Pyramidal connectivity along with increase (blue arrow) in external excitatory inputs. PYR - Pyramidal cell, BAS - Basket Cell, OLM - Oriens-Lacunosum Moleculare interneuron.

Scenario 3

Along with reduction in dendritic inhibition and enhancement in reception of external excitatory inputs by pyramidal cells (Scenario 2), the strengths of connection between different neuron types were changed in a stepwise manner **(Figure 3.4)**. There was no quantitative information from literature about the extent of possible changes in the strength of these synapses. Also, it was not known *how much* change in synaptic strength *in vivo* or *in vitro* leads to hippocampal hyperexcitability, leading to epilepsy. Therefore, the changes in synaptic strengths between neurons were arbitrarily assumed. While reducing the pyramidal dendritic inhibition (numbered 1 in parenthesis, Fig 3.4), the following network connectivity changes were assumed and systematically simulated **(Figure 3.4)**

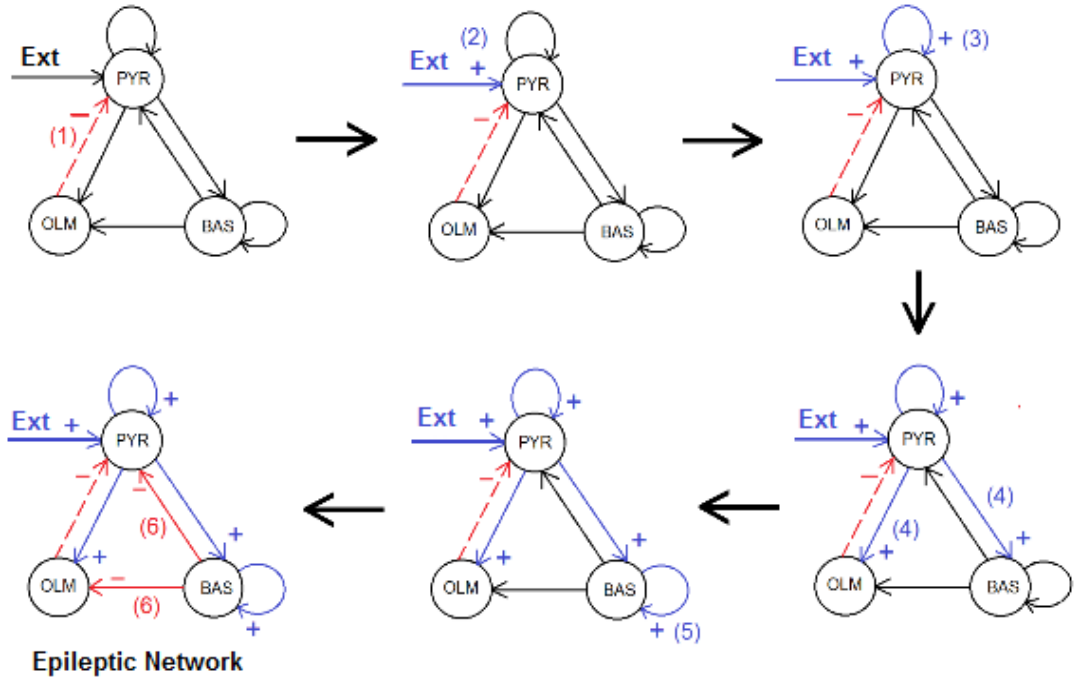

Figure 3.4: Stepwise simulation of network connectivity changes leading to epileptic activity in a CA3 network. Blue arrows with '+' sign show strengthened synaptic responses, red arrows with '-' sign show weakened synaptic responses. The dashed arrow from OLM to pyramidal cell shows input condition - reduced dendritic inhibition. The number in parenthesis show sequence of network changes. PYR - pyramidal cell, BAS - basket cell, OLM - Oriens-Lacunosum Moleculare interneuron.

> The excitability of pyramidal cells is increased due to increased reception of external excitatory inputs. (numbered (2), Fig 3.4)

> The enhanced excitability of pyramidal cells along with their mutual recurrent connectivity strengthens the communication between them. This increases the overall excitatory output from pyramidal cell population and excites the connected cells (3).

> The highly excited pyramidal cells strongly excite basket cells and OLM interneurons (4)

> The increased excitability of basket cells increases the recurrent inhibition between them, further disinhibiting the pyramidal cells (5 & 6).

The increased excitability of pyramidal cells increases the drive to OLM

interneurons but the reduced strength of connection from OLM interneurons to pyramidal cells prevents effective dendritic inhibition of pyramidal cells. These set of processes lead to overall hyperexcitability in the network. The increase in reception of external excitatory inputs by the pyramidal cells due to sprouting and spine formation in their distal apical dendrites has been reported in the literature (McAllister, 2000) and hence justifies the simulation.

Based on these proposed network changes, two representative conditions are shown - reduction of OLM interneuron to pyramidal cell connectivity to:

1) 50% (50% impairment of dendritic inhibition) of the baseline **(Figure 3.5 (a))** and

2) 30% (70% impairment of dendritic inhibition) **(Figure 3.5 (b))** of the baseline along with corresponding changes in strength of connectivity between the other neurons.

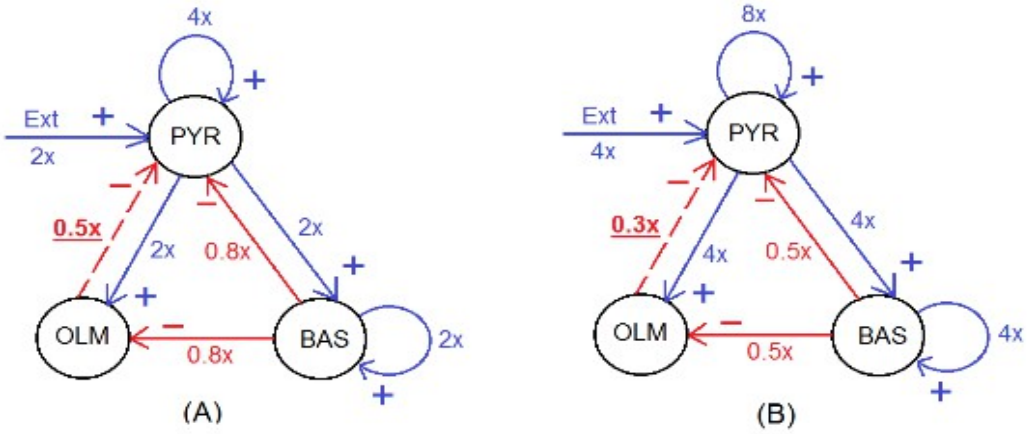

Figure 3.5: Network connectivity changes when dendritic inhibition reduces to 50% (0.5x) of the baseline (A) and 30% (0.3x) of the baseline (B). PYR-pyramidal cell, OLM-Oriens-Lacunosum Moleculare interneuron, BAS- Basket Cell.

The following changes in connectivity were simulated while reducing the connectivity from OLM to pyramidal cells to 50% of the baseline (50% impairment).

Compared to baseline normal levels,

> the reception of external excitatory inputs by pyramidal cells at their distal apical

dendrites doubled (2x)

> the recurrent connectivity between pyramidal cells strengthened by four times (4x)

> the excitatory drive received by OLM interneurons and basket cells from pyramidal cells strengthened twice (2x)

> basket cell to basket cell inhibitory interactions strengthened twice (2x)

> inhibition received by pyramidal cells and OLM interneurons from basket cells reduced to 80% of baseline (0.8x)

The changes in connectivity simulated with reduction of OLM to pyramidal cell connectivity to 30% of baseline (70% impairment) are as follows. **Compared to baseline normal levels,**

> external excitatory inputs received by pyramidal cells at their distal apical dendrites increased by four times (4x)

> the recurrent connectivity between pyramidal cells strengthened by eight times (8x)

> the excitatory drive received by OLM interneurons and basket cells from pyramidal cells strengthened by four times (4x)

> basket cell to basket cell inhibitory interactions strengthened by four times (4x)

> inhibition received by pyramidal cells and OLM interneurons from basket cells reduced to 50% of baseline (0.5x)

3.5 SIMULATING HIGH EXTRACELLULAR POTASSIUM CONDITION

The enhancement of extracellular potassium $[K+]_O$ levels in the network was simulated as an effect of overall excitatory activity in the network. With enhanced extracellular potassium concentration, two important parameters were considered – the reversal potential of potassium E_K and the reversal potential of inhibitory

synapses, E_{GABA}. The changes in extracellular potassium affects chloride (Cl-) transport. High extracellular potassium is reported to increase Cl− influx through the sodium-potassium-chloride co-transporter NKCC1 (Id Bihi et. al, 2005). This results in depolarization of E_GABA which could impair inhibitory control of recurrent excitations in hippocampal networks.

After characterizing the baseline activity of the normally connected network (theta-modulated gamma oscillations), the reduction of OLM to pyramidal cell connectivity was simulated in two steps - 20% impairment in dendritic inhibition (80% OLM to pyramidal connectivity, **Figure 3.6** (left)) and 30% impairment in dendritic inhibition (70% OLM to pyramidal connectivity, **Figure 3.6** (right)) with increase in extracellular potassium levels accordingly. The details are as below:

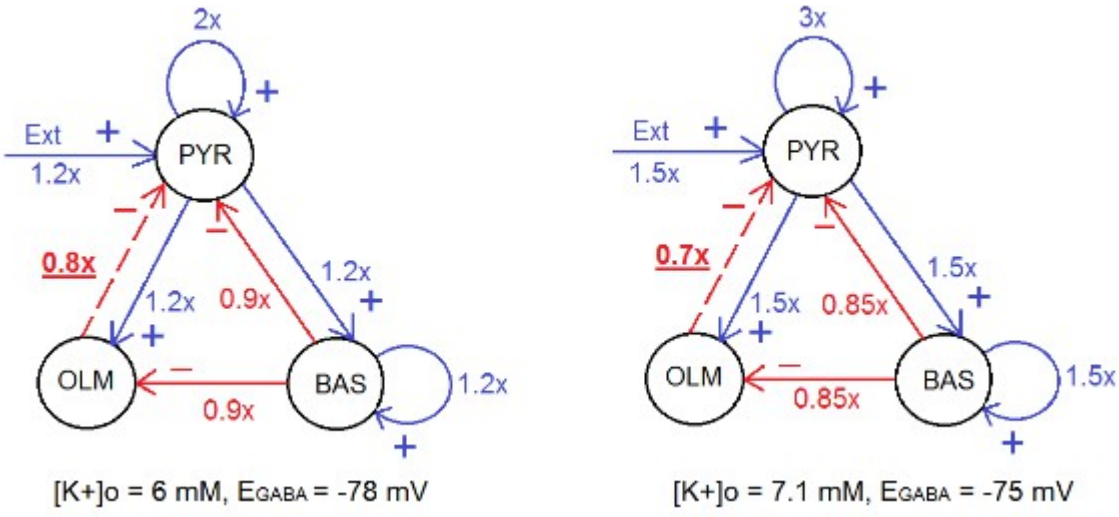

Figure 3.6: Scheme of connectivity in the CA3 network. Left: Network changes due to 20% impaired dendritic inhibition (OLM – Pyr connectivity 80% (0.8X), underlined); Right: Network changes due to 30% impaired dendritic inhibition (OLM – Pyr connectivity 70% (0.7X),underlined). The extracellular potassium concentrations [K+]o and reversal potential of GABA (E_{GABA})are shown for each case.

First, in the baseline model, the strength of OLM to pyramidal cell connection was reduced to 80% of baseline connectivity (20% impaired dendritic inhibition). In this condition, compared to baseline levels,

> The external excitatory input reception by pyramidal cells enhanced by 20% (1.2x)

> The strength of recurrent connectivity between pyramidal cells was doubled (2x)

> The strength of connectivity of pyramidal cell to basket cells, basket cell to basket cell and pyramidal to OLM cells were also enhanced by 20% (1.2x)

> The strength of connectivity from basket cell to pyramidal and basket cell to OLM interneurons was reduced to 90% of baseline (0.9x)

> The extracellular potassium levels were increased to 6 mM (E_K = -85 mV, applying Nernst Equation) and E_{GABA} was made slightly more positive to -78 mV from the baseline of -80 mV.

Second, in the baseline model, the strength of OLM to pyramidal cell connection was reduced to 70% of baseline connectivity (30% impairment). In this condition, **compared to baseline levels,**

> The external excitatory input reception by pyramidal cells enhanced by 50% (1.5x)

> The strength of recurrent connectivity between pyramidal cells was tripled (3x)

> The strength of connectivity of pyramidal cell to basket cells, basket cell to basket cell and pyramidal to OLM cells were also enhanced by 50% (1.5x).

> The strength of connectivity from basket cell to pyramidal and basket cell to OLM interneurons was reduced to 85% of baseline (0.85x)

> The extracellular potassium levels was increased to 7.1 mM (E_K = -80 mV, applying Nernst Equation) and E_{GABA} was made slightly more positive to -75 mV from the baseline of -80 mV.

3.6 SIMULATING THE EFFECT OF ENHANCED HCN CONDUCTANCE g(Ih) IN THE NETWORK

3.6.1 Effect on normal baseline network.

To study the effect of enhancing g(Ih) in the network, initially its value was changed in one type of neuron at a time. This approach was taken to isolate the role of Ih for that type of cell and its contribution in epileptogenesis. First, g(Ih) was enhanced to two, four and six times the baseline in pyramidal neurons alone, followed by changes in basket cells alone and then in OLM cells alone. Thereafter, g(Ih) was simultaneously enhanced in all three neuron types simultaneously to two, four and six times its baseline value.

3.6.2 Effect on epileptic network.

The effect of enhanced (g(Ih)) was tested on the network which generated epileptiform activity due to 30% impairment in dendritic inhibition **(Figure 3.6, Right)**. This was done to study the expected effect of g(Ih)-modifying drugs. The g(Ih) was increased in all three neuron types simultaneously by two, four and six times the baseline values to study changes in network activity.

The effect of enhanced (g(Ih)) was further tested on the networks with 50% and 70% impairment in dendritic inhibition with extracellular potassium levels maintained at 7.1 mM itself **(Figure 3.7)**. The g(Ih) was enhanced in all three neuron types uniformly by two, four and six times the baseline values in these networks.

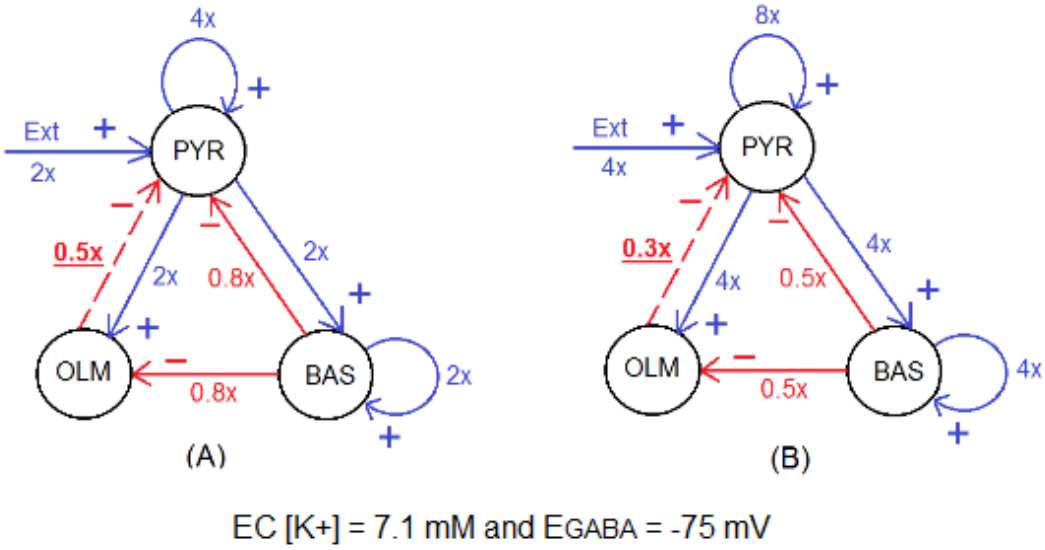

Figure 3.7 The networks with 50% and 70% impairment in dendritic inhibition (A and B respectively) with extracellular potassium levels maintained at 7.1 mM itself to test effect of enhanced g(Ih).

3.7 SIMULATIONS AND ANALYSIS

The simulations were run on a quad core 2.66 GHz Linux based 64-bit system using the NEURON simulator with Python interpreter (Hines et al, 2009; Carnevale & Hines, 2006). A single simulation (5s, 1200 neurons) with a time step of 0.1 ms took about 5 minutes to run. More than 1000 simulations have been done for the entire study. For the part of the study on increased extracellular potassium and effect of drugs, a single simulation (3.2 s, 1200 neurons) took approximately 3.5 minutes to run with a fixed time step of 0.1 ms. The output of the simulations including the individual cell firing patterns and local field potentials were saved as text files. The data were imported to the software pClamp v.10 (Molecular Devices Inc, USA) for analysis. In all the simulated outputs, the first 200 ms of data required for baseline stabilization was discarded. Analysis of the data included average firing frequency of each type of neuron, synchronous activity between the neuron types, changes in firing rates of individual cell types, theta and gamma frequencies and their power.

CHAPTER 4

RESULTS

4.1 CHANGES IN NEURONAL CONNECTIVITY IN THE NETWORK

4.1.1 Baseline Network Activity

The baseline CA3 network comprising of pyramidal cells, basket cells, and OLM interneurons generated theta-modulated gamma oscillations with inputs from Medial Septum **(MS)** as simulated in the Local Field Potential **(Figure 4.1)**. The inhibitory interactions between pyramidal and basket cells and those between basket cells generated gamma rhythms. The interactions between pyramidal cells and OLM interneurons produced theta rhythms (Neymotin et al., 2011). Though the OLM and basket cells were equally driven by the inputs from MS, the effect on basket cells was lesser due to the excitatory drive received by basket cells from pyramidal cells and the interactions between basket cells themselves.

The periodic MS inputs provided to the inhibitory neurons every 150 ms primarily turned off OLM activity **(Figure 4.2,** Raster Plot**)**. This disinhibited pyramidal cells as seen from the gradual increase in firing of pyramidal cells after MS inputs. The pyramidal cells drove both OLM interneurons and basket cells. The basket cell activation contributed to the amplitude of gamma oscillations. As OLM interneurons were excited by pyramidal cells, they again start inhibition of pyramidal cell activity, which reduced LFP and gamma amplitude, until the next MS inputs are received by the interneurons. The LFP is computed by a sum of differences in membrane potential between the most distal apical and the basal dendritic compartment over all pyramidal cells. The theta and gamma waves generated was a

result of pyramidal-basket, basket-basket and pyramidal-OLM interactions. Their obtained amplitude pattern was similar to that in previous model by Neymotin et. al (2011). Due to these sequence of interactions between neuron types, the network activity reflected an imposed theta oscillation of 6.7 Hz frequency from the periodic medial septal activation at every 150 ms. The basket-basket and basket-pyramidal interactions resulted in gamma activity and measured ~33 Hz in the LFP. The average firing rates **(FR)** were: 2.36 +/- 0.02 Hz for pyramidal cells, 16.05 +/- 0.15 Hz for basket cells and 0.96 +/- 0.03 Hz for OLM interneurons.

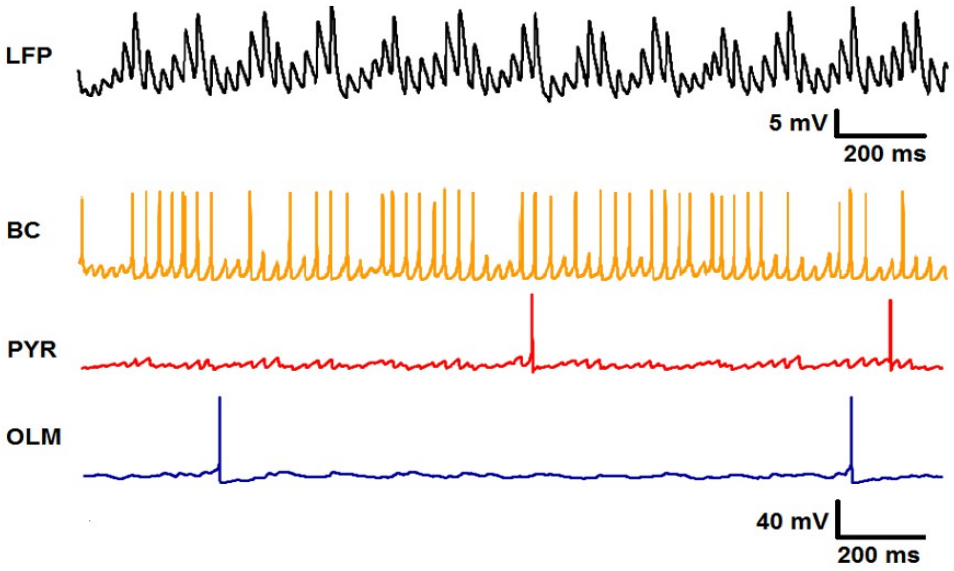

Figure 4.1 The baseline theta-modulated gamma oscillations and activity of individual cell types. LFP - Local Field Potential, OLM - OLM Interneurons, BC - Basket Cells, PYR - Pyramidal Cells

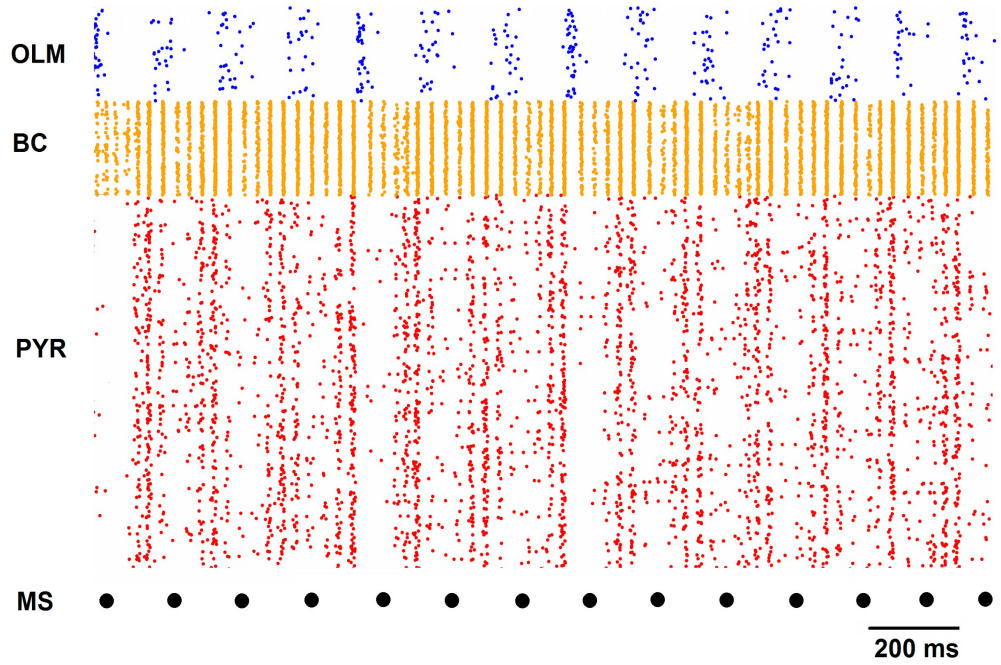

Figure 4.2 Raster Plot showing the spiking activity of 800 pyramidal cells (PYR), 200 basket cells (BC) and 200 OLM interneurons (OLM) in the network. The black dots represent the medial septum (MS) inputs to OLM and BC every 150 ms. Many spikes not be visible due to vertical overlap.

4.1.2 Scenario 1: Effect of reducing dendritic inhibition onto distal dendrites of CA3 pyramidal neurons.

The strength of connection from OLM interneurons to pyramidal cells was reduced step by step from 100% to 0%. The FR of all individual cell types increased with reduction in OLM to pyramidal cell connectivity. Specifically, there was a significant increase in firing activity in all three cell types when OLM – pyramidal cell connectivity was less than 5% **(Table 4.1)**. The FR of pyramidal and basket cells nearly doubled when the OLM – pyramidal cell connectivity was reduced to 0%: from 2.36 +/-0.02 Hz at baseline to 4.19 +/-0.04 Hz for pyramidal cells and 16.05 +/- 0.15 Hz to 30.98 +/-0.07 Hz for basket cells. The FR of OLM interneurons almost tripled, from 0.96 +/- 0.03 Hz to 2.7 +/- 0.03 Hz.

The theta and gamma frequencies remained unchanged at about 6.7 Hz and

32-33 Hz respectively (similar to baseline) till the OLM - pyramidal connectivity was reduced to 5%. The theta component of the LFP disappeared when the OLM to pyramidal cell connectivity was reduced to 0% which is total impairment of dendritic inhibition **(Figure 4.3)**.

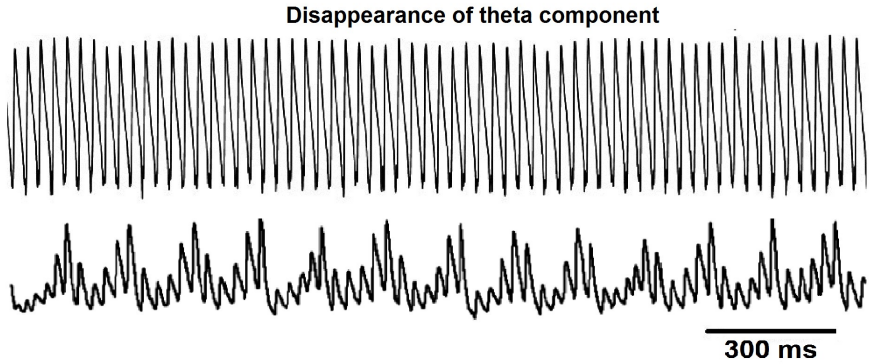

Figure 4.3 The local field potential record showing the disappearance of theta component when the OLM - pyramidal connectivity is reduced to 0% (top). The baseline theta-modulated gamma oscillations are shown for comparison (bottom). The gamma frequency remained the same at around 33 Hz in both cases, but the power of gamma oscillations increased from 2.55 mV^2/Hz at baseline to 8.7 mV^2/Hz at total impairment of dendritic inhibition.

With the reduction of OLM to pyramidal cell connectivity, the powers of theta and gamma oscillations varied in inverse fashion. The theta power reduced from 5.35 mV^2/Hz (baseline) to 0.95 mV^2/Hz when OLM – pyramidal connectivity was reduced to 5%. Further, it reduced to 0 at total lack of dendritic inhibition (0% OLM - pyramidal cell connectivity). On the other hand, the gamma power increased from 2.55 mV^2/Hz (baseline) to 8.7 mV^2/Hz at total lack of dendritic inhibition. It was also observed that the gamma power remained fairly stable around 4 mV^2/Hz when OLM to pyramidal cell connectivity varied between 10% to 40% **(Table 4.1)**.

Table 4.1 The average firing rate (FR) of cell types, theta and gamma frequency components in the LFP and their powers, when dendritic inhibition alone is reduced stepwise (Scenario 1).

OLM to Pyr. Weight	Pyr (Hz)	BC (Hz)	OLM (Hz)	Theta Freq (Hz)	Theta Power (mV^2/Hz)	Gamma Freq (Hz)	Gamma Power (mV^2/Hz)
100%	2.36+/-0.02	16.05+/-0.15	0.96+/-0.03	6.7	5.35	33.2	2.55
80%	2.43+/-0.03	15.96+/-0.16	0.98+/-0.03	6.7	4.6	33.9	1.18
60%	2.51+/-0.03	17.46+/-0.15	0.95+/-0.03	6.7	4.2	32.7	1.3
40%	2.62+/-0.03	18.56+/-0.16	0.95+/-0.03	6.7	4.1	32	3.7
20%	2.76+/-0.03	19.87+/-0.15	1.03+/-0.03	6.7	2.85	32	3.9
10%	2.87+/-0.03	21.62+/-0.15	1.18+/-0.03	6.7	1.45	31.5	4.2
5%	3.08+/-0.03	23.17+/-0.13	1.37+/-0.03	6.7	0.95	31.1	7.8
0%	4.19+/-0.04	30.98+/-0.07	2.7+/-0.04	0	0	32.4	8.7

On reducing OLM to pyramidal cell connectivity, the FR for all three neuron types increased. The theta frequency was constant at 6.7 Hz (except at 0% connectivity), while gamma frequency varied slightly. At total impairment of dendritic inhibition (0% OLM to pyramidal cell connectivity), theta power reduced from 5.35 to 0 mV^2/Hz while gamma power increased from 2.55 to 8.7 mV^2/Hz.

4.1.3 Scenario 2: Effect of increased external inputs received at distal dendrites along with loss of dendritic inhibition

With stepwise decrement of OLM to pyramidal cell connectivity, proportional increments were simulated in the reception of external inputs by pyramidal cells through AMPA and NMDA synapses. The dendritic inhibition was systematically reduced from 100% to 80%, 60%, 40%, 20%, 10%, 5% and 0% (total impairment). The reception of external inputs by the pyramidal cells at their distal apical compartment was correspondingly increased from 100% to 120%, 140%, 160%, 180%, 190%, 195% and 200% respectively.

Until the reduction of OLM to pyramidal connectivity to 20% of baseline, all the neuron types – pyramidal, basket and OLM interneurons, showed synchronous activity. Reducing the OLM - pyramidal cell connectivity to 10% resulted in tighter synchrony of activity of basket cells among themselves **(Figure 4.4, top)**. Further reduction of this connectivity to 5% of baseline resulted in desynchronization among basket cells **(Figure 4.4, middle)**. The desynchronization of basket cells was more prominent at total lack of OLM – pyramidal cell connectivity **(Figure 4.4, bottom)**. The synchrony between OLM cells and pyramidal cells was maintained since the connectivity from pyramidal cells to OLM cells was not affected.

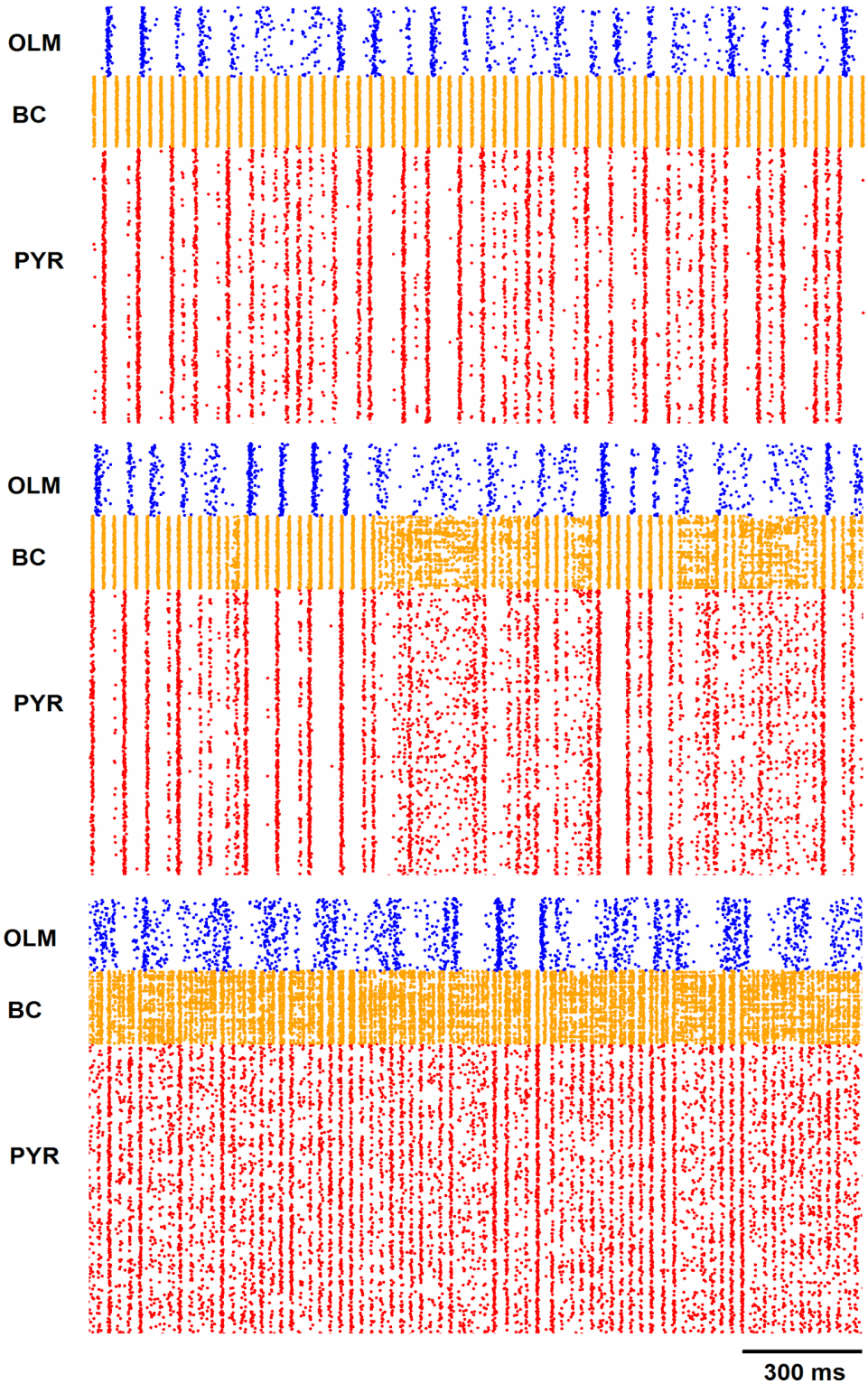

Figure 4.4: Synchrony between the neuron types when strength of OLM to pyramidal cell connectivity is 10% (top), 5% (middle), and 0% (bottom). At 10% connectivity, all cell types showed synchronous activity; at 5% connectivity, Basket Cells (BC) starts to undergo desynchrony. At 0%, the BCs show a high lack of synchrony while, OLM and Pyramidal cells (PYR) still maintain synchronous activity.

To quantify the change in synchrony among basket cells, correlation of activity of two arbitrary basket cells (50th and 100th in the network) was analysed at 100% and 0% OLM to pyramidal connectivity. Two different time periods - 5 seconds and 1 second was taken for correlation analysis for 100% and 0% OLM to pyramidal cell connectivity.

The Pearson's formula was used for computing correlation. The coefficient of correlation r is given by

$$r = \frac{\sum_i (x_i - \bar{x})(y_i - \bar{y})}{\sqrt{\sum_i (x_i - \bar{x})^2 \sum_i (y_i - \bar{y})^2}}$$

$\bar{x}$ and $\bar{y}$ are averages of x and y; they being the two sets of data-points defining the signals of interest (basket cell activity). The correlation was taken as a measure of how synchronous the activity of an arbitrary pair of basket cells was in the network.

On computing the cross-correlation for five seconds of data, at 100% OLM-Pyramidal cell connectivity, the correlation of the activities of basket cells (50^{th} to 100^{th}) was 57.7% with a lag time of +0.2 ms. At 0% connectivity, it was 33.5% with lag time of -0.2 ms. Computing similarly for one second of data, at 100% OLM - pyramidal cell connectivity, the correlation was 56.5% with a lag time of +0.1 ms. For 0% connectivity, the correlation reduced to 31.3% with lag time of -0.3 ms. Overall, this indicates noticeably reduced correlation and thus reduced synchronization of firing activity between basket cells at different connectivities.

With reduction in OLM - pyramidal cell connectivity and simultaneous increase in the reception of external excitatory inputs by pyramidal cells, the

individual cell FRs showed fairly linear increment **(Table 4.2)**. The FR at 100% and 0% OLM to pyramidal cell connectivity respectively were 2.36 +/- 0.02 Hz and 6.14 +/- 0.05 Hz for pyramidal cells, 16.05 +/-0.15 Hz and 24.26 +/-0.44 Hz for basket cells and 0.96 +/-0.03 Hz and 4.98 +/-0.04 Hz for OLM interneurons. This qualitative observation from Table 4.2 is justified by performing regression analysis. For pyramidal cell FR, the $R^2 = 0.75$; for basket cell FR, the $R^2 = 0.72$ and for OLM interneurons FR, the $R^2 = 0.84$ **(Figure 4.5)**

Table 4.2 Changes in cell firing rates (FR), theta and gamma frequencies and their power in when dendritic Inhibition is reduced and reception of external inputs by pyramidal cells increased simultaneously.

OLM to Pyr. Weight	Ext. excit. i/p	Pyr (Hz)	BC (Hz)	OLM (Hz)	Theta Freq Hz	Theta Power mV^2/Hz	Gamma Freq Hz	Gamma Power mV^2/Hz
100%	100%	2.36+/-0.02	16.05+/-0.15	0.96+/-0.03	6.7	5.35	33.2	2.55
80%	120%	2.66+/-0.03	19.88+/-0.14	1.11+/-0.03	6.7	5.4	32.5	2.4
60%	140%	2.9+/-0.03	21.04+/-0.15	1.42+/-0.03	6.7	4.1	32.4	5.3
40%	160%	3.19+/-0.03	22.15+/-0.15	1.93+/-0.03	6.7	2.2	31.7	3.6
20%	180%	3.67+/-0.04	23.97+/-0.15	2.64+/-0.04	6.7	2	32.7	6.5
10%	190%	4.24+/-0.04	26.08+/-0.15	3.35+/-0.03	6.7	1.16	33.9	11.4
5%	195%	4.5+/-0.04	21.08+/-0.25	3.69+/-0.03	6.7	0.65	37.8	1.55
0%	200%	6.14+/-0.05	24.26+/-0.44	4.98+/-0.04	0	0	38.8	1.32

The FR of pyramidal and OLM cells increased while that of basket cells showed an initial increase and then a decrease. The theta frequency remained at 6.7 Hz except at 0% connectivity. The gamma frequency varied from 33.2 Hz at 100% connectivity to 38.8 Hz at 0% connectivity. The theta power reduced from 5.35 to 0 mV^2/Hz; gamma power increased from 2.55 at 100% connectivity to 6.5 mV^2/Hz at 20% connectivity and dropped to 1.32 mV^2/Hz at 0% connectivity.

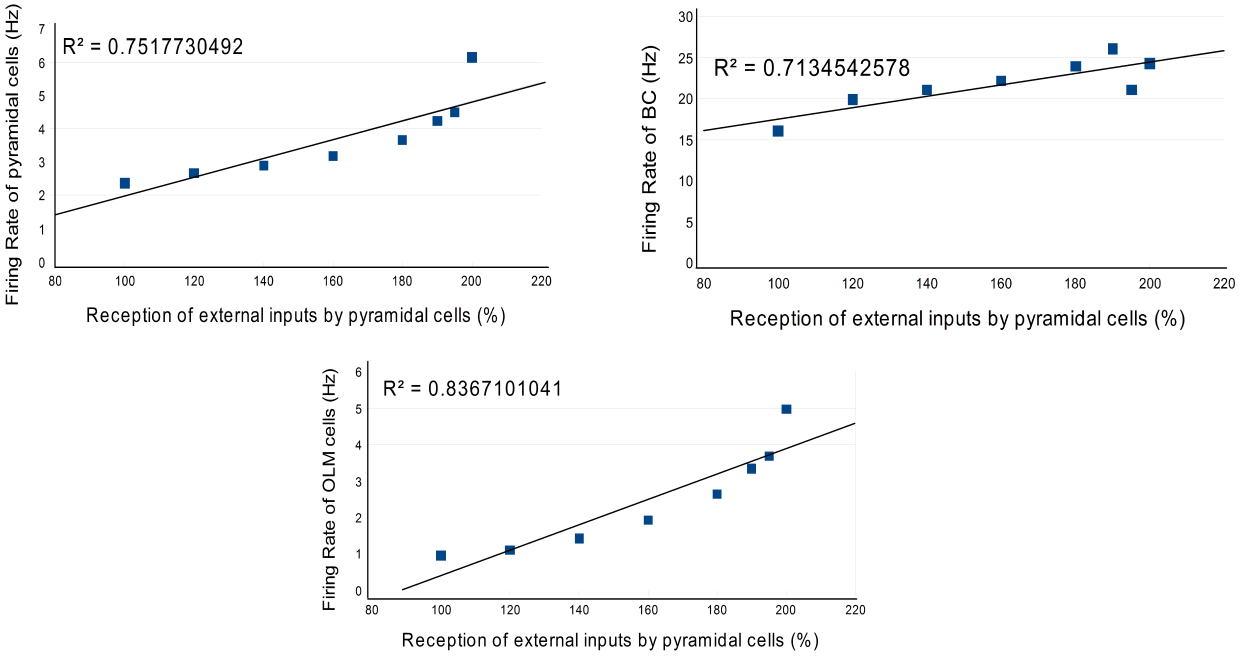

Figure 4.5: Regression analysis confirming the linear increment in firing activity of each cell type under Scenario 2

The theta oscillations had a constant frequency of 6.7 Hz till the OLM to pyramidal connectivity was reduced to 5% of the baseline, owing to strong pacing from MS at this frequencyA. t lower than 10% of this connectivity, the gamma frequency increased from around 33 Hz to 38-39 Hz. As in scenario 1, the theta power dropped down from 5.35 mV^2/Hz to 0 at total loss of dendritic inhibition. The power of gamma oscillations showed a notable increase from 6.5 mV^2/Hz to 11.4 mV^2/Hz with reduction of OLM – pyramidal cell connectivity from 20% to 10%. But, at 5% of this connectivity, the gamma power dropped sharply to 1.55 mV^2/Hz.

Special Condition: From the above observations, it was felt that 10% connectivity from OLM to pyramidal cells was a notable level of impairment where transition of network behaviour occurred. Hence, a special condition was tested at this point. The reception of external excitatory inputs by the pyramidal cells at their distal apical

dendritic compartment was increased by eight times over and above the already set increment of 1.9 times (190%), thus making an overall increase of their reception by about 15 times the baseline levels. This resulted in **depolarization block (DB) of basket cells**, a state where the capability of basket cells to generate action potentials is blocked due to excessive excitatory drive from the pyramidal cells. This DB of basket cells started 1.45 seconds after the start of the simulation. The output LFP showed a characteristic epileptic pattern **(Figure 4.6).** This simulated epileptic pattern was comparable to published experimental results (Cymerblit-Sabba & Yitzhak Schiller (*J Neurophysiol* 107:1718-1730, 2012, Fig.2, p.1721 – Ictal Phase-I); Isaev et. al (*Hippocampus* 17:210–219,2007, Fig.6B-b (left panel), p.216)). The synchrony between OLM cells and pyramidal cells was maintained since the connectivity from pyramidal cells to OLM cells was not affected **(Figure 4.7)**.

The individual cell FR before the depolarization block of basket cells were 10.45+/-0.1 Hz for pyramidal cells, 44.2+/-0.24 Hz for basket cells and 11.52+/-0.07 Hz for OLM interneurons. After the DB of basket cells, the firings rates were 19.09+/-0.09 Hz for pyramidal cells and 18.56+/-0.03 Hz for OLM interneurons.

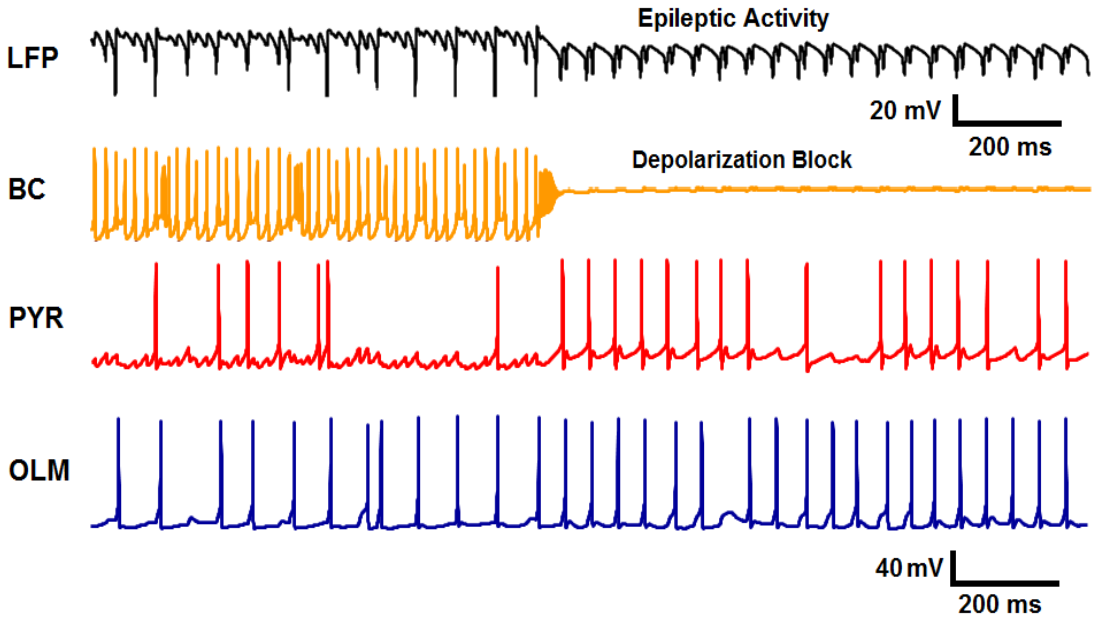

Figure 4.6 The depolarization block (DB) of basket cells (BC) leading to epileptic pattern in the local field potential (LFP) record. The DB was caused when the reception of external excitatory inputs by the pyramidal cells at their apical dendrites was increased by about 15 times the baseline levels simultaneous with 90% impairment in dendritic inhibition. The firing of OLM interneurons (OLM) and pyramidal cells (PYR) are also shown.

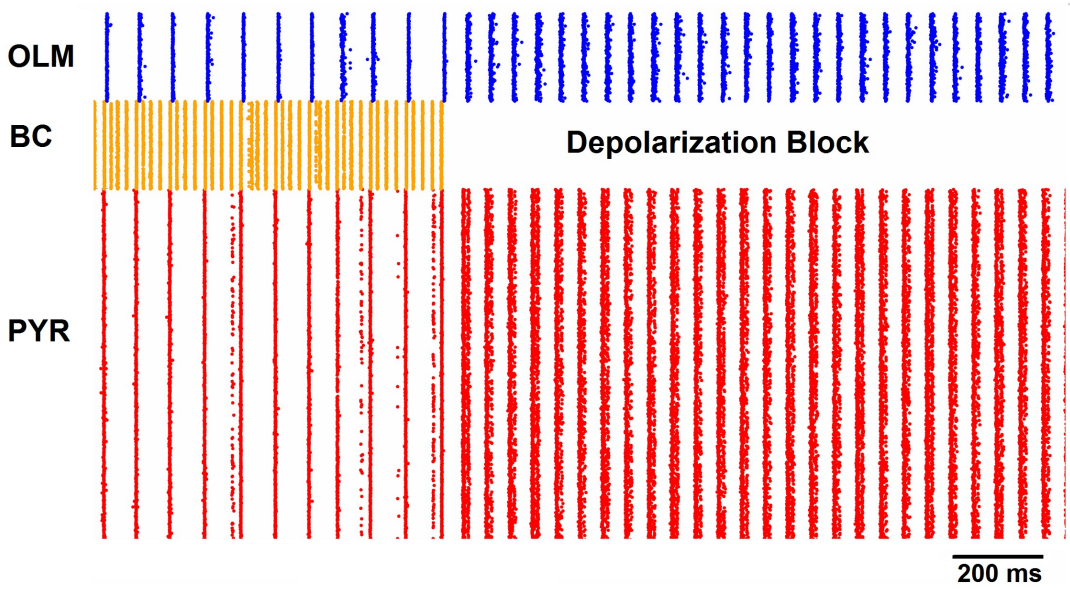

Figure 4.7 Raster plot showing the DB of basket cells (BC) and maintenance of synchronous activity between the OLM interneurons (OLM) and pyramidal cells (PYR).

It is observed that 90% impairment of dendritic inhibition combined with about 15 times increment in the reception of external excitatory inputs by pyramidal cells led to depolarization block of basket cells and ensuing epileptic activity in the network due to impaired dendritic inhibition (structural change). No changes were further simulated at the synapses between the various types of neurons in the network.

4.1.4 Scenario 3: Effect of changes in connectivity at all synapses in the network.

In this scenario, two conditions were simulated: reduction of OLM interneuron to pyramidal cell connectivity initially to 50% (50% impairment of dendritic inhibition) and then to 30% (70% impairment of dendritic inhibition). Changes in strength of connectivity at all synapses were simulated as detailed in Figure 3.5 (page 34) in the chapter 'Materials and Methods'.

Reducing the OLM to pyramidal cell connectivity to 50% of the baseline, the FR for pyramidal cells, basket cells and OLM cells changed from baseline values to 1.93 +/- 0.02 Hz, 10.58 +/- 0.24 Hz and 3.52 +/- 0.04 Hz respectively. The theta component in the LFP had a frequency of 6.8 Hz and gamma component had a frequency of 34.9 Hz. The powers of theta and gamma components were 0.4 mv^2/Hz and 0.36 mv^2/Hz respectively. The baseline theta modulated gamma oscillations were disrupted (not specifically shown); the basket cells showed desynchrony among themselves and with other neurons in the network **(Figure 4.8)**.

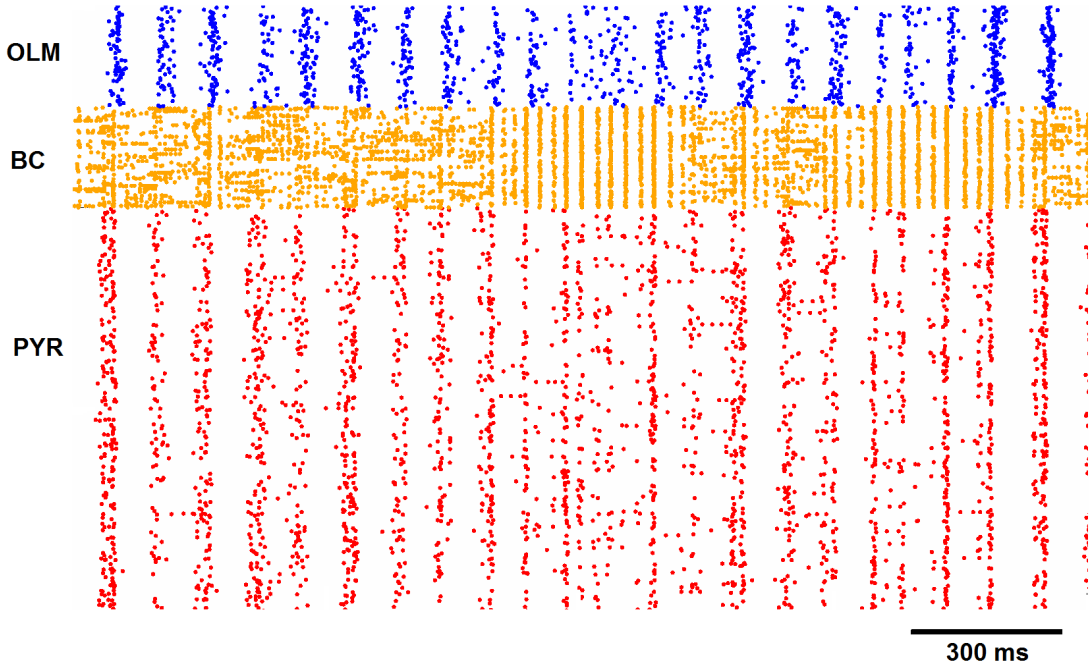

Figure 4.8 Intermittent desynchrony of basket cells due to 50% impairment in dendritic inhibition with simultaneous changes in network connectivity in Scenario 3.

On reducing the OLM to pyramidal cell connectivity to 30% (70% impairment of dendritic inhibition), along with other changes in network connectivity (detailed in 'Materials and Methods', page 34), the basket cells were observed to enter DB similar to Scenario 2. The DB of basket cells started 1.3 seconds after the start of the simulation. The simulated network response (LFP) showed a characteristic epileptic (ictal-tonic) pattern **(Figure 4.9)**. The corresponding raster plot is shown in **(Figure 4.10)**. This is comparable to published experimental results (Isaev et.al, 2007; Cymerblit-Sabba & Schiller, 2012).

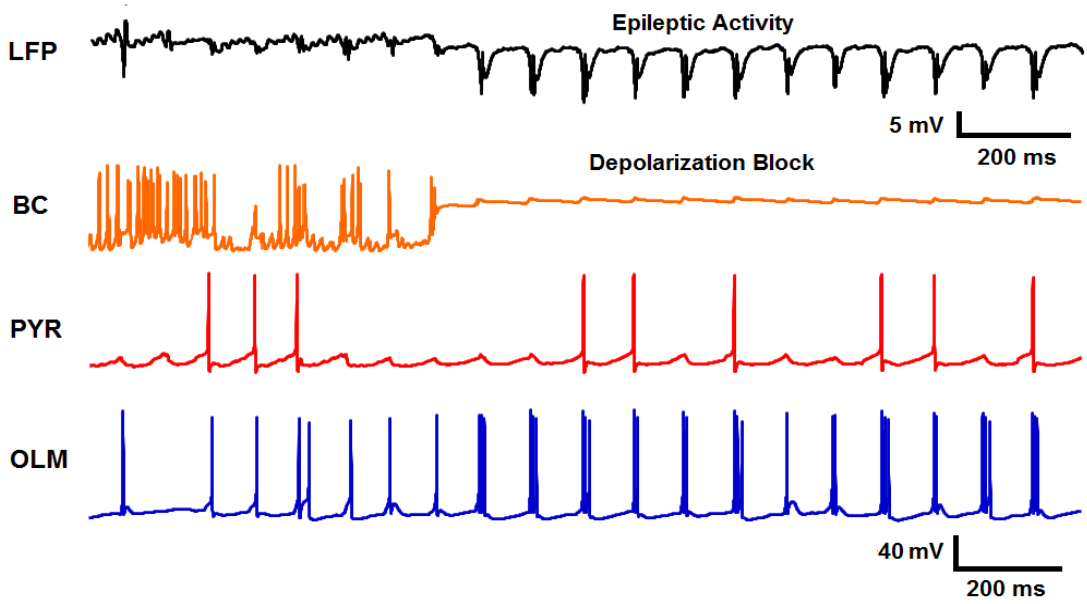

Figure 4.9 The depolarization block (DB) of basket cells (BC) leading to epileptic pattern in the local field potential (LFP) record. The DB was caused when the OLM to pyramidal cell connectivity was reduced to 30% of baseline (70% impaired dendritic inhibition), and simultaneous changes in connection strengths at all synapses in the network (Fig. 3.5, Materials and Methods, page 34). The firing of OLM interneurons (OLM) and pyramidal cells (PYR) are also shown

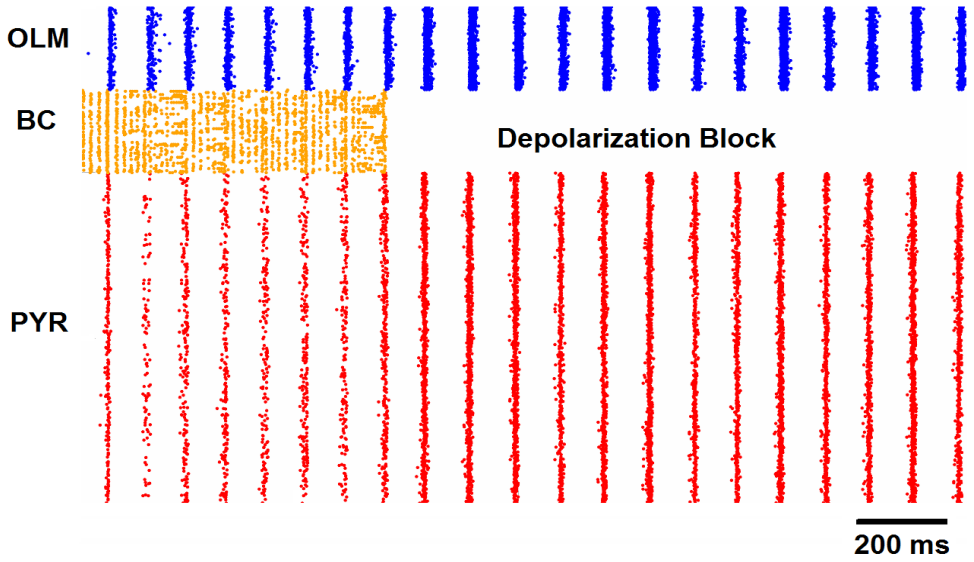

Figure 4.10 Raster plot showing the DB of basket cells (BC) and continuing synchronous activity between the OLM interneurons (OLM) and pyramidal cells (PYR).

The FR of the various cell types before DB of basket cells were: 3.14 +/- 0.06 Hz for pyramidal cells, 13.9 +/- 0.39 Hz for basket cells and 11.6 +/- 0.11 Hz for OLM interneurons. The frequency of theta and gamma components were 10 Hz and

32.7 Hz respectively, and their powers 0.175 mv^2/Hz and 0.0075 mv^2/Hz respectively. After the DB of basket cells, the FR of pyramidal and OLM cells increased to 7.17 +/- 0.03 Hz and 23.8 +/- 0.05 Hz respectively, which were more than double the values before the DB. The theta frequency remained at 10 Hz while its power increased to 5.4 mv^2/Hz. The basket cells being inactive, the gamma frequency power components were absent in the LFP.

Therefore, 70% impairment in dendritic inhibition and four times increment in reception of external excitatory inputs by pyramidal cells along with plasticities at all the synapses in the network led to depolarization block of basket cells and ensuing epileptic activity in the network due to impaired dendritic inhibition (structural change).

4.2 CHANGES IN CHEMICAL ENVIRONMENT: INCREASE IN EXTRACELLULAR POTASSIUM

The increase in extracellular potassium is a realistic effect of hyperexcitability in neuronal network. This effect was simulated to investigate its influence on network behaviour and its contribution to generation of epileptic activity. For this part of the work, HCN channel conductance was incorporated into basket cells to make the model more neurobiologically realistic. The baseline activity was simulated first and then the effect of increased extracellular potassium was investigated.

4.2.1 Baseline Network Activity

The baseline CA3 neuronal network produced theta-modulated gamma oscillations in the LFP **(Figure 4.11)**, with synchrony between the cell types **(Figure 4.12)**. This was found to be similar to the baseline activity mentioned earlier in this

thesis (Figure 4.1, page 41). The inhibitory interactions between soma-inhibiting basket cells and pyramidal cells and those between basket cells produced gamma rhythms, while the interactions between pyramidal cells and OLM cells produced theta rhythms (Neymotin et. al, 2011; Sanjay et. al, 2015). The network generated a fixed theta frequency of 6.7 Hz due to MS inputs at every 150 ms to OLM and basket cells while the gamma frequency component was 34.2 Hz. As previously mentioned, effect of MS inputs on basket cells was lower due to interactions between basket cells themselves and an increased drive provided to basket cells by pyramidal cells. The FR of the cell types were 2.32 +/- 0.03 Hz for pyramidal cells, 15.19 +/- 0.22 for basket cells and 1.03 +/- 0.04 Hz for OLM interneurons. The powers of theta and gamma components in the LFP were 2.95 mV^2/Hz and 0.52 mV^2/Hz respectively.

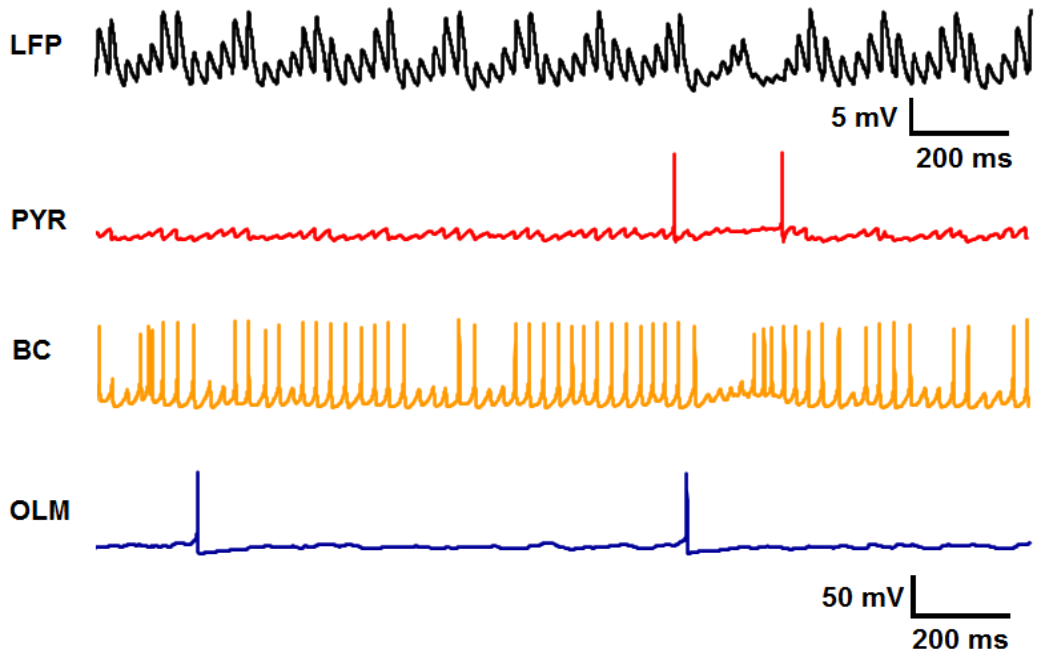

Figure 4.11 The baseline activity of normal intact network after incorporating HCN channel conductances in basket cells along with the individual cell-type activities: PYR - Pyramidal Cells, OLM - OLM Interneurons, BC - Basket Cells

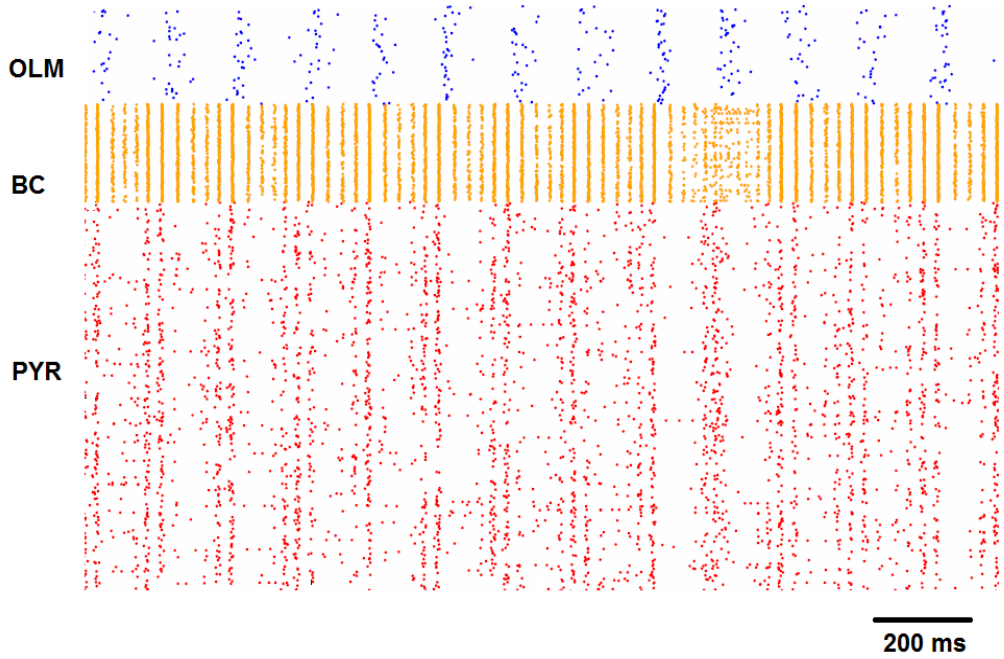

Figure 4.12 Raster plot showing synchronous activity between the neuron types in the normal baseline network. OLM - OLM interneurons, BC - Basket Cells, PYR - Pyramidal Cells

4.2.2 Impairment of dendritic inhibition by 20%

The strength of connectivity from OLM to pyramidal cells was reduced to 80% of baseline (20% impairment in dendritic inhibition), external inputs received by the pyramidal cells was simultaneously enhanced by 20%, connectivity changes were simulated at all synapses in the network and extracellular potassium was enhanced to 6 mM (Fig. 3.6, Materials and Methods, page 36). In this condition, the FR of pyramidal and basket cells were 2.25 +/- 0.03 and 16.95 +/- 0.23 Hz, which were close to baseline values. However, the FR of OLM cells increased by about twice the baseline values to 1.93 +/- 0.04 Hz. The theta and gamma frequencies remained the same at 6.7 Hz and 34.2 Hz respectively. However, the theta power reduced from baseline 2.95 mV^2/Hz to 1.22 mV^2/Hz and gamma power from baseline 0.52 mV^2/Hz to 0.45 mV^2/Hz. The LFP record showed minor variations as compared to the baseline activity **(Figure 4.13)**.

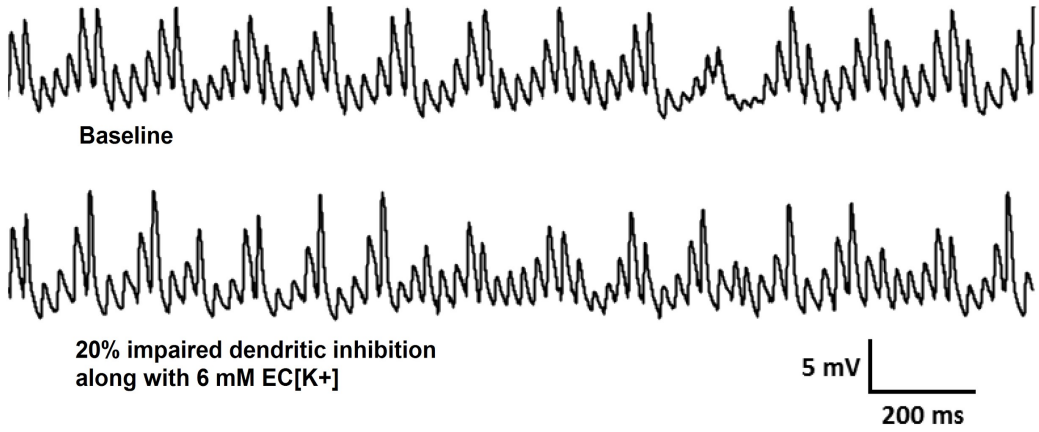

Figure 4.13 Local Field Potential (LFP) record when there is 20% impaired dendritic inhibition and associated network and chemical changes (bottom trace), compared with the baseline LFP (top trace)

4.2.3 Impairment of dendritic inhibition by 30%

The strength of connectivity from OLM to pyramidal cells was reduced to 70% of baseline (30% impairment in dendritic inhibition), external inputs received by the pyramidal cells simultaneously enhanced by 50%, connectivity changes were simulated at all synapses in the network and extracellular potassium was enhanced to 7.1 mM (Fig. 3.6, Materials and Methods, page 36). In this condition, the basket cells entered a state of depolarization block **(DB)**.The output LFP showed characteristic epileptic activity **(Figure 4.14)**. The pyramidal cells and OLM interneurons displayed synchronous activity with each other **(Figure 4.15)**. This DB was observed at the start of simulation itself. The FR for the pyramidal cells and OLM interneurons during this state were 4.85 +/- 0.04 Hz and 9.5 +/- 0.03 Hz respectively. Hence, it can be interpreted that the pyramidal cell activity close to 5 Hz drove the basket cells to DB. The simulated epileptic activity is similar to the experimental results (Cymerblit-Sabba and Schiller, Fig.2, p.1721 – Ictal Phase-I and Isaev et. al ,Fig.6B-b (left panel), p.216).

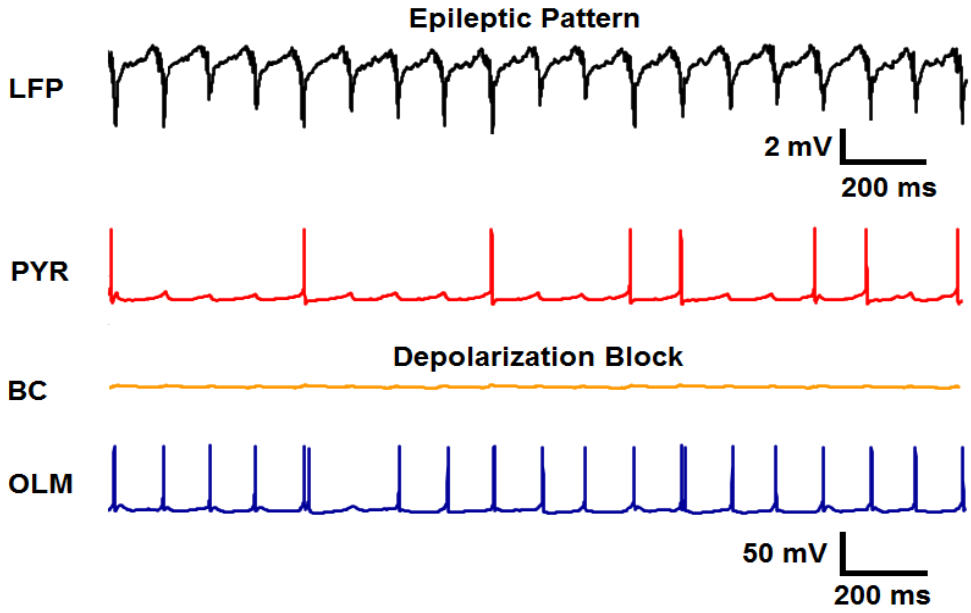

Figure 4.14 Firing activity of three types of cells along with the local field potential (LFP) record in the epileptic network. The depolarization block of basket cells due to excessive excitatory drive from pyramidal cells was observed right from the start of the simulation. PYR - Pyramidal Cell, BC - Basket Cell, OLM - OLM Interneuron

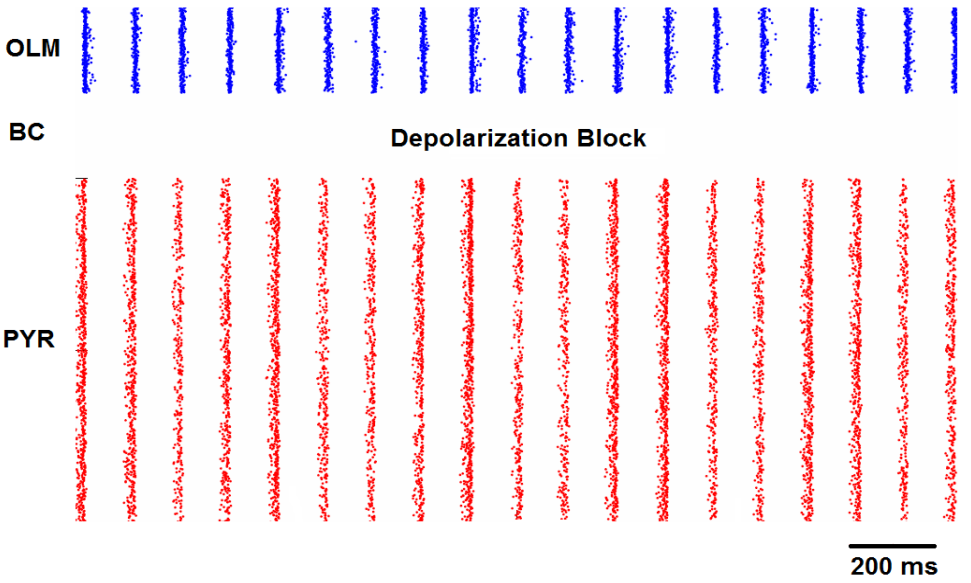

Figure 4.15 The depolarization block of basket cells (BC) due to excessive excitatory drive from pyramidal cells (PYR). The synchronous activity between OLM interneurons (OLM) and pyramidal cells can be seen.

Hence, it can be concluded that changes in chemical environment viz., enhancement in extracellular potassium concentration in this case had a much significant role in causing hyperexcitability in the network. While 70% of impairment in dendritic inhibition along with network connectivity changes led to a pathological state in the previous part of the study, it is observed that enhanced extracellular potassium (chemical change) led to a pathological state at 30% impairment in dendritic inhibition (structural change) itself.

4.3 CONTROL OF EPILEPTIC ACTIVITY

Drugs like gabapentin and lamotrigine used to treat epilepsy, act by increasing HCN currents by increasing the channel conductance, g(Ih) without changing other parameters significantly (Poolos et.al, 2002; Surges et.al, 2003). Increased dosage of these drugs increases Ih conductance in neurons. In this part of the study, the effect of enhancing this conductance in any one type of cell (Pyramidal/OLM/BC) in the normal baseline network was initially studied , while keeping it unchanged in other cell types. This approach was taken to study in isolation the role of g(Ih) for that type of cell and its contribution in epileptogenesis. Next, g(Ih) was uniformly changed in all three cell types in the normal network to study the changes in network behaviour. Finally, g(Ih) was enhanced uniformly in all neurons in the epileptic network.

4.3.1 Effect of enhanced g(Ih) on different neuron types of the normal baseline network.

When g(Ih) was increased in pyramidal cells alone to twice, four times and six times its baseline, it led to enhanced firing activity and that of connected basket

and OLM cells in the network, consistent with published results (Neymotin et al, 2013). However, there was no DB of the basket cells despite increased drive from pyramidal cells (> 5 Hz). When g(Ih) was increased to twice, four times and six times the baseline in basket cells alone, it led to their enhanced firing activity while other two cells did not show large changes. When g(Ih) was increased to twice, four times and six times the baseline in OLM cells alone, the pyramidal and basket cell activity was suppressed. Thus, it signifies the relatively high inhibitory effect of OLM interneurons in the whole network. **Table 4.3** summarises the FR of cells for the above conditions.

Table 4.3 Change in firing rates (FR) of individual cell types when g(Ih) is enhanced separately in each type of neuron.

Change in g(Ih) in pyr. cell alone	Pyramidal Cell FR (Hz)	Change in g(Ih) in BC alone	Basket Cell FR (Hz)	Change in g(Ih) in OLM cell alone	OLM FR (Hz)
1x	2.32 +/- 0.03	1x	15.19 +/- 0.22	1x	1.03 +/- 0.04
2x	2.65 +/- 0.03	2x	18.34 +/- 0.18	2x	3.05 +/- 0.03
4x	3.86 +/- 0.02	4x	19.79 +/- 0.15	4x	6.81 +/- 0.02
6x	5.36 +/- 0.02	6x	21.8 +/- 0.17	6x	10.2 +/- 0.02

It is seen that all three types of neurons generally had increased excitability with enhanced g(Ih) in them. 1x: baseline value; 2x, 4x, 6x: two, four and six times the baseline, respectively.

4.3.2 Effect of enhanced g(Ih) on the whole baseline normal network.

When g(Ih) was increased to twice the baseline in all three cell types simultaneously without making any changes in their connectivity, the FR of pyramidal cell reduced to about two-thirds, and basket cells to three-fourths of their respective baseline values. However, the FR of OLM interneurons increased by about four-times from its baseline value **(Table 4.4).**

Table 4.4 Change in firing rates of individual cell types when g(Ih) is enhanced simultaneously in all types of neurons in a normal baseline network.

Change in g(Ih)	Pyramidal Cell (Hz)	Basket Cell (Hz)	OLM Interneuron (Hz)
1x	2.32 +/- 0.03	15.19 +/- 0.22	1.03 +/- 0.04
2x	1.53 +/- 0.03	11.7 +/- 0.15	3.66 +/- 0.03
4x	1.1 +/- 0.02	11.35 +/- 0.12	7.24 +/- 0.02
6x	0.23 +/- 0.01	4.3 +/- 0.08	10.2 +/- 0.02

It is seen that OLM interneurons had notably increasing rates of firing with increase in g(Ih) that led to decreased firing of pyramidal neurons and connected basket cells.1x: baseline value; 2x, 4x, 6x: two, four and six times the baseline, respectively.

When g(Ih) was further increased to four times the baseline value, the pyramidal cells FR further dropped to 1.1 Hz (< ½ of the baseline pyramidal FR). The basket cells, FR showed a decrement to 11.35 HZ while the OLM cells showed a seven times increase compared to baseline values (7.24 Hz as against 1.03 Hz). Increasing g(Ih) further to six times the baseline value almost silenced pyramidal cells (FR 0.23 Hz) . The basket cell activity also dropped down to about one-fourth of its baseline value (4.3 Hz as compared to 15.2 Hz baseline), while the OLM interneuron FR increased to 10.2 Hz which is about ten times the baseline FR.

This implies that enhancing g(Ih) in all three cell types simultaneously and without making any changes in network connectivity led to increased firing of OLM interneurons but decreased FR of pyramidal and basket cells. Clearly, increased g(Ih) led to considerable increased FR of OLM, leading to significant control of excitability of pyramidal cells. This reduction in FR of pyramidal cells, reduced the excitatory drive to basket cells and hence the decrement in their FR as well. Importantly, OLM interneurons have considerable influence over the network under both conditions i.e increment in g(Ih) in OLM alone or uniformly in the entire

network. This suggests that OLM interneurons exert considerable control over the excitatory activity of pyramidal cells and the network.

4.3.3 Effect of enhanced g(Ih) in an epileptic network.

To simulate the effect of drugs like gabapentin and lamotrigine, g(Ih) was enhanced uniformly in all the cells in the epileptic network (30% impaired dendritic inhibition). The DB of basket cells and the typical epileptiform activity were abolished when g(Ih) was increased to twice the baseline values **(Figures 4.16)** and the pyramidal cells started driving other cells in the network, restoring normal network activity **(Figure 4.17)**. The FR of pyramidal, basket and OLM interneurons were 1.42 +/- 0.02 Hz, 12.13 +/- 0.21 Hz and 5.92 +/- 0.03 Hz respectively. The frequencies of theta and gamma oscillations were 6.8 Hz and 33.3 Hz respectively and spectral powers were 0.4 mV^2/Hz and 0.14 mV^2/Hz respectively **(Table 4.5)**.

Table 4.5: Change in firing rates of individual cell types when g(Ih) was enhanced simultaneously in all types of neurons in an epileptic network caused due to 30% impairment of dendritic inhibition.

Change in g(Ih)	Pyramidal Cell (Hz)	Basket Cell (Hz)	OLM Interneuron (Hz)
1x	4.85 +/- 0.04	0 +/- 0 **(DB)**	9.7 +/- 0.03
2x	1.42 +/- 0.02	12.1 +/- 0.21	5.92 +/- 0.03
4x	0.84 +/- 0.01	9.36 +/- 0.11	9.88 +/- 0.03
6x	1.71 +/- 0.01	12.08 +/- 0.11	14.48 +/- 0.02

As in previous cases, OLM interneurons had notably increased firing rates with increase in g(Ih), even though their connectivity to pyramidal cells was reduced by 30%. This led to decreased pyramidal cell firing and hence the controlled overall network activity. DB - Depolarization Block. 1x: baseline value; 2x, 4x, 6x: two, four and six times the baseline, respectively.

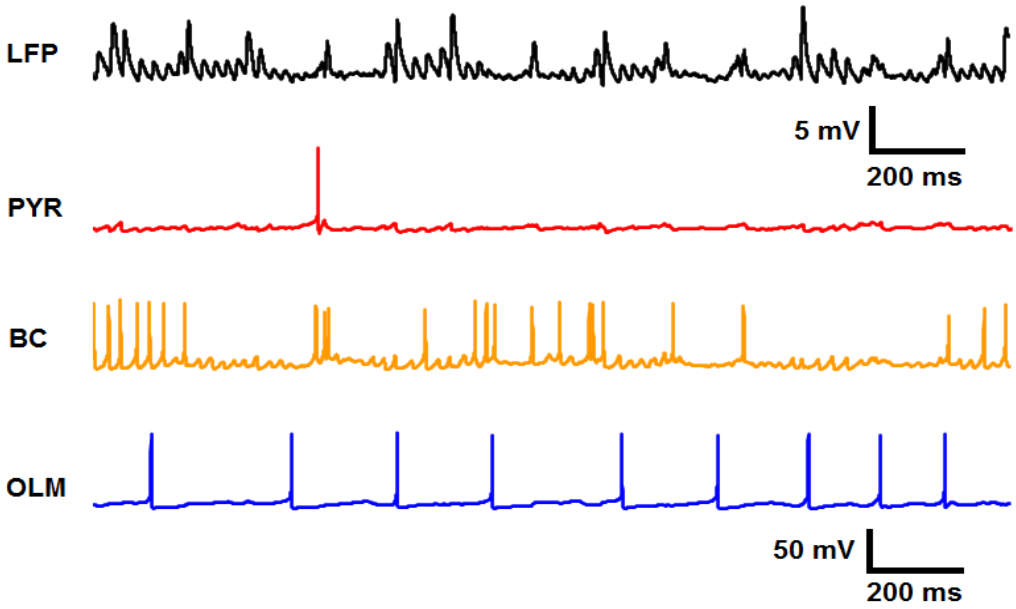

Figure 4.16 Firing activity of the three types of cells along with the local field potential record in a recovered network when g(Ih) is increased to twice the baseline. On increasing g(Ih) in the whole network, the depolarization block of basket cells is eliminated and the interactions between the three cell types are re-established with modified firing patterns.

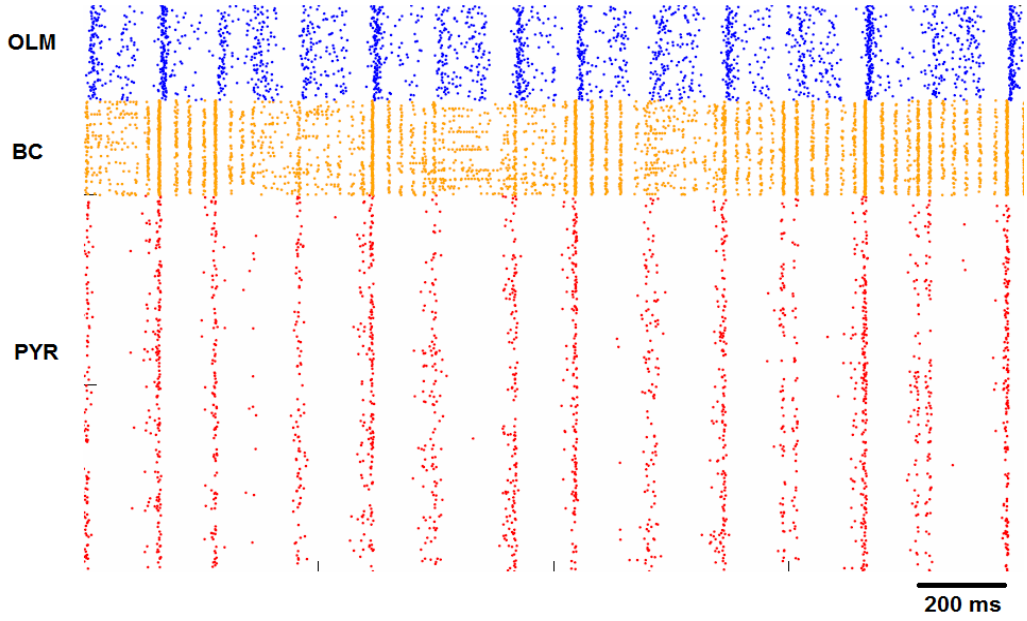

Figure 4.17 Raster plot showing the firing activity of three types of cells in a recovered network when g(Ih) was increased to twice the baseline in all cells in the network. The depolarization block of basket cells is eliminated and the interactions between three cell types are re-established with the pyramidal cells driving the other cells in the network.

The OLM interneurons seemed to play a significant role in eliminating DB. The enhanced FR of OLM interneurons exerted considerable inhibition on the excitatory activity of pyramidal cells thereby reducing the excitatory inputs to basket cells, relieving them from DB. With this, the network dynamics change further and the interactions between all three types of neurons are re-established, leading to modified FR of the cells as described above. The enhanced FR of OLM interneurons due to increased g(Ih), enabled them to control hyperexcitability even when the inhibition was reduced by 30% (70% OLM to pyramidal connectivity maintained).

When g(Ih) was increased to four and six times the baseline value, the DB of basket cells was eliminated, thus abolishing typical epileptiform activity. At g(Ih) = 4x, the frequency and power of theta component was 6.8 Hz and 0.11 mV^2/Hz, however frequency and power weren't distinctly clear for the gamma component. At g(Ih) = 6x, the frequencies of theta and gamma oscillations were 6.8 Hz and 35.5 Hz respectively and had spectral powers of 0.22 mV^2/Hz and 0.3 mV^2/Hz, respectively.

To further understand the ability of g(Ih) to bring the network out of DB, the effect of enhanced g(Ih) on networks with 50% and 70% impaired dendritic inhibition with enhanced extracellular potassium was tested. The extracellular potassium level was maintained at 7.1 mM itself and E_{GABA} at -75 mV itself in these networks. The g(Ih) was increased to twice, four times and six times the baseline values in all the constituent neurons in these two networks. It was observed that the DB of basket cells and epileptic activity in the LFP were abolished in the network with 50% impaired dendritic inhibition. However, the elimination of basket cell DB and suppression of epileptiform activity were NOT observed in the network with 70% impaired dendritic inhibition **(Figure 4.18)**.

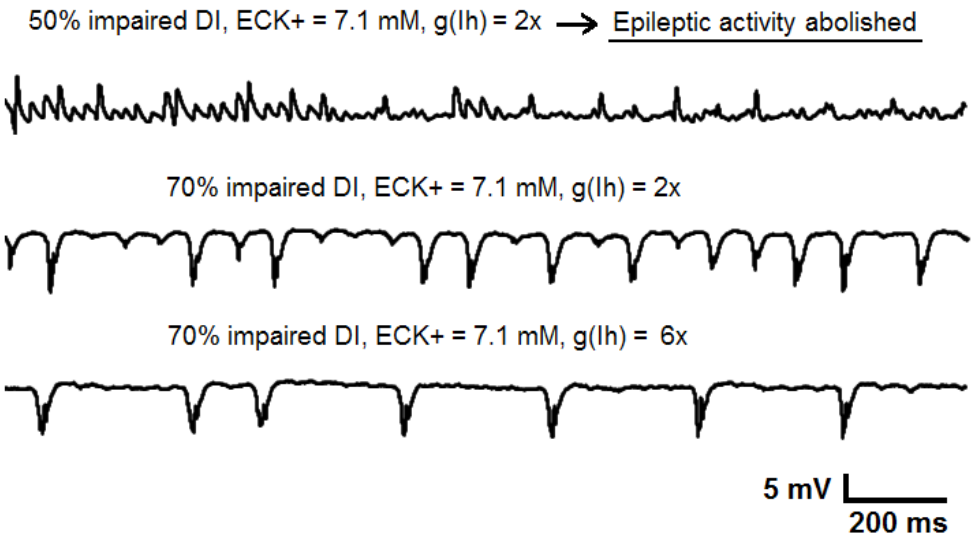

Figure 4.18: Local Field Potential records showing the effect of increased HCN channel conductance g(Ih) in networks with 50 and 70% impairments in dendritic inhibition and associated chemical changes as shown above each trace (DI - Dendritic Inhibition, 2x and 6x - twice and six times the baseline values). It may be noted that the epileptic activity could not be eliminated even with increasing the g(Ih) six times the baseline level in the network with highly impaired (70%) DI.

These results (summarized in **Table 4.7**) show that the elimination of DB of basket cells happens due to the reduced drive they receive from pyramidal cells, which in turn, is due to enhanced dendritic inhibition of pyramidal cells. At high impairments of dendritic inhibition, the pyramidal cells are unable to reduce the excitatory drive of basket cells. Hence, the basket cells sustain DB and the epileptiform activity persists.

Therefore, it is observed that the OLM interneurons played a prominent role in controlling the hyperexcitability and recovery of balanced network activity due to enhanced HCN channel conductance, even when the dendritic inhibition provided by them was impaired. The recovery of balanced network activity was limited to about 50% impairment of dendritic inhibition and associated chemical changes and not applicable at higher impairments of dendritic inhibition.

The following tables **4.6** and **4.7** summarize the conditions tested and those leading to generation of epileptiform activity and recovery in the simulations.

Table 4.6 Overall summary of conditions tested and those leading to generation of epileptic activity in the CA3 network

Section No.	Condition Tested	Epileptic Activity
4.1.2	Impairment in dendritic inhibition alone without changes in reception of external excitatory inputs by pyramidal cells	NO
4.1.3	Impairment in dendritic inhibition along with proportionate increase in reception of external excitatory inputs by pyramidal cells	NO
4.1.3 Special Condition	15 times (excessive high input) reception of external excitatory inputs at 90% impairment of dendritic inhibition	**YES**
4.1.4	50% impairment in dendritic inhibition, proportionate increment in reception of external excitatory inputs by pyramidal cells and connectivity changes in the network	NO
4.1.4	70% impairment in dendritic inhibition, proportionate increment in reception of external excitatory inputs by pyramidal cells and connectivity changes in the network	**YES**
4.2.2	20% impairment in dendritic inhibition, proportionate increment in reception of external excitatory inputs by pyramidal cells, connectivity changes in the network and increased extracellular potassium to 6 mM	NO
4.2.3	30% (and above) impairment in dendritic inhibition, proportionate increment in reception of external excitatory inputs by pyramidal cells, connectivity changes in the network and increased extracellular potassium to 7.1 mM	**YES**

Table 4.7 Conditions showing recovery of balanced network activity due to the enhanced HCN channel conductance, g(Ih).

Section No.	Condition tested	Increment in g(Ih)	Recovery
4.3.2	30% impairment in dendritic inhibition, associated network changes and increased extracellular potassium to 7.1 mM	twice, four times and six times the baseline level	**YES**
4.3.2	50% impairment in dendritic inhibition, associated network changes and increased extracellular potassium to 7.1 mM	twice, four times and six times the baseline level	**YES**
4.3.2	70% impairment in dendritic inhibition, associated network changes and increased extracellular potassium to 7.1 mM	twice, four times and six times the baseline level	NO

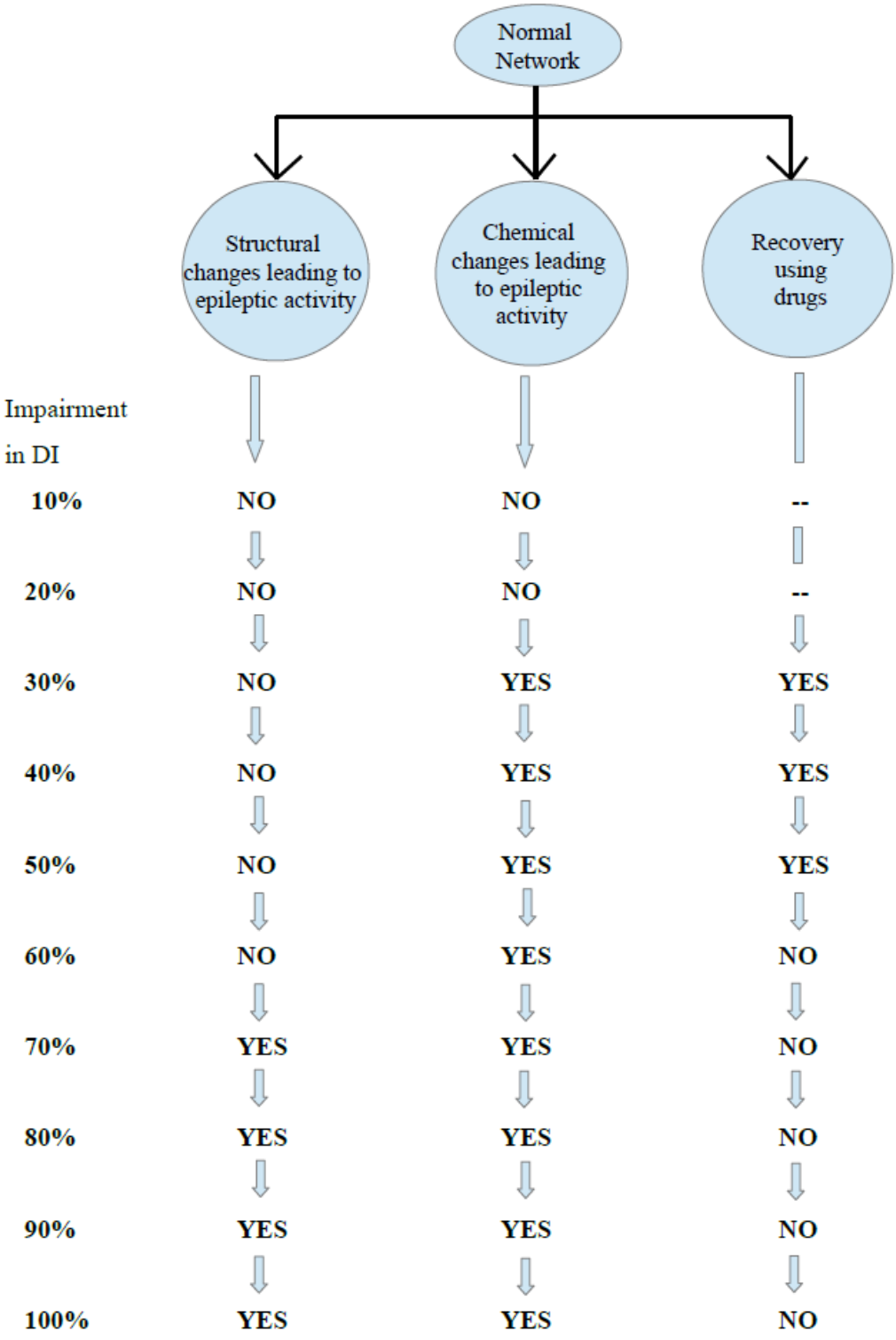

Figure 4.19: The overall picture of the various conditions tested and the results observed. DI - Dendritic Inhibition.

CHAPTER 5

DISCUSSION

In this research work, an in-silico model was used to investigate how impaired dendritic inhibition of the excitatory pyramidal neurons of the vulnerable CA3 subfield of hippocampus leads to hyperexcitability, a characteristic feature of epileptic activity. The network generated theta-modulated gamma oscillations. While theta oscillations occur during spatial navigation and motor behaviour, the gamma oscillations occur during processes like learning and memory. Though different cell assemblies generate these oscillations, they co-occur in synchrony in field potentials (Colgin & Moser, 2010). In this study, the strength of connectivity from OLM interneurons to pyramidal neurons was reduced to simulate impairment in dendritic inhibition. In the next part of the study, the increment in extracellular potassium levels was simulated as a consequence of hyperexcitability due to impaired dendritic inhibition. Thereafter, the effect of antiepileptic drugs like gabapentin was modelled by enhancing the conductance of HCN channels to study how the epileptic CA3 network responds to various levels of drug dosage. To make this part of the study realistic, the effect of drugs was tested on the network that generated epileptic activity due to the combined effect of neurodegeneration (impaired dendritic inhibition) and chemical imbalance (high extracellular potassium).

5.1 MODEL ASSUMPTIONS AND OBSERVATIONS

To study how impaired dendritic inhibition leads to epileptiform activity, three scenarios were considered and simulated. First, the dendritic inhibition to pyramidal cells was reduced systematically from the baseline 100% connectivity to

total impairment 0%, without any other changes in the network. Second, a simultaneous and proportional increase in the reception of external excitatory inputs at the distal apical dendritic compartment of pyramidal cells was simulated assuming this to be a consequence of reduced dendritic inhibition from the OLM neurons. The relationship between impaired dendritic inhibition and increase in reception of these external excitatory inputs was assumed to be linear for the purpose of the model due to unavailability of supporting literature. Third, in addition to above changes, the strengths of connectivity between different neuron types was also modified. These scenarios were simulated in a stepwise manner to study systematically the contribution of changes in connectivity and inputs to the behaviour of the CA3 network and determine what extent of these changes lead to epileptic activity. Medial Septum **(MS)** inputs were simulated as rhythmic GABAergic inhibitory mechanisms provided to OLM interneurons and basket cells at every 150 ms in all the scenarios. These rhythmic inputs paced theta oscillations in the baseline network. The theta rhythms were resilient to modifications in network connectivity, partially due to the strong pacing of interneurons due to MS inputs.

In the first scenario, on simulating impaired dendritic inhibition without adding any other network changes, the pyramidal cells were disinhibited and increased their activity as indicated by their enhanced FR. The basket and OLM interneuron activity increased due to enhanced drive from pyramidal cells. The increased basket cell activation raised the gamma power while the decreased influence of OLM interneurons on pyramidal cells lowered the theta power in the LFP. The simulated LFP showed disruption of baseline network activity, leading to total disappearance of theta component at 100% impairment of dendritic inhibition.

In the second scenario, the reception of external excitatory inputs at the distal apical dendritic compartments of pyramidal cells was increased. These simulated excitatory inputs model those from extra-hippocampal areas, predominantly the entorhinal cortex. The pyramidal cells increased their activity as evidenced from their enhanced FR. The basket cells received increased drive from the pyramidal cells. Their activity also increased but to a lesser extent compared to the first scenario (Eg., about 24 Hz in second scenario compared to about 31 Hz in first scenario, at total impairment of dendritic inhibition). This may be contributed by the enhanced recurrent GABAergic inhibition (Cutsuridis et.al, 2010) of basket cells. However, the OLM interneurons showed much higher activation due to pyramidal cells as compared with first scenario.

The reduction of OLM to pyramidal cell connectivity to 10% was of particular significance. This resulted in change in frequency and power of the gamma oscillations. On reducing this connectivity from 20% to 10%, the frequency of gamma oscillations increased from 33 Hz to ~38 Hz and their power from 6.5 to 11.4 mV^2/Hz. This could be due to tighter synchrony of the basket cells as seen in the raster plot **(**Results, Figure 4.4 top, page 45**)**. Further reduction of this connectivity and increase in reception of external excitatory inputs by pyramidal cells led to loss of synchrony of basket cell activity and sharp drop of gamma power to 1.55 mV^2/Hz.

A special condition was tested at 10% OLM to pyramidal cell connectivity by increasing the reception of external excitatory inputs by pyramidal cells to 15 times the baseline. The basket cells were observed to enter the state of depolarization block **(DB)**, whereby there were unable to fire action potentials due to excessive drive from the pyramidal cells. **Thus, the result was further inhibition of an otherwise intact**

and functional inhibitory mechanism. The simulated overall network response (LFP) showed a pattern characteristic of epileptic activity (ictal-tonic pattern). This indicated that at such low connectivity (or high impairments of dendritic inhibition - 90% in this case), a high input received from extra-hippocampal regions could trigger pathological activity in the hippocampus. Mainly these external inputs are received by the CA3 subfield of hippocampus from the adjoining entorhinal cortex, which in turn receives input from other cortical areas (Amaral, 1993; Witter, 2007). Hence, such high inputs in the form of visual or auditory stimuli could perhaps trigger hyperexcitability in the vulnerable hippocampus (Manganotti et al, 1998; Seddigh et. al, 1999).

In addition to impaired dendritic inhibition and increased reception of external excitatory inputs by pyramidal cells, a change in strength of connectivity was simulated across all synapses in the network (third scenario). A recording from the distal apical dendritic compartment of a representative pyramidal neuron confirms this increase. Occasionally, this enhanced excitatory input reception led to short periods of tetanic response **(Figure 5.1)**. The high recurrent connectivity among CA3 pyramidal cells enhanced the excitatory output from the pyramidal cell population, which further activated the connected basket and OLM interneurons. The mutual inhibition among the basket cells reduced the inhibitory output which are received by pyramidal neurons. This further disinhibited pyramidal cells and resulted in an overall increase of excitatory activity in the network. A total imbalance between excitatory and inhibitory responses ensued in the network due to the high excitatory responses.

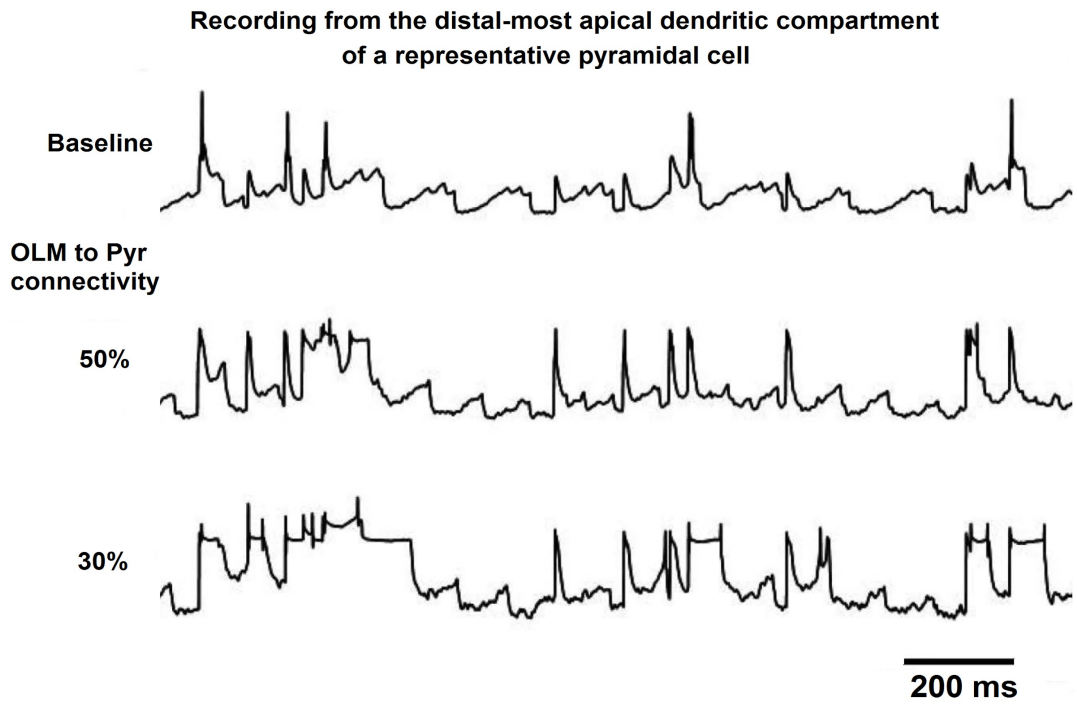

Figure 5.1 Inputs received by the distal dendritic compartment of a representative pyramidal neuron from external sources at baseline connectivity, 50% and 30% OLM to pyramidal cell connectivity (50% and 70% impaired dendritic inhibition respectively).The increase in the received inputs is clear, especially at 30% OLM to pyramidal cell connectivity with intermittent tetanic states.

When the OLM to pyramidal cell connectivity was reduced to 50% and connectivity changes simulated accordingly at other synapses, the network activity showed a notable change. The basket cells were seen to intermittently lose synchrony in the network (Results, Figure 4.7, page 51). Presumably, the network activity had entered a stage of transition to epileptiform activity. On further reduction of OLM to pyramidal cell connectivity to 30% (70% impairment of dendritic inhibition), the basket cells entered DB and a pattern characteristic of epileptic activity (ictal-tonic activity) was observed in the LFP. Compared to the first and second scenarios (changing the OLM to pyramidal connectivity alone), the third scenario generated a characteristic pathological activity at a comparatively earlier stage, i.e., at 30% OLM to pyramidal cell connectivity or 70% impaired dendritic inhibition. The simulated

epileptic response in the LFP was comparable to the ictal activity reported in the literature (Cymerblit-Sabba and Schiller, 2012; Isaev et al, 2007).

5.2 NETWORK CHANGES LEADING TO EPILEPTIC ACTIVITY

When impairment of dendritic inhibition alone was simulated without any changes effected at any other synapse (Scenario 1), the network response changed from the baseline theta-modulated gamma pattern to a full gamma pattern. Simultaneous gradual increase of external excitatory inputs received at the distal dendritic compartment of pyramidal cells (Scenario 2) led to a notable change in the network response at 10% OLM to pyramidal cell connectivity. At this point, a 15 times increment of baseline levels of external excitatory inputs received by pyramidal cells was simulated. The basket cells entered a state of DB and the synchronous activity due to residual connectivity between the pyramidal and OLM cells generated a characteristic epileptic pattern.

The inactivity of basket cells due to their DB seemingly contributed to the ictal-tonic pattern of activity in the simulations that generated them. Comparison of FR of pyramidal cells before and after DB of basket cells in the second scenario (10.45 +/- 0.1 Hz and 19.09 +/- 0.09 Hz) and third scenario (3.14 +/- 0.06 Hz and 13.9 +/- 0.39 Hz) shows that the FR of pyramidal cells after the DB of basket cells in the third scenario (changes in strengths of connectivities at synapses) is less than that in the second scenario (only increase of external inputs along with decrease of dendritic inhibition) i.e 13.9 +/- 0.39 Hz as against 19.09 +/- 0.09 Hz. The third scenario refers to the plasticity at connections between all neurons of the CA3 network while second scenario refers to increased external input reception by the

pyramidal cells without any other potentiation of activity between neurons. Also, in the third scenario, the DB of basket cells set in about 1.3 seconds after the start of simulation while the same occurred about 1.45 seconds after the start of simulation in the second scenario. Hence, it may be concluded that synaptic plasticities including axonal and dendritic sprouting significantly contribute to pathological states like temporal lobe epilepsy. This may be linked to situations like traumatic brain injury and cerebral ischemia that lead to loss of neurons or their impaired activity. Epileptic activity also has been observed to occur in these incidents.

Enhanced neuronal activity and potentiation of network activity has been observed in different models of epileptic activity generation in temporal lobe structures including hippocampus (Leite et. al, 2005). Similarly, McAllister et.al (2000) has described about the enhanced activity in neuronal networks due to sprouting at pyramidal cell dendrites, having implications in epileptic activity generation. Enhanced neuronal activity due to long-term potentiation has been observed to cause epileptic activity in human subjects as well (Cook and Bliss, 2006). Presumably, the network changes occurring at gross levels in the brain across various neuronal circuits leads to faster generation of pathological states like epilepsy than those at specific connections.

5.3 GENERATION OF EPILEPTIC ACTIVITY DUE TO INCREASED EXTRACELLULAR POTASSIUM

This part of the study showed that when the dendritic inhibition was reduced even by 30% (70% connectivity maintained from OLM to pyramidal cells) along with other network changes as described, the network generated a characteristic

epileptiform activity in accordance with observed experimental studies (Isaev et. al, 2007; Cymerblit-Sabba & Schiller, 2012). The threshold for epileptic activity generation due to impaired dendritic inhibition and simultaneous changes in chemical environment was much lower compared to our previous observations (Sanjay et. al, 2015). In the previous part, 70% impairment of dendritic inhibition was required to generate a similar epileptiform activity. This suggests that by the time epilepsy manifests in its presentable form, a significant extent of neurodegeneration (30% impairment of dendritic inhibition in our model) would have already occurred. It also indicates that changes in the chemical environment plays a significant contributing role in producing network dynamics that may predispose to pathological conditions like epilepsy.

5.4 EFFECT OF ENHANCED HCN CHANNEL CONDUCTANCE g(Ih) IN NORMAL AND EPILEPTIC NETWORKS

In a normal network, when g(Ih) was increased in each cell type one at a time, their individual excitabilities increased in different amounts, with the OLM interneurons showing the highest increase in firing rates. However, when g(Ih) was uniformly enhanced in all three types of cells, the overall network activity was suppressed and the OLM interneurons showed highest FR. Hence, OLM interneurons had prominent inhibitory effect on the excitatory activity of pyramidal cells, which led to reduced basket cell activity. The net result showed reduced LFP amplitude, signifying the prominent role of OLM cells in controlling network excitability.

To understand how excitability of pyramidal cells change, the recordings from the distal-most apical dendritic compartment (AD3), the pyramidal cell soma

and the local field potential were recorded for a baseline network, the epileptic network (with 30% impaired dendritic inhibition) and the network with increased g(Ih). Compared to baseline conditions, when impaired dendritic inhibition led to epileptic activity, the external inputs received at the distal dendritic compartment (AD3) of the pyramidal cells and generation of action potentials in it increased **(Figure 5.2 A,B)**. When g(Ih) was enhanced uniformly in all the cells in the epileptic network, the pyramidal cells' AD3 compartment showed a decrease in depolarization **(Figure 5.2 C)** reducing pyramidal cell FR (~5 Hz to 1.41 Hz). The *recovered* network activity also displayed theta and gamma frequency oscillations (6.8 and 33.3 Hz) comparable to baseline values (6.7 and 34.2 Hz) but the oscillatory powers were lower (theta: 0.4 Vs 2.95 mv^2/Hz; gamma: 0.14 Vs 0.45 mv^2/Hz).

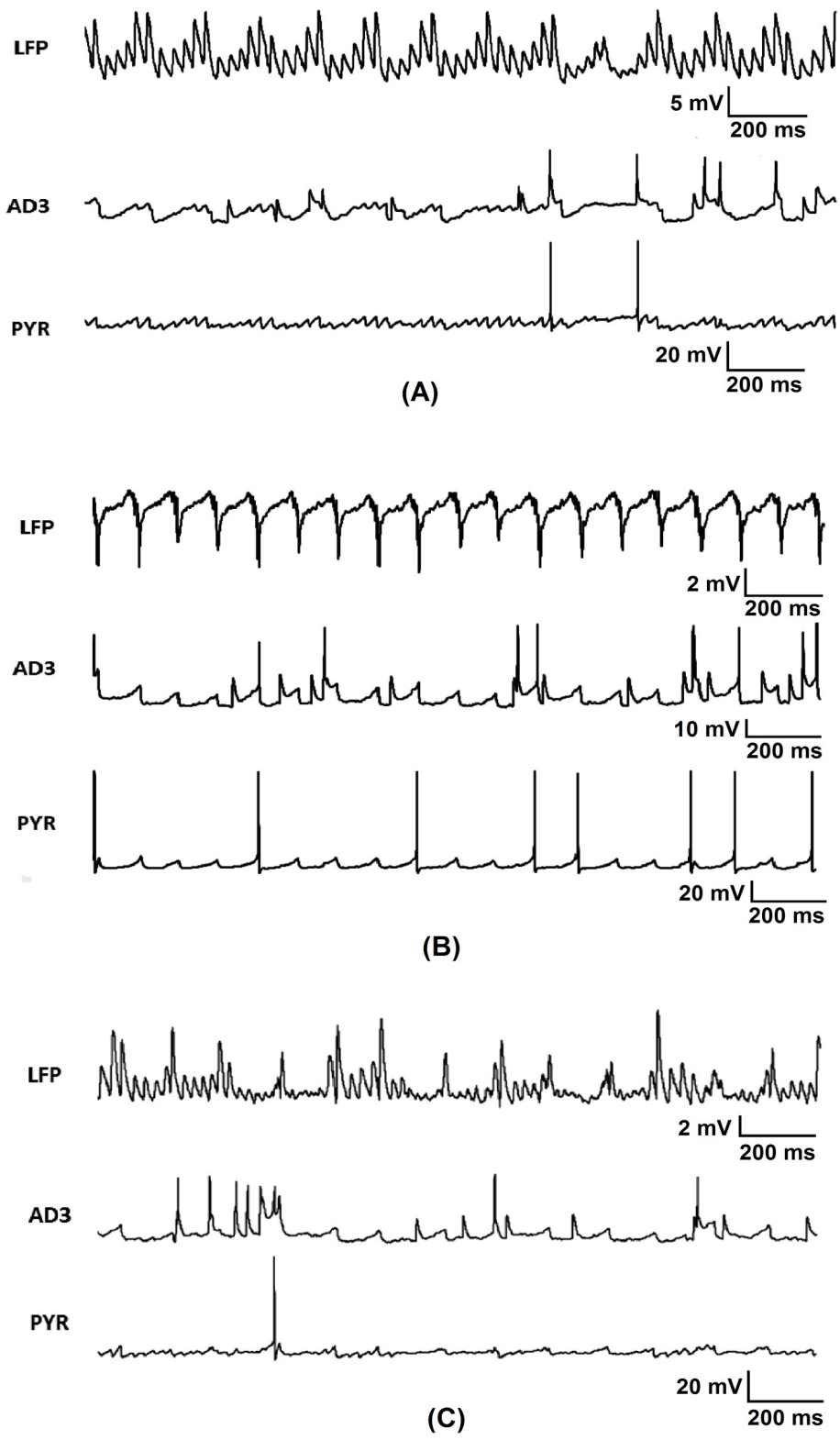

Figure 5.2: The Local Field Potential, activity at the distal most compartment of apical dendrite (AD3) and the somatic recording from pyramidal cell in a baseline network (A), an epileptic network due to 30% impaired dendritic inhibition and enhanced extracellular potassium (B) and network showing recovery when g(Ih) was increased to twice the baseline values in all cells of the network.

Enhancing g(Ih), increased network-wide inhibition via interactions between OLM, pyramidal, and basket cells, thereby re-establishing baseline network dynamics (Figure 5.3-C). In the epileptic network, pyramidal cells were disinhibited due to impaired dendritic inhibition, which led to depolarization block of basket cells. After enhancing g(Ih), the FR of OLM cells increased by 5-6 times from baseline (5.5 vs 1.0 Hz). This increase, even with 30% reduction in their connectivity to pyramidal cells, provided sufficient inhibition to reduce network hyperexcitability. The increased OLM firing rate reduced the excitatory activity of pyramidal cells and thereby reduced the excitatory drive to basket cells, thus eliminating their DB. However, at severe degradation of dendritic inhibition (70% impairment), g(Ih) was not able to reduce hyperexcitability sufficiently. The basket cells therefore continued to be in DB even with large enhancement of g(Ih) in the network.

5.5 EFFECT OF DRUGS ON NORMAL AND EPILEPTIC NETWORKS

HCN channel conductance has been implicated in many neurobiological function, and its alteration plays a role in pathological conditions (Noam et. al, 2011; Kase & Imoto, 2012). Studies have shown that antiepileptic drugs, gabapentin and lamotrigine restore normal network function by increasing HCN channel conductance (Poolos et. al, 2002; Surges et. al, 2003). Our model predicts that in a normal network, enhancing g(Ih) leads to overall suppression of network activity although individual cell FR increased with increase in g(Ih) in them individually. It was observed that a six times increment in g(Ih), almost silenced the pyramidal cells by reducing their FR to about one-tenth of the baseline levels. This is a result of tight inhibitory control of these cells due to excessive firing of OLM interneurons. Hence,

drugs that increase this conductance can have detrimental effects on normal network areas. These adverse effects include somnolence, dizziness, fatigue, nausea, headache etc (Brodie, 2010; French & Gazzola, 2011, Al-Bachari et. al, 2013). Hence, it is important that one is aware of their dual effects.

In the conditions leading to epileptic activity, enhancing g(Ih) by two times the baseline is sufficient to abolish depolarization block of basket cells and abolish the epileptiform activity produced by the network. This shows the importance of the OLM cells in controlling the excitatory activity of pyramidal neurons. The basket cells were driven to DB when the pyramidal cell FR were at relatively large values (~5 Hz). When the dendritic inhibition was reduced by 70%, the OLM cells were not effective in reducing the pyramidal excitatory activity despite significant enhancement of g(Ih). This inability to control pyramidal activity drove basket cells into DB, resulting in epileptic activity.

5.6 DEPOLARIZATION BLOCK OF BASKET CELLS

A significant observation from this study is the depolarization block **(DB)** of basket cells leading to a pathological state in the CA3 network. It is observed that this DB was caused by enhanced activation of pyramidal cells which was in turn due to their disinhibition. The DB of neurons has been observed in different experimental studies, causing pathological states.

Karlocai et.al (2014) describes a set of reasons for this DB. One is the perisomatic organization of basket cells facilitating their faster activation due to increased pyramidal cell activity. Second is their high reception of synaptic input from recurrently connected pyramidal cells. Third is the absence of K^+ channel

mediated hyperpolarizing currents and M-currents in basket cells. In their experimental work, Karlocai et.al (2014) observed DB of basket cells in three epileptogenic treatments – high extracellular potassium, zero-magnesium and addition of 4-amino-pyridine in hippocampal CA3 subfield. They observed increased firing of pyramidal cells and interneurons during these treatments eventually leading to DB of basket cells due to their high excitation compared to other neurons of the network. The pyramidal cells and dendrite-inhibiting interneurons continued their firing after the DB of basket cells.

Similar inactivation of basket cells due to mossy cell loss leading to epileptic activity has been reported in studies on dentate gyrus (Sloviter, 1991; Zhang & Buckmaster, 2009). Here, loss of mossy cells reduced basket cell excitation leading to a dormant state for the basket cells. However, this concept termed *dormant basket cell hypothesis* has been much debated (Sloviter et.al, 2003). Basket cell dysfunction has been reported to reduce pyramidal cell inhibition due to deficient GABA release, leading to psychological disorders like schizophrenia (Curley & Lewis, 2012).

The DB could result from other factors and involvement of other neurons. Experimental models of epilepsy using 4-Aminopyridine combined with low-magnesium showed generation of epileptic activity in the CA1 subfield of hippocampus due to DB of OLM interneurons. The suppression of inhibitory spike generation in these neurons led to an ictal-like activity in the network (Ziburkus et.al, 2006). In studies on epileptic activity generation using high extracellular potassium combined with low extracellular calcium, DB of pyramidal cells was observed to cause ictal activity pattern in the network (Su et al, 2001; Bikson et.al, 2003).

The above mentioned studies show that the suppression of activity of neurons

other than basket cells can also lead to similar pathological state observed in this thesis.

5.7 PYRAMIDAL CELL ACTIVITY IN NORMAL AND PATHOLOGICAL STATES

The rate of firing of pyramidal cells is worth noting from the results. As already mentioned it is the increased excitatory drive received by the basket cells from pyramidal cells that led to their depolarization block. As seen from the results, in the special condition (excessive external excitatory input to pyramidal cells) in Scenario 2 (Results, Section 4.1.3), the FR of pyramidal cells was 19.09 +/- 0.09 Hz during the basket cell DB. In Scenario 3 with 70% impairment in dendritic inhibition and changes in connectivity across all synapses in the network (Results, Section 4.1.4), the FR was 7.17 +/- 0.03 Hz during the basket cell DB and resulting epileptic activity.

In high extracellular potassium condition with 30% impairment in dendritic inhibition (Results, Section 4.2.3), the FR of pyramidal cells was 4.85 +/- 0.04 Hz during the basket cell DB. At 50% and 70% impairment in dendritic inhibition and elevated potassium in the network, the FR of pyramidal cells were 5.45 +/- 0.03 and 8 +/- 0.02 Hz respectively during the DB of basket cells, resulting epileptic activity. High pyramidal cell firing of the order of 6 to 14 Hz has been observed in various studies involving human subjects and in-vitro recordings from rat brain slices (Ziburkus et. al, 2006; Motamedi et. al, 2012). This study also finds similar excitabilities in pyramidal cells during the pathologic state. The rates of firing vary due to the in-vivo nature of the network and also depending on the condition tested.

5.8 COMPARISON WITH OTHER MODELS

Though CA3 subfield is known to be a vulnerable area for generating pathological conditions, computational models of this subfield have been lesser in number compared to CA1. This is probably due to the heterogeneous neuronal connectivity patterns within CA3 and lack of knowledge of exact biophysical parameters. Modellers have attempted to incorporate parameters applicable to CA1 neurons and modify them to simulate the experimentally observed activity of CA3 neurons (eg., Lazarewicz et.al, 2002). The model presented in this thesis generates theta-modulated gamma oscillations as the baseline activity which is observed to undergo significant changes in pathological states.

Many studies have attempted to explain the generation of abnormal activity caused due to excitation-inhibition imbalance (Wittner et. al, 2005; El-Hassar et. al, 2007). This study shows that inhibitory activity is compromised in the network. It is demonstrated here that a particular extent of impairment (threshold of connectivity changes) of inhibition makes the network hyperexcitable (90% impaired dendritic inhibition alone with excessive external stimulus or 70% impaired dendritic inhibition along with other network connectivity changes or 30% impaired dendritic inhibition with enhanced extracellular potassium (structural and chemical changes combined)). When changes in strength of connection were simulated at synapses between various neurons in network, hyperactivity was observed at an earlier point in time, as compared to other changes in the network. The strength of this study is that with the proposed set of network changes, hyperactivity in the network could be simulated, comparable to experimental observations.

5.9 LIMITATIONS OF THE STUDY

Similar to other computational models, this work also has its limitations. Though there are a number of experimental studies on epileptic activity generation in different areas of the brain, the exact mechanisms of epileptic activity generation and or how a network of neurons becomes epileptic is not properly understood. Assumptions had to be made as to how the external excitatory inputs received by pyramidal neurons undergo changes with stepwise decrement in dendritic inhibition. These along with other changes in network connectivity were tested systematically. While studying the effect of high extracellular potassium, it was assumed that changes in the reversal potential of $GABA_A$ synapses occur in a range of 10% from -80 mV to -72 mV for all three types of cells in our network.

This model was able to demonstrate epileptic activity with dynamics similar to those observed in experimental conditions by including three major types of cells, though in reality interplay between other types of cells in the *in vivo* network might lead to different outcomes. Although pyramidal to OLM and pyramidal to basket neuron synapses are facilitative and depressive, respectively (e.g.Sylwestrak and Ghosh, 2012), to study the effect of modulating synaptic weights in a systematic and controlled manner, the extra complexities in plasticity were left out. Though only some factors have been considered that play a role in the process of epileptogenesis, and many not considered, including biochemical pathways that may be involved, it is interesting to note that these factors were sufficient to produce simulated epileptic dynamics.

5.10 FUTURE WORK

This accepted computational model of CA3 network (Sanjay et. al, 2015) used in this study successfully generates theta-modulated gamma oscillations as the baseline activity. The individual neuron types in this model contain several biophysical parameters which are comparable to those incorporated in models of other neurons and networks which display normal physiology. A number of such models can be obtained from ModelDB (https://senselab.med.yale.edu/modeldb). Adding more biophysical and other contributing parameters to the model could help to simulate the neurophysiology of the network as such in more detail and improve our understanding of their influence on network activity. The hippocampus connects to various other regions of the brain. If the inputs from these sources are incorporated, then the model could be more realistic. For example, Dentate Gyrus inputs (which haven't been explicitly modelled). The CA3 and DG are known to form excitatory-inhibitory loops. This determines the inputs received by CA3 pyramidal cells from external sources and also produces oscillatory activity (Schafman, 2007). Degeneration of interneurons in DG has also been reported to lead to circuit hyperexcitability resulting in epileptic activity. Hence, elaborating the model to include the influence of other connected areas could make the study more realistic from pathophysiological point of view.

Since hippocampal CA3 subfield plays a significant role in learning, memory encoding and retrieval, cognitive processes, and spatial navigation, the changes in the network could potentially lead to impairment of these processes in an affected individual. In the future, studies could be performed to quantify the extent of impairment of dendritic inhibition and validate whether and to what extent of

impairment could lead to generation of abnormal activity. How network oscillations change in relation to network modifications in pathological states could be another interesting area of research. A significant future challenge is to devise methods to control the epileptic activity generation. Electrophysiological studies involving cell cultures could be planned to understand the influence of drugs increasing g(Ih) on specific cell types and networks formed by these cells. This could be useful for drug titration to determine what dosage of drug can bring recovery for a specific severity of neurodegeneration. Future models can link hippocampal network activity to electroencephalography and further study the effect of drugs.

CHAPTER 6

SUMMARY AND CONCLUSION

In this thesis, the excitatory and inhibitory interactions between neurons in the comparatively less studied, anatomically diverse and pathologically vulnerable CA3 subfield of hippocampus is studied using computational modelling, taking epilepsy as an example. This subfield has been known to have a low threshold for generating epileptic activity. But, the exact mechanisms leading to the generation of epileptic activity has not been fully understood. This research has attempted to propose a mechanism of epileptic activity generation caused due to hippocampal sclerosis (structural change) and ensuing abnormal chemical environment (high extracellular potassium - chemical change).

A stepwise approach was taken to systematically study how 1) impaired dendritic inhibition of pyramidal cells alone, 2) impaired dendritic inhibition combined with increased reception of external excitatory inputs by pyramidal cells, 3) network connectivity changes throughout the network and 4) abnormal chemical environment (high extracellular potassium resulting from hyperactivity due to sclerosis) lead to generation of epileptic activity in the vulnerable CA3 subfield. Thereafter, the action of drugs on HCN channel conductance to control the network hyperexcitability was studied.

The insilico CA3 network consisting of 800 pyramidal cells, 200 basket and 200 OLM interneurons along with inputs from the medial septum generated theta-modulated gamma oscillations as the baseline activity. When the strength of connectivity from OLM interneurons to pyramidal cells alone was reduced step by step, the network response simulated as Local Field Potential (LFP), showed

decrease in theta component and its absence at total loss of OLM to pyramidal cell connectivity. When increase in reception of external excitatory inputs by pyramidal cells was simultaneously simulated along with decrease in dendritic inhibition, a network response similar to earlier case was observed. But at 90% dendritic inhibition, when the reception of external excitatory input by pyramidal cells was highly increased (about 15 times the baseline), a characteristic ictal activity was simulated in the output LFP, which was comparable with published experimental results. When changes in connectivity between all neurons in the network were simulated as an effect of decreased dendritic inhibition and enhanced reception of external excitatory inputs by pyramidal cells, the network activity showed a characteristic ictal response at 70% impairment of dendritic inhibition. When a rise of extracellular potassium was simulated as a consequence of the structural changes, the epileptic activity occurred at 30% impairment of dendritic inhibition and associated network changes. In all these cases, the epileptic activity was a consequence of basket cell depolarization block thereby compromising the somatic inhibitory mechanisms in the network. Hence, low levels of impaired dendritic inhibition combined with changes in chemical environment makes neuronal networks easily susceptible to epileptic activity. It was worth noting that the firing rates (FR) of pyramidal cells was close to or above 5 Hz in all conditions leading to epileptic activity, consistent with published experimental observations.

The effect of anti-epileptic drugs like gabapentin and lamotrigine was simulated by increased conductance of HCN channels (g(Ih)). It was found that when this conductance was increased independently in each cell type in a normal network, their respective FR increased, with the FR of OLM interneurons showing the

maximum increase. On increasing g(Ih) uniformly in all neuron types in the normal network, the overall activity was suppressed due to the influence of increased OLM interneuron firing. Therefore, it can be summarized that though increased HCN channel conductance increase individual cell type activity, it suppresses the activity at network level.

When g(Ih) was increased systematically in the epileptic networks with high extracellular potassium due to 30, 50 and 70% impairments in dendritic inhibition, it was seen that the epileptic activity was abolished in the networks with 30% and 50% impaired dendritic inhibition and NOT in the one with 70% impairment in dendritic inhibition. It was also observed that whenever the epileptic activity was abolished due to increased g(Ih), the pyramidal cell FR was lower than that during normal network function. This implies that though the drugs acting on HCN channels could control hyperexcitabilities in the network, it can also have side-effects (somnolence, headache, giddiness, lowered cognitive function etc). It can also be noted that though OLM interneurons have played a significant role in abolishing epileptic activity, it is limited by the extent of impairment in dendritic inhibition.

To conclude: The balance between excitatory and inhibitory interactions in hippocampus and other areas of the brain are important for the normal function of a living being. Derangements in these intereactions can lead to a variety of disorders like epilepsy as discussed in this thesis. Much more needs to be studied about these interactions in health and disease to have a better understanding and devise therapeutic methods. Computational Neuroscience will be a highly promising area which could help in such studies by lessening the burden of technically challenging experiments and required expertise. Computational modelling along with

experimental and clinical studies in combination could immensely help in better understanding the nervous system at various levels of its organization - molecular, cellular, network and systems level and to design strategies to contain the disorders that may arise. This study suggests that therapies designed to restore lost excitatory-inhibitory balance would be particularly promising in reducing pathological dynamics. Hence, the potential of computational studies combined with future experiments is quite promising to advance our present knowledge and develop therapeutic strategies for neurodegenerative disorders.

BIBLIOGRAPHY

Al-Bachari S, Pulman J, Hutton JL et. al. (2013) Gabapentin add-on for drug-resistant partial epilepsy. *Cochrane Database of Systematic Reviews* Issue 7. Art. No.: CD001415.

Amaral DG (1993) Emerging principles of intrinsic hippocampal organization. *Current Opinion in Neurobiology* 3: 225-229

Arts WF, Brouwer OF, Peters AC, Stroink H, Peeters EA, Schmitz PI, van Donselaar, CA, Geerts, AT. (2004) Course and prognosis of childhood epilepsy: 5-year follow-up ofthe Dutch study of epilepsy in childhood. *Brain* 127(Pt 8):1774-84.

Asconape JJ. (2002) Some common issues in the use of antiepileptic drugs. *Semin. Neurol.* 22: 27-39

Balasubramani PP, Chakravarthy VS, Ali M, Ravindran B, Moustafa AA (2015) Identifying the Basal Ganglia Network Model Markers for Medication-Induced Impulsivity in Parkinson's Disease Patients. *PLoS ONE* 10(6): e0127542. doi:10.1371/journal.pone.0127542

Barbarosie M and Avoli M. (2003) CA3-Driven Hippocampal-Entorhinal Loop Controls Rather than Sustains *In Vitro* Limbic Seizures. *J Neurosci*, 17(23):9308–9314.

Bartos M, Vida I, Frotscher M, Meyer A, Monyer H, Geiger JRP, Jonas P (2002) Fast synaptic inhibition promotes synchronized gamma oscillations in hippocampal interneuron networks. *PNAS* 99 (20):13222–13227.

Bazhenov M, Timofeev I, Fro¨hlich F, Sejnowski TJ. (2008) Cellular and network mechanisms of electrographic seizures. *Drug Discov Today Dis Models* 5(1):45–57.

Ben-Menachem, E. (2007) Weight issues for people with epilepsy - A review. *Epilepsia* 48 (Suppl. 9), 42-45

Bender RA, Baram TZ. (2008) Hyperpolarization activated cyclic-nucleotide gated (HCN) channels in developing neuronal networks. *Prog. Neurobiol.* 86:129–140.

Berényi A, Belluscio M, Mao D, Buzsáki G (2012) Closed-Loop Control of Epilepsy by Transcranial Electrical Stimulation. *Science* 10 Aug 2012: 735-737

Bikson M, Hahn PJ, Fox JE Jeffrys JG (2003) Depolarization Block of Neurons During Maintenance of Electrographic Seizures. *J Neurophysiol* 90: 2402–2408.

Biton V. (2003) Effect of antiepileptic drugs on bodyweight: overview and clinical implications for the treatment of epilepsy. *CNS Drugs* 17, 781-791. 104.

Borhegyi Z, Varga V, Szilágyi N, Fabo D, Freund TF (2004) Phase Segregation of Medial Septal GABAergic Neurons during Hippocampal Theta Activity. *J Neurosci* 24(39) 8470 – 8479

Bragin A, Jando G, Nadasdy Z, Hetke J, Wise K, Buzsaki G. (1995) Gamma (40–100 Hz) oscillation in the hippocampus of the behaving rat. *J Neurosci* 15: 47–60.

Bragin A, Mody I, Wilson CL, Engel J Jr (2002) Local generation of fast ripples in epileptic brain. *J Neurosci* 22:2012–2021.

Brodie MJ (2010) Antiepileptic drug therapy the story so far. *Seizure* 19(10):650-5.
Buhl EH, Halasy K, Somogyi P (1994) Diverse sources of hippocampal unitary inhibitory postsynaptic potentials and the number of synaptic release sites. *Nature* 368: 823 – 828

Buzsaki G, Leung LW, Vanderwolf CH (1983) Cellular bases of hippocampal EEG in the behaving rat. *Brain Res* 287: 139–171.

Buzsaki G (1989) Two-stage model of memory trace formation: A role for noisy brain states. *Neuroscience* 31(3): 551-570.

Buzsaki G (2002) Theta Oscillations in the Hippocampus. *Neuron* 33:325–340

Carnevale NT and Hines ML (2006) The NEURON Book. Cambridge University Press.

Case M, Soltesz I (2011) Computational Modeling of Epilepsy. *Epilepsia* 52(Suppl 8): 12–15.

Cobb SR, Halasy K, Vida KI, Nyiri G, Tamas G, Buhl EH and Somogyi P (1997) Synaptic Effects Of Identified Interneurons Innervating Both Interneurons And Pyramidal Cells In The Rat Hippocampus. *Neuroscience* 79:3, 629–648.

Colgin LL, Moser EI. (2010) Gamma Oscillations in the Hippocampus. *Physiology* 25: 319-329.

Cooke SF, Bliss TVP (2006) Plasticity in the human central nervous system, *Brain* 129 (7):1659–1673

Cossart R , Dinocourt C , Hirsch JC, Merchan-Perez A, J. De Felipe, Ben-Ari Y, Esclapez M Bernard C. (2001) Dendritic but not somatic GABAergic inhibition is decreased in experimental epilepsy. *Nat Neurosci* 4 (1): 52 – 62.

Cramer J, Vachon L, Desforges C, Sussman NM. (1995) Dose frequency and dose interval compliance with multiple antiepileptic medications during a controlled clinical trial. *Epilepsia* 36, 1111-1117.

Curley AA and Lewis DA (2012) Cortical basket cell dysfunction in schizophrenia. *J Physiol* 590.4: 715-724.

Cutsuridis V, Graham BP, Cobb S, Vida I (Eds) (2010) Hippocampal Microcircuits: A computational modeler's resource book. Springer-Verlag, New York.

Cymerblit-Sabba A, Schiller Y. (2012) Development of hypersynchrony in the cortical network during chemoconvulsant-induced epileptic seizures in vivo. *J Neurophysiol* 107:1718–1730

Destexhe A, Rudolph M, Paré D. (2003) The high-conductance state of neocortical neurons in vivo. *Nat Rev Neurosci.* 4:739–751.

Dinocourt C, Petanjek Z, Freund TF, Ben-Ari Y and Esclapez M (2003) Loss of Interneurons Innervating Pyramidal Cell Dendrites and Axon Initial Segments in the CA1 Region of the Hippocampus following Pilocarpine-Induced Seizures. *J Comp Neurol* 459:407–425.

Dragoi G, Carpi D, Recce M, Csicsvari J and Buzsáki G (1999) Interactions between Hippocampus and Medial Septum during Sharp Waves and Theta Oscillation in the Behaving Rat. *J Neurosci* 19(14) 6190 – 6199.

Dyhrfjeld-Johnsen J, Morgan RJ, Soltesz I (2009) Double trouble? Potential for hyperexcitability following both channelopathic up- and downregulation of Ih in epilepsy. *Front. Neurosci.* 3, 25–33.

Dzhala VI and Staley KJ. (2003) Transition from Interictal to Ictal Activity in Limbic Networks *In Vitro. J Neurosci* 23(21):7873–7880.

El-Hassar L, Milh M, Wendling F, Ferrand N, Esclapez M, Bernard C (2007) Cell Domain-Dependent Changes in the Glutamatergic and GABAergic Drives during Epileptogenesis in the Rat CA1 Region *J Physiol* 578(Pt 1):193–211.

Fertziger AP, Ranck JB Jr. (1970) Potassium accumulation in interstitial space during epileptiform seizures. *Exp Neurol.* 26(3):571–85.

Fisher RS, Pedley TA, Moody Jr WJ, Prince DA (1976) The Role of Extracellular Potassium in Hippocampal Epilepsy. *Arch Neurol*. 33(2):76-83.

Fisher RS, Webber WR, Lesser RP, Arroyo S, Uematsu S (1992) High-frequency EEG activity at the start of seizures. *J Clin Neurophysiol.* 9(3):441-8.

Fisher RS, Velasco AL (2014) Electrical brain stimulation for epilepsy. *Nat Rev Neurol.* 10(5): 261–270.

Florence G, Pereira T, Kurths J. (2012) Extracellular potassium dynamics in the

hyperexcitable state of the neuronal ictal activity, *Commun Nonlinear Sci Numer Simulat* 17:4700–4706.

French JA & Gazzola DM (2011) New generation antiepileptic drugs: what do they offer in terms of improved tolerability and safety? *Therapeutic Advances in Drug Safety* 2(4):141-158.

French, J. A. (2007) Refractory epilepsy: clinical overview. *Epilepsia* 48 (Suppl.1), 3-7.

Frohlich F, Timofeev I, Sejnowski T, Bazhenov M. (2007) Extracellular potassium dynamics and epileptogenesis. In: Soltesz I, Staley KJ, editors. *Computational neuroscience in epilepsy.* San Diego: Elsevier. pp. 407–39.

Fröhlich F, Bazhenov M, Iragui-Madoz V, Sejnowski TJ (2008) Potassium Dynamics in the Epileptic Cortex: New Insights on an Old Topic. The Neuroscientist?: a review journal bringing neurobiology, neurology and psychiatry 14(5):422-433.

Furman M (2013) Seizure Initiation and Propagation in the Pilocarpine Rat Model of Temporal Lobe Epilepsy. *J Neurosci* 33(42):16409 –16411.

Gayatri NA, Livingston JH (2006) Aggravation of epilepsy by anti-epileptic drugs. *Dev Med Child Neurol.* 48(5):394-8

Gloveli T, Dugladze T, Rotstein HG, Traub RD, Monyer H, Heinemann U, Whittington MA and Kopell NJ. (2005) Orthogonal arrangement of rhythm-generating microcircuits in the hippocampus. PNAS 102 (37): 13295 – 13300.

González-Ramírez LR, Ahmed OJ, Cash SS, Wayne CE, Kramer MA (2015) A Biologically Constrained, Mathematical Model of Cortical Wave Propagation Preceding Seizure Termination. *PLoS Comput Biol* 11(2): e1004065. doi:10.1371/journal.pcbi.1004065

Green JD. (1964) The hippocampus. *Physiol Rev*44:561–608 .

Greenwood, R. S. (2000) Adverse effects of antiepileptic drugs. *Epilepsia*, 41 (Suppl. 2), S42-S52. 93

Hangya B, Borhegyi Z, Szilagyi N, Freund T, Varga V. (2009) GABAergic neurons of the medial septum lead the hippocampal network during theta activity. *J Neurosci.* 29:8094–8102

Hemond P, Epstein D, Boley A, Migliore M, Ascoli GA, Jaffe DB. (2008) Distinct classes of pyramidal cells exhibit mutually exclusive firing patterns in hippocampal area CA3b. *Hippocampus*. 18(4):411-424.

Heurta PT, Lisman JE (1993) Heightened synaptic plasticity of hippocampal CA1 neurons during a cholinergically induced rhythmic state. *Nature* 364: 723-725.

Hines ML, Davison AP, Muller E (2009) NEURON and Python *Front Neuroinform 3:*1

Iasemidis LD (2003) Epileptic seizure prediction and control. *IEEE Trans Biomed Eng.* 50(5):549-58.

Id Bihi R, Jefferys JGR, and Vreugdenhil M. (2005) The Role of Extracellular Potassium in the Epileptogenic Transformation of Recurrent GABAergic Inhibition. *Epilepsia* 46(Suppl. 5):64–71.

Isaev D, Isaeva E, Khazipov R et al. (2007) Shunting and Hyperpolarizing GABAergic Inhibition in the High-Potassium Model of Ictogenesis in the Developing Rat Hippocampus. *Hippocampus* 17:210–219

Jacobs J (2014) Hippocampal theta oscillations are slower in humans than in rodents: implications for models of spatial navigation and memory. *Phil Trans R Soc B* 369:20130304

Jensen MS, Yaari Y (1997) Role of intrinsic burst firing, potassium accumulation, and electrical coupling in the elevated potassium model of hippocampal epilepsy. *J Neurophysiol.* 77(3):1224-33.

Jobst BC, Darcey TM, Thadani VM, Roberts DW. (2010) Brain stimulation for the treatment of epilepsy. *Epilepsia.* 51:88–92

Karlocai MR, Kohus Z, Kali S, Ulbert I, Szabo G, Mate Z, Freund TF and Gulyas AI. (2014) Physiological sharp wave-ripples and interictal events in vitro: what's the difference? *Brain* 137:463-485

Kase D and Imoto K (2012) The Role of HCN Channels on Membrane Excitability in the Nervous System. *J Signal Transduct* 2012:619747. Epub 2012 Aug 13.

Kitayama, M. (2003) et al. Ih blockers have a potential of antiepileptic effects. *Epilepsia* 44:20–24.

Klassen T, Davis C, Goldman A, et al. (2011) Exome sequencing of ion channel genes reveals complex variant profiles confounding personal risk assessment in epilepsy. *Cell*. 145(7):1036-1048.

Korn SJ , Giacchino JL , Chamberlin NL et al. (1987) Epileptiform burst activity induced by potassium in the hippocampus and its regulation by GABA-mediated inhibition. *J Neurophysiol* 57(1): 325-340.

Lanerolle N.C. de , Kim JH, Robbins R.J. et al. (1989) Hippocampal interneuron loss and plasticity in human temporal lobe epilepsy. *Brain Res* 495: 387-395.

Lazarewicz MT, Migliore M, Ascoli GA. (2002) A new bursting model of CA3

pyramidal cell physiology suggests multiple locations for spike initiation. *BioSystems* 67:129 – 137.

Lega B, Burke J, Jacobs J, Kahana, MJ (2016) Slow-Theta-to-Gamma Phase–Amplitude Coupling in Human Hippocampus Supports the Formation of New Episodic Memories. *Cereb. Cortex* 26(1):268-278

Leite JP, Neder L, Arisi GA, Carlotti Jr. CG, Assirati A, and Moreira E. (2005) Plasticity, Synaptic Strength, and Epilepsy: What Can We Learn from Ultrastructural Data? *Epilepsia*, 46(Suppl. 5):134–141

Leppik, I. E (1992) Intractable epilepsy in adults. *Epilepsy Res.* (Suppl.) 5:7-11.

Leppik, I. E (2001) Issues in the treatment of epilepsy. *Epilepsia*, 42 Suppl 4:1-6.

Leppik, I. E & Schmidt, D. (1988) Consensus statement on compliance in epilepsy. *Epilepsy Res.* Suppl, 1: 179-182

Liu Y, Yu F, Liu W, He X, Peng B (2014) Dysfunction ofhippocampal interneurons in epilepsy. *Neurosci Bull* 30(6): 985–998.

Loup. F (2006) $GABA_A$ receptors in human temporal lobe epilepsy. *Epileptologie* 23: 187-194

Lytton WW, Hellman KM, Sutula TP (1998) Computer models of hippocampal circuit changes of the kindling model of epilepsy. *Artif Intell Med* 13(1-2):81-97.

Lytton WW (2008) Computer modeling of epilepsy. *Nat Rev Neurosci.* August ; 9(8): 626–637.

Lytton WW, Orman R, Stewart M. (2005). Computer simulation of epilepsy: implications for seizure spread and behavioral dysfunction. Epilepsy Behav. 7(3): 336–344.

Manganotti P, Miniussi C, Santorum E, Tinazzi M, Bonato C, Marzi CA, Fiaschi A, Bernardina DB, Zanette G (1998) Influence of somatosensory input on paroxysmal activity in benign rolandic epilepsy with ‘extreme somatosensory evoked potentials’. *Brain* 121: 647–658.

McAllister KA. (2000) Cellular and Molecular Mechanisms of Dendritic Growth. *Cerebral Cortex* 10: 963 – 973.

McBain CJ (1994) Hippocampal inhibitory neuron activity in the elevated potassium model of epilepsy. *J Neurophysiol*. 72(6):2853-63.

Migliore M, Cook EP, Jaffe DB, Turner DA, Johnston D. (1995) Computer simulations of morphologically reconstructed CA3 hippocampal neuron. *J Neurophysiol* 73(3):1157-1158.

Mora GN, Bramanti P, Osculati F, Chakir A, Nicolato E, Marzola P, Sbarbati A, Fabene PF. (2009) Does Pilocarpine-Induced Epilepsy in Adult Rats Require Status epilepticus? *PlosOne* 4(6): e5759.

Morgan RJ, Soltesz I. (2008) Nonrandom connectivity of the epileptic dentate gyrus predicts a major role for neuronal hubs in seizures. *Proceedings of the National Academy of Sciences of the United States of America*. 105(16):6179-6184.

Motamedi GK., Gonzalez-Sulser A, Dzakpasu R & Vicini S (2012). Cellular Mechanisms of Desynchronizing Effects of Hypothermia in an In Vitro Epilepsy Model. *Neurotherapeutics* 9:199–209

Neymotin SA, Hilscher MM, Moulin TC, Skolnick Y, Lazarewicz MT, Lytton WW (2013) *Ih* Tunes Theta/Gamma Oscillations and Cross-Frequency Coupling In an *In Silico* CA3 Model. PLoS ONE 8(10): e76285.

Neymotin SA, Lazarewicz MT, Sherif M, Contreras D, Finkel LH, and Lytton WW (2011) Ketamine Disrupts Theta Modulation of Gamma in a Computer Model of Hippocampus. The *J Neurosci* 31(32):11733–11743.

Noam Y, Bernard C, Baram TZ (2011) Towards an integrated view of HCN channel role in epilepsy. *Current Opinion in Neurobiology* 21(6):873-879.

O'Sullivan-Greene E, Mareels I, Freestone D, Kulhmann L, Burkitt A. (2009) A paradigm for epileptic seizure prediction using a coupled oscillator model of the brain. *Conference Proceedings – IEEE Engineering in Medicine and Biology Society* 6428–31

Park J, Lee H, Kim T, Park GY, Lee EM, Baek S, Ku J, Kim IY, Kim SI, Jang DP, Kang JK (2014) Role of low- and high-frequency oscillations in the human hippocampus for encoding environmental novelty during a spatial navigation task. *Hippocampus*. 24(11):1341-52.

Patsalos PN, Berry DJ, Bourgeois BF, Cloyd JC, Glauser TA, Johannessen SI, Leppik IE, Tomson T, Perucca E (2008) Antiepileptic drugs--best practice guidelines for therapeutic drug monitoring: a position paper by the subcommission on therapeutic drug monitoring, ILAE Commission on Therapeutic Strategies. *Epilepsia* 49: 1239-1276

Poolos NP, Migliore M, Johnston D (2002). Pharmacological upregulation of h-channels reduces the excitability of pyramidal neuron dendrites. *Nat Neurosci* 5 (8): 767-774

Poolos NP (2004) The yin and yang of the H-channel and its role in epilepsy. *Epilepsy Curr.* 4, 3–6 .

Postea O, Biel M (2011) Exploring HCN channels as novel drug targets. *Nat. Rev. Drug Discov.* 10:903-914

Regesta G, Tanganelli P (1990) Clinical aspects and biological bases of drug-resistant epilepsies. *Epilepsy Res* 34(2-3):109-22.

Ren H, Shi Y, Lu Q, Liang P, Zhang P (2014). The role of the entorhinal cortex in epileptiform activities of the hippocampus. *Theoretical Biology and Medical Modelling* 11:14

Robbins RJ, Brines ML, Kim JH et al. (1991) Selective Loss of Somatostatin in the Hippocampus of Patients with Temporal Lobe Epilepsy. *Ann Neuro* 20:325-332.

Stefanescu RA, Shivakeshavan RG, Talathi SS (2012) Computational models of epilepsy. *Seizure* 21:748–759

Sanjay M., Neymotin SA., and Krothapalli SB.(2015) Impaired dendritic inhibition leads to epileptic activity in a computer model of CA3. *Hippocampus* 25 (11): 1336-1350

Scharfman HE: The CA3 "backprojection" to the dentate gyrus. *Prog Brain Res* 2007, 163: 627-637

Seddigh S, Thomke F and Vogt TH. (1999) Complex partial seizures provoked by photic stimulation. *J Neurol Neurosurg Psychiatry* 66:801-802

Sloviter RS, Zappone CA, Harvey BD, Bumanglag A V, Bender RA, Frostscher M. (2003) "Dormant basket cell" hypothesis revisited: relative vulnerabilities of dentate gyrus mossy cells and inhibitory interneurons after hippocampal status epilepticus in the rat. *J Comp Neurol* 459(1):44-76.

Sloviter, R. S (1987) Decreased hippocampal inhibition and a selective loss of interneurons in experimental epilepsy. *Science* 235:73–76

Somjen GG (2004) Ions in the brain: normal function, seizures, and stroke. Oxford University Press, New York.

Spencer SS (2002) When should temporal-lobe epilepsy be treated surgically? *Lancet Neurol.* 1,375-382.

Squire LR (2009). The Legacy of Patient H.M. for Neuroscience. *Neuron* 61(1), 6–9.

Stacey W, Lazarewicz M, Litt B. (2009) Synaptic noise and physiological coupling generate high-frequency oscillations in a hippocampal computational model. *J Neurophysiol.* 102:2342–2357.

Stewart M, Fox SE. (1990). Do septal neurons pace the hippocampal theta rhythm?

Trends Neurosci 13:163–168.

Stoop R, Pralong E (2000) Functional connections and epileptic spread between hippocampus, entorhinal cortex and amygdala in a modified horizaontal slice preparation of the rat brain. *Eur J Neurosci* 12: 3651 – 3663.

Su H, Alroy G, Kirson ED et al. (2001) Extracellular Calcium Modulates Persistent Sodium Current-Dependent Burst-Firing in Hippocampal Pyramidal Neurons. *J Neurosci* 21(12):4173–4182

Surges R, Freiman TM, Feuerstein TJ (2003) Gabapentin Increases the Hyperpolarization-activated Cation Current Ih in Rat CA1 Pyramidal Cells. *Epilepsia* 44(2):150–156, 2003

Sylwestrak EL, Ghosh A (2012) Elfn1 regulates target-specific release probability at CA1-interneuron synapses. *Science* 338(6106):536-40.

Timofeev I, Steriade M. (2004) Neocortical seizures: initiation, development and cessation *Neuroscience* 123:2, 299–336

Tort AB, Rotstein HG, Dugladze T, Gloveli T, Kopell NJ. 2007. On the formation of gamma-coherent cell assemblies by oriens lacunosum moleculare interneurons in the hippocampus. *Proc Natl Acad Sci USA* 104:13490–13495.

Traub RD, Whittington MA, Buhl EH, LeBeau FE, Bibbig A, Boyd S, Cross H, Baldeweg T. (2001) A possible role for gap junctions in generation of very fast EEG oscillations preceding the onset of, and perhaps initiating, seizures. *Epilepsia* 42(2):153-70.

Uhlhaas PJ, Singer W (2006) Neuralsynchronyinbraindisorders:relevance for cognitive dysfunctions and pathophysiology. Neuron 52:155–168.

Wahab A, Albus K, Gabriel S, Heinemann U (2010) In search for models of pharmacoresistant epilepsy: A review. *Epilepsia* 51 (Suppl. 3), 154-159

Wang X (2002) Pacemaker Neurons for the Theta Rhythm and Their Synchronization in the Septohippocampal Reciprocal Loop *J Neurophysiol* 87: 889–900.

White J, Banks M, Pearce R, Kopell N. (2000) Networks of interneurons with fast and slow γ-aminobutyric acid type A (GABAA) kinetics provide substrate for mixed gamma-theta rhythm. *Proc Nat Acad Sci* 97:8128–8133

Whittington MA, Traub RD and Jefferys JGR. (1995) Erosion of inhibition contributes to the progression of low magnesium bursts in rat hippocampal slices. *J Physiol* 486(3), 723-734.

Wilby J, Kainth A, Hawkins N, Epstein D, McIntosh H, McDaid C, Mason A,

Golder S, O'Meara S, Sculpher M, Drummond M, Forbes C (2005) Clinical effectiveness, tolerability and cost-effectiveness of newer drugs for epilepsy in adults: a systematic review and economic evaluation. *Health Technol.Assess.* 9(15):1-157 iii-iv.

Witter MP (2007) Intrinsic and extrinsic wiring of CA3: Implications for connectional heterogeneity. *Learn. Mem.* 14: 705-713.

Wittner L, Eross L, Czirja´k S, Hala´sz P, Freund T. F. & Zs. Maglo´czky (2005) Surviving CA1 pyramidal cells receive intact perisomatic inhibitory input in the human epileptic hippocampus. *Brain* 128 (Pt 1):138-152. Epub 2004 Nov 17.

Zaccara G, Franciotta D, Perucca E (2007) Idiosyncratic adverse reactions to antiepileptic drugs. *Epilepsia 48*, 1223-1244.

Zhang H, Jacobs J (2015) Traveling Theta Waves in the Human Hippocampus The *J Neurosci* 35(36): 12477-12487

Zhang W, Buckmaster PS. (2009) Dysfunction of the dendate basket cell circuit in a rat model of temporal lobe epilepsy. *J Neurosci* 29(24):7846 –7856.

Ziburkus J, Cressman JR, Barreto E, Schiff SJ (2006) Interneuron and Pyramidal Cell Interplay During In Vitro Seizure-Like Events *J Neurophysiol* 95: 3948–3954.

LIST OF PUBLICATIONS FROM THESIS

PUBLICATIONS IN JOURNALS

Sanjay M., Neymotin SA., and Krothapalli SB (2015) Impaired dendritic inhibition leads to epileptic activity in a computer model of CA3. *Hippocampus* 25 (11): 1336-1350. (Impact Factor 4.302)

INVITED BOOK CHAPTERS - UPCOMING

1) **M. Sanjay** and K. Srinivasa Babu. Modelling Epileptic Activity In Hippocampal CA3. In: Hippocampal Microcircuits. A computational Modeler's Resource Book. 2nd Volume. Springer NY. Edited by Vassilis Cutsuridis et.al *(Submitted, in press)*

2) **M Sanjay**, Samuel A Neymotin, K Srinivasa Babu, William W Lytton. Multiscale Computer Modeling Of Epilepsy. In: Computational Models of Brain and Behavior. To be published by Wiley-Blackwell in 2016. *(Submitted, in press)*

CURRICULUM VITAE - M SANJAY

EDUCATION

Ph.D Bioengineering (2009 - 2016) at Christian Medical College Vellore, affiliated to Sree Chitra Tirunal Institute for Medical Sciences and Technology, Trivandrum.

MS Bioengineering (2007 - 2009) at Christian Medical College Vellore, affiliated to Sree Chitra Tirunal Institute for Medical Sciences and Technology, Trivandrum.

B.Tech Electronics and Biomedical Engineering (2000 - 2004) at Model Engineering College Ernakulam affiliated to Cochin University of Science and Technology, Kochi.

WORK EXPERIENCE

Lecturer, Dept. of Electronics and Communication Engg, Nehru College of Engg & Research Centre, Thiruvilwamala, Thrissur District, Kerala (July 2005 to July 2007).

MAJOR CONFERENCES / WORKSHOPS ATTENDED

1. **IAN Clinical Neurophysiology subsection workshop on Electro-neuro-myography and Autonomic Disorders,** CMC Vellore from 28th to 30th August 2014

2. **Okinawa Institute of Science and Technology – Computational Neuroscience Course (OCNC) 2013** at Okinawa Institute of Science and Technology, Okinawa, Japan from 17th June to 4th July 2013 and presented a poster related to Ph.D research work.

3. **National Workshop,** Indian National Node for Neuro Informatics jointly at IIT Madras and Institute of Mathematical Sciences Chennai from 5-7 November 2012.

4. **Organizing Committee Member** of the **National Workshop** in Experimental Physiology conducted jointly by the Departments of Physiology and Bioengineering, CMC Vellore from 3-5 September 2008.

PUBLICATIONS IN JOURNALS

1) Sivadasan, A., **Sanjay, M**., Alexander, M., Devasahayam, S. R. and Srinivasa B. K, (2013) Utility of multi-channel surface electromyography in assessment of focal hand dystonia, *Muscle and Nerve*, 48: 415-422.

2) **Sanjay, M.**, Neymotin, S. A., and Krothapalli, S. B (2015). Impaired dendritic inhibition leads to epileptic activity in a computer model of CA3. *Hippocampus* 25: 1336-1350.

GRANTS RECEIVED

Institutional Fluid Research Grant from Christian Medical College Vellore during the MS Thesis research work (2008 – 2009)

MEMBERSHIP OF SOCIETIES

1) Life Member – Biomedical Engineering Society of India (No. L 793)
2) Life Member – Indian Society for Technical Education (No. 51481**)**

ACHIEVEMENTS

Qualified GATE 2007 in Instrumentation Engineering (Score 363).

APPENDIX

A1: PUBLICATION RELATED TO THE THESIS WORK - Sanjay et. al (2015)

A2: INSTITUTIONAL REVIEW BOARD APPROVAL

HIPPOCAMPUS 25:1336–1350 (2015)

Impaired Dendritic Inhibition Leads to Epileptic Activity in a Computer Model of CA3

M. Sanjay,[1,2] Samuel A. Neymotin,[3,4] and Srinivasa B. Krothapalli[1]*

ABSTRACT: Temporal lobe epilepsy (TLE) is a common type of epilepsy with hippocampus as the usual site of origin. The CA3 subfield of hippocampus is reported to have a low epileptic threshold and hence initiates the disorder in patients with TLE. This study computationally investigates how impaired dendritic inhibition of pyramidal cells in the vulnerable CA3 subfield leads to generation of epileptic activity. A model of CA3 subfield consisting of 800 pyramidal cells, 200 basket cells (BC) and 200 Oriens—Lacunosum Moleculare (O-LM) interneurons was used. The dendritic inhibition provided by O-LM interneurons is reported to be selectively impaired in some TLEs. A step-wise approach is taken to investigate how alterations in network connectivity lead to generation of epileptic patterns. Initially, dendritic inhibition alone was reduced, followed by an increase in the external inputs received at the distal dendrites of pyramidal cells, and finally additional changes were made at the synapses between all neurons in the network. In the first case, when the dendritic inhibition of pyramidal cells alone was reduced, the local field potential activity changed from a theta-modulated gamma pattern to a prominently gamma frequency pattern. In the second case, in addition to this reduction of dendritic inhibition, with a simultaneous large increase in the external excitatory inputs received by pyramidal cells, the basket cells entered a state of depolarization block, causing the network to generate a typical ictal activity pattern. In the third case, when the dendritic inhibition onto the pyramidal cells was reduced and changes were simultaneously made in synaptic connectivity between all neurons in the network, the basket cells were again observed to enter depolarization block. In the third case, impairment of dendritic inhibition required to generate an ictal activity pattern was lesser than the two previous cases. Moreover, the ictal like activity began earlier in the third case. Hence, our study suggests that greater synaptic plasticity occurring in the whole network due to increase in reception of external excitatory inputs (due to impaired dendritic inhibition) makes the network more susceptible to generation of epileptic activity. © 2015 Wiley Periodicals, Inc.

KEY WORDS: temporal lobe epilepsy; hippocampus; oscillations; basket cells; depolarization block; ictal activity

[1] **Neurophysiology Unit, Department of Neurological Sciences, Christian Medical College, Vellore, India;** [2] **Department of Bioengineering, Christian Medical College, Vellore, India;** [3] **Department of Physiology and Pharmacology, State University of New York, Downstate Medical Center, Brooklyn, New York;** [4] **Department of Neurobiology, Yale University School of Medicine, New Haven, Connecticut**

Grant sponsor: National Hub for Health Care Instrumentation Development Project; Grant number: IDP/Med Hub/2009-10; Department of Science and Technology;; Grant sponsor: Dr. Marcus Devanandan Endowment Fund; Grant number: 22E065; Christian Medical College Vellore India.

*Correspondence to: Dr. K Srinivasa Babu, Senior Scientist, Neurophysiology Unit, Department of Neurological Sciences, Christian Medical College Vellore, Tamilnadu, India. E-mail: srinivas@cmcvellore.ac.in

Accepted for publication 10 March 2015.
DOI 10.1002/hipo.22440
Published online 10 April 2015 in Wiley Online Library (wileyonlinelibrary.com).

INTRODUCTION

Epilepsy is a neurological disorder caused by an imbalance between excitatory and inhibitory interactions among the neurons in a network. In temporal lobe epilepsy (TLE), the CA3 subfield of hippocampus is known to initiate epileptic activity which then spreads to other areas. The mechanism involved in the generation of epileptic activity is still not fully understood. The CA3 subfield of hippocampus and the entorhinal cortex are two areas which are reported to generate independent epileptiform activity (Lytton et al., 2005). The CA3 subfield has a very high degree of recurrent neuronal connectivity (Witter, 2007), which reduces its activation threshold and makes it easily hyperexcitable. Though there have been many experimental studies on the CA3 subfield, computational studies involving biophysically detailed models have been fewer, compared to CA1.

Different animal models are used to study the various aspects of epileptic activity viz., its generation, route of spread, severity, specific patterns, etc. These studies have been in vivo or in vitro, extracellular or intracellular. Epileptic activity is induced using various methods including electrical stimulation, elevating the levels of potassium in artificial cerebrospinal fluid (aCSF) (Dzhala and Staley, 2003; Id Bihi et al., 2005), eliminating magnesium from aCSF (Barbarosie and Avoli, 1997; Wittington et al., 1995), adding convulsive agents like bicuculline to aCSF (Stoop and Pralong, 2000), or intraperitoneal administration of pilocarpine (Dinocourt, 2003; Cymerblit-Sabba and Schiller, 2012). The mechanism of epileptic activity generation differs in all these methods. Limited computational modeling studies are done with biophysical and network connectivity details to investigate mechanisms of hyperexcitability (Lytton, 2008).

This study uses a computer model to investigate how changes in connectivity between neurons of the hippocampal CA3 subfield leads to generation of abnormal network activity, a characteristic of epilepsy, with a focus on the role of loss of dendritic inhibition. Loss of dendritic inhibition is a significant change in connectivity that is reported in certain experimental models of epilepsy. Pilocarpine treated rats have been

reported to undergo loss of dendritic inhibition as evident from histological studies (Dinocourt, 2003; Cymerblit-Sabba and Schiller, 2012). This is also reported to cause dendritic sprouting in pyramidal cells (McAllister, 2000; Ren et al., 2014) and thus leading to increased excitatory external input being received by the pyramidal cells. These inputs are received mainly from the entorhinal cortex. The pilocarpine model gains significance due to the fact that abnormal patterns of neuronal activity observed could be compared to those observed in human patients with epilepsy (Mora et al., 2009; Moran Furman, 2013).

In this study we propose a set of mechanisms that leads to an altered network that generates experimentally observed patterns, characteristic of epileptic activity in the CA3 subfield. We have adopted a computer model of the CA3 network (Neymotin et al., 2011) consisting of 800 pyramidal cells, 200 O-LM interneurons and 200 basket cells. The model has sufficient biophysical detail to generate theta-modulated gamma oscillations at baseline. While theta oscillations play a significant role in spatial navigation and motor behaviour, gamma oscillations are important in learning, and memory encoding and retrieval (Colgin and Moser, 2010). In the course of leading to epileptiform activity development, the changes occurring in the baseline oscillatory behavior is also studied. In this model we explored how: (1) loss of connectivity between the O-LM and pyramidal cells alone influences the behaviour of other types of neurons and its overall effect on the network, (2) changes in external inputs received by pyramidal neurons affect the activity, and (3) how changes at synapses between the neurons affect the overall network activity in the CA3 subfield.

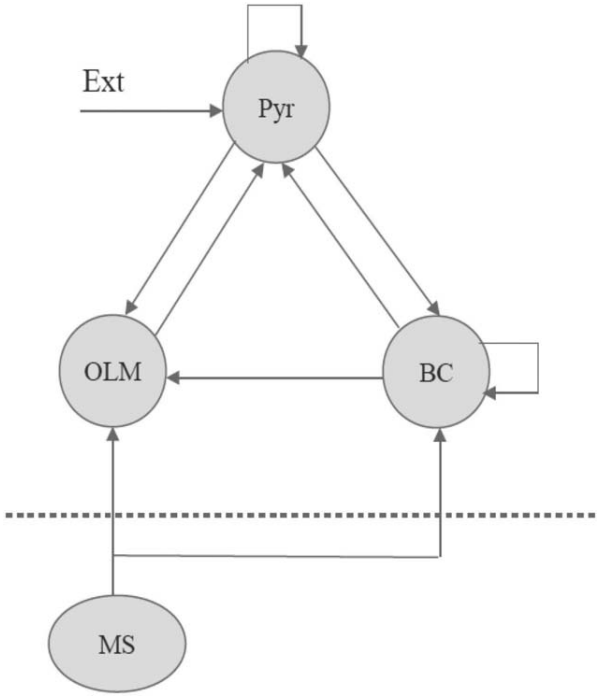

FIGURE 1. Schematic connectivity between Pyr—pyramidal cells, BC—basket cells (soma-inhibiting), OLM—oriens lacunosum moleculare interneurons (dendrite-inhibiting), Ext—external inputs to pyramidal cells (mainly from entorhinal cortex), MS—medial septum. The basket and OLM cells receive excitatory inputs from pyramidal cells. The pyramidal cells receive inhibitory inputs from basket and OLM cells. The recurrent connections between pyramidal cells are excitatory while those between basket cells are inhibitory. OLM cells receive inhibitory inputs from basket cells. The medical septum provides inhibitory inputs every 150 ms to basket and OLM cells.

METHODOLOGY

In our study, we have used a computer model of a network of neurons in the CA3 subfield of hippocampus (Neymotin et al., 2011) consisting of 800 five-compartment pyramidal cells (three apical dendrites, one basal dendrite, soma), 200 one-compartment O-LM interneurons and 200 one-compartment basket cells. The full source code of the model is available on ModelDB (http://senselab.med.yale.edu/modeldb/ShowModel.asp?model=139421). The model generates theta-modulated gamma oscillations as a baseline activity. To this model we added additional connections from basket cells to O-LM cells, consistent with anatomical data (Cobb et al., 1997). However, this connectivity did not noticeably alter baseline activity.

Current injections (pyramidal cells: 50 pA; OLM cells: −25 pA) were added to obtain baseline activity. All cells contained leak current, transient sodium current I_{Na}, and delayed rectifier current I_{K-dr} to allow for action potential generation. Pyramidal cells contained potassium type A current I_{K-A} for rapid inactivation, and hyperpolarization-activated current I_h. The O-LM cells had a simple calcium-activated potassium current I_{KCa} to allow long lasting inactivation after bursting, high-threshold calcium current I_L to augment bursting and to activate I_{KCa}, hyperpolarization-activated current I_h for bursting, and intracellular calcium concentration dynamics. These current selections were based on the published work by Tort et al. (2007).

Synaptic Connectivity in the Normal CA3 Network

The CA3 network used in the study is shown in Figure 1. Three main types of neurons in the CA3 subfield are considered—pyramidal cells (Pyr), soma-inhibiting basket cells (BC), and dendrite-inhibiting Oriens-Lacunosum Moleculare (O-LM) interneurons. The pyramidal cells and basket cells are recurrently connected. The pyramidal cell activity drives the basket cells and O-LM cells. The basket cells and O-LM interneurons connect to pyramidal cells and produce inhibitory responses in the network, preventing hyperactivity. The basket cells and O-LM interneurons receive inhibitory inputs from the medial septum (MS) once every 150 ms to model the function of medial septum as a pacemaker (Stewart and Fox, 1990, Dragoi et al.,

TABLE 1.

Synaptic Parameters for the Connectivity Between Neurons in the Model

Presynaptic	Postsynaptic	Receptor	τ_1 (ms)	τ_2 (ms)	Conductance (nS)
Pyramidal	Pyramidal	AMPA	0.05	5.3	0.02
Pyramidal	Pyramidal	NMDA	15	150	0.004
Pyramidal	Basket	AMPA	0.05	5.3	0.36
Pyramidal	Basket	NMDA	15	150	1.38
Pyramidal	OLM	AMPA	0.05	5.3	0.36
Pyramidal	OLM	NMDA	15	150	0.7
Basket	Pyramidal	GABA-A	0.07	9.1	0.72
Basket	Basket	GABA-A	0.07	9.1	4.5
Basket	OLM	GABA-A	0.07	9.1	0.0288
OLM	Pyramidal	GABA-A	0.2	20	72
MS	Basket	GABA-A	20	40	1.6
MS	OLM	GABA-A	20	40	1.6

1999, Borhegyi et al., 2004). Basket and O-LM cells also received external random inputs. The pyramidal cells receive external inputs at the distal dendritic compartment that represents inputs from the entorhinal cortex. Their soma also receives random external inputs.

The pyramidal cell to O-LM connectivity, the pyramidal cell to basket cell connectivity, and the recurrent connectivity between pyramidal cells are modeled through NMDA and AMPA synapses (Table 1). The O-LM and basket cells and soma of pyramidal cells receive background random excitatory and inhibitory inputs through AMPA and GABA-A receptors. Similar inputs received at the distal dendritic compartment of pyramidal cells are through AMPA, NMDA and GABA-A receptors. The O-LM to pyramidal cell, basket to pyramidal cell, basket-basket recurrent connections, and MS to O-LM and basket cell connections is through GABA-A receptors. Synapses were modeled by standard NEURON double-exponential mechanism. Magnesium block in NMDA receptors used the experimental scaling factor from Jahr and Stevens, (1990). The baseline network produced theta modulated gamma oscillations. The local field potential (LFP) was simulated by a sum of differences in membrane potential between the most distal apical and the basal dendritic compartment over all pyramidal cells.

The loss of dendritic inhibition and its effect on the network were studied in three steps. First, the strength of connectivity from O-LM to pyramidal cells alone was reduced step by step to observe the changes occurring in the baseline activity of the network. In addition to this condition the effect of increased external excitatory inputs received by the pyramidal neurons was studied. In addition to the above two conditions, the synaptic strength was changed in the network and its effect was studied.

In the first scenario, the weight of connection from O-LM cells to pyramidal neurons was reduced from the baseline 100% (1×) to 80% (0.8×), 60% (0.6×), 40% (0.4×), 20% (0.2×), 10% (0.1×), 5% (0.05×) and total absence/loss, 0% (0×) (Fig. 2A). In the second scenario, as dendritic inhibition changes from 1× (100%) to 0.8×, 0.6×, 0.4×, 0.2×, 0.1×, 0.05×, and 0×, the external inputs received by the distal dendritic compartment of pyramidal cells were increased from 1× to 1.2×, 1.4×, 1.6×, 1.8×, 1.9×, 1.95×, and 2× (200%), respectively (Fig. 2B).

In the third scenario, a proportionate increment in the synaptic strength between all the neurons is affected. Basically, reduction in dendritic inhibition was assumed to enhance the network activity by strengthening the communication between different neurons. A set of changes to the network described below were performed to test this scenario.

Proposed mechanism of in vivo abnormal network activity generation

When the dendritic inhibition is reduced:

- The continuous external excitatory inputs that are received at the distal dendrites of pyramidal neurons reach soma and increase their excitability.
- The recurrent connectivity between the pyramidal neurons in the network makes the network more excitable and the synaptic communications between the pyramidal neurons are strengthened.
- The pyramidal neurons provide stronger excitation to the basket cells and O-LM cells.
- The increased recurrent inhibition between basket cells makes pyramidal cells more disinhibited.
- Though the O-LM cells are also excited by the increased activity of pyramidal cells, the reduction in connectivity of O-LM to pyramidal cells prevents O-LM cells to further inhibit pyramidal cells.
- The external inputs received by the pyramidal neurons are increased since sprouting and formation of spines could happen in the distal apical dendrites of pyramidal cells due to disinhibition, as reported in the literature (McAllistair, 2000).

Based on these proposed changes in the network, two conditions were tested—reduction of OLM to pyramidal cell connectivity to 50% (50% impairment of dendritic inhibition) and 30% (70% impairment of dendritic inhibition) of the baseline along with changes in strength of connectivity between the other neurons to test the model. With reduction in O-LM to pyramidal cell connectivity to 50% of the baseline, the excitatory external inputs as received by the pyramidal cells were doubled and the pyramidal cell to pyramidal cell recurrent connectivity is strengthened by four times the baseline. The pyramidal cell to O-LM interneuron, pyramidal cell to basket cells and basket to basket interactions are strengthened to twice the baseline connectivity. As BC to BC interactions are mutually inhibitory, the output from BC to other cells, that is, BC to pyramidal cell inhibition and BC to O-LM inhibiton are reduced to 80% of baseline (Fig. 2C).

When the OLM to pyramidal cell connectivity was reduced to 30% (70% impairment of dendritic inhibition), bigger

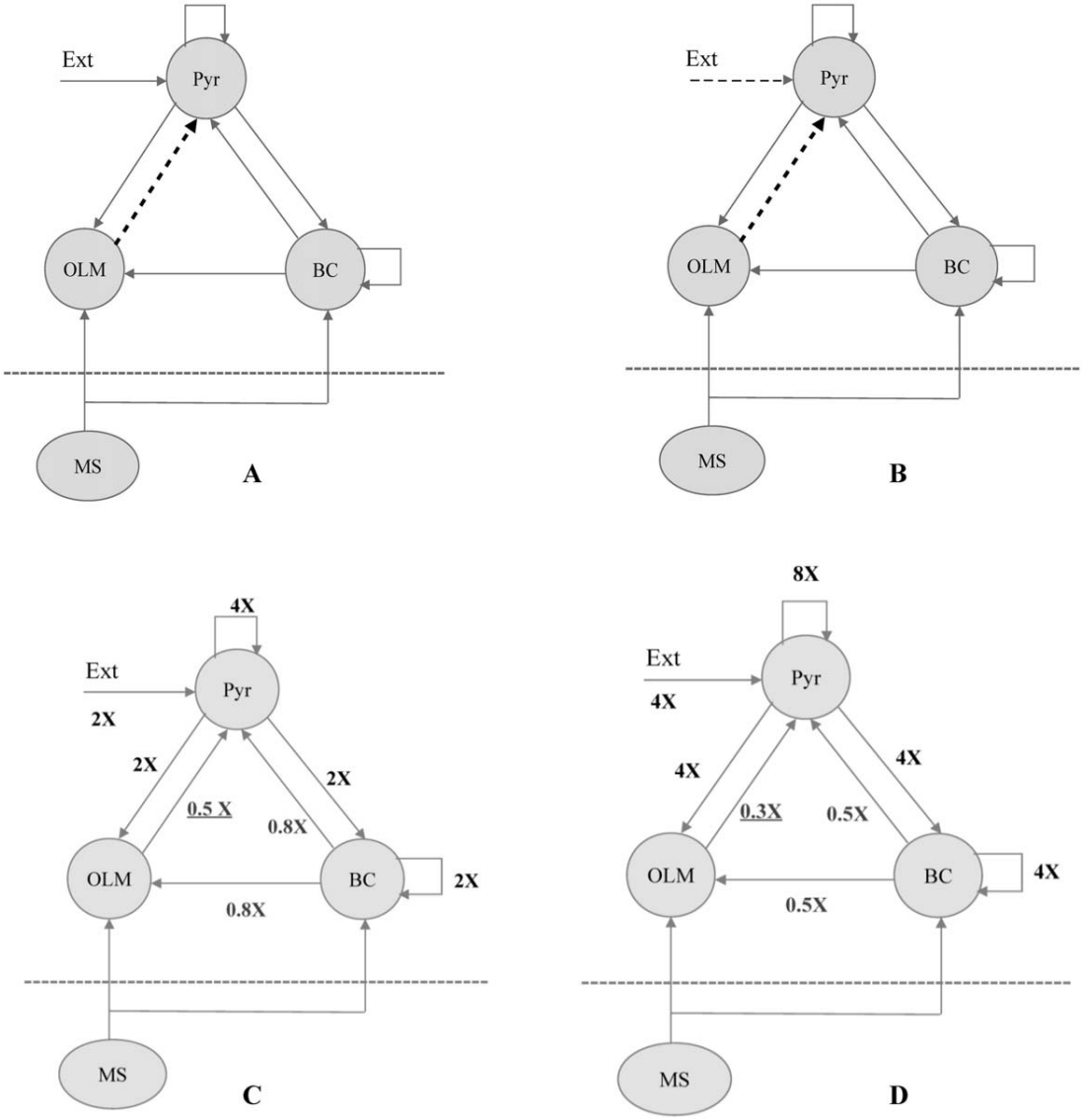

FIGURE 2. Changes in connectivity under different scenarios. (A) Scenario 1—strength of connectivity between OLM and pyramidal cells alone changed (dark dotted line with arrow). (B) Scenario 2—In addition to condition in scenario 1, external inputs are also increased. (C) and (D) Scenario 3—strength of connections between all neurons in the network are changed when OLM—Pyr connectivity was reduced to 50% (0.5×) and 30% (0.3×), respectively. The numbers along the arrows shows the extent of change in strength between the connected neurons as compared to baseline strength, e.g., 4× means four times the normal baseline. All the neurons receive random excitatory and inhibitory inputs (not specifically shown).

changes in connectivity between the other neurons were effected as follows. The excitatory external inputs received by the pyramidal cells was increased to four times the normal and the pyramidal cell to pyramidal cell recurrent connectivity was strengthened by eight times. The pyramidal cell to OLM interneuron, pyramidal cell to basket cell and basket to basket interactions were strengthened by four times the baseline connectivity. The output from BC to other cells, that is, BC to OLM and BC to pyramidal cell connectivity were reduced to 50% of that in the baseline network (Fig. 2D).

The changes in synaptic connectivity, induced uniformly across all neurons, were both a modeling simplification as well as a minimal assumption since it is not known exactly what the synaptic weights change *in vivo* or *in vitro* that predispose the hippocampal microcircuits towards epilepsy.

Simulations and Analysis

The simulations were run on a quad core 2.66 GHz Windows 7 based 64-bit system using the NEURON simulator with Python interpreter (Carnevale and Hines, 2006; Hines et al., 2009). A single simulation (5 s, 1,200 neurons) took ~5 min to run with a fixed time step of 0.1 ms. More than 500 simulations were run for this study. The neuronal responses including the local field

potentials were saved as text files for analysis. The data was then imported to the software pClamp v.10 developed by Molecular Devices. The average firing frequency of each type of neuron that was displayed at the end of the simulation was noted. The data was analysed for synchronous activity between the neuron types, cross-correlations, changes in firing rates of individual cell types, theta and gamma frequencies and their power.

RESULTS

Baseline Network Activity

The baseline CA3 neuronal network comprised of pyramidal cells, basket cells, and O-LM interneurons that produced theta modulated gamma oscillations in the local field potentials (LFP), while receiving inputs from Medial Septum (MS). The inhibitory interactions between soma-inhibiting basket cells and pyramidal cells and those between basket cells produced gamma rhythms, while the interactions between pyramidal cells and the dendrite-inhibiting O-LM cells produced theta rhythms (Neymotin et al., 2011). The average firing rates were 2.36 ± 0.024 Hz for pyramidal cells, 16.05 ± 0.15 Hz for basket cells and 0.96 ± 0.027 Hz for O-LM interneurons. Because of medial septum inputs at every 150 ms provided to O-LM and basket cells, a fixed theta frequency of 6.7 Hz was generated in the network. The gamma frequency component of the LFP was ~33 Hz. The basket cells were also equally driven by the MS inputs but the effect of these MS inputs is much lesser due to interactions between basket cells themselves and an increased drive from pyramidal cells.

Scenario 1: effect of reducing dendritic inhibition onto distal dendrites of CA3 pyramidal neurons

All three types of neurons—pyramidal cells, basket cells and O-LM interneurons showed synchronous activity in the network which is similar to baseline activity even when the OLM to pyramidal cell connectivity was completely reduced to 0% (Fig. 3).

With reduction in O-LM to pyramidal cell connectivity, the firing rates of all individual cell types increased. As shown in Table 2 and Figure 4A, there was a significant increase in firing activity in all three cell types when O-LM–pyramidal cell connectivity was <5%. From Table 2, it can be seen that the rate of firing of pyramidal and basket cells almost doubled when there was a total loss of O-LM–pyramidal cell connectivity; 2.36 ± 0.024 Hz at baseline to 4.19 ± 0.04 Hz for pyramidal cells, 16.05 ± 0.15 Hz to 30.98 ± 0.07 Hz for basket cells, while the firing rate of O-LM interneurons almost tripled, from 0.96 ± 0.027 Hz to 2.7 ± 0.034 Hz.

Until connectivity was reduced to 5% between OLM to pyramidal cells (Fig. 4B), the frequency of gamma oscillations remained fairly constant around 32–33 Hz and the frequency of theta oscillations remained nearly constant at 6.7 Hz. These are comparable to the baseline frequencies when there is 100% OLM cell to pyramidal cell connectivity. At total lack of O-LM to pyramidal cell connectivity, the theta oscillations died out due to lack of input from O-LM cells to pyramidal cells.

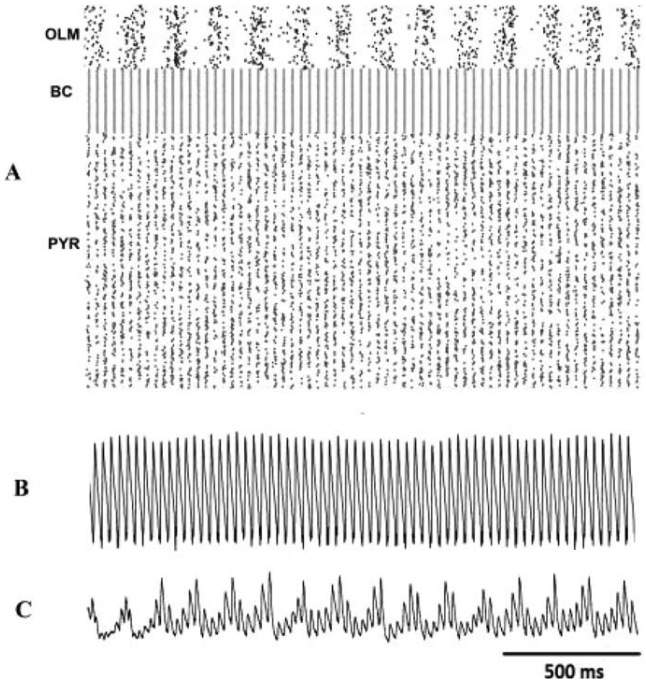

FIGURE 3. (A) Scenario 1, with OLM to pyramidal cell connectivity totally lacking. The pyramidal cell to OLM connectivity is unaffected and hence OLM cells continue to be activated by the pyramidal cells. Because mutual connectivity was between pyramidal and basket cells, only gamma component exists in the local field potential record (B). The baseline activity—theta modulated gamma oscillations, is shown for comparison (C).

As O-LM to pyramidal cell connectivity was reduced, the power of theta and gamma oscillations changed in inverse fashion. The theta power reduced from the baseline of 5.35 $mV^2\ Hz^{-1}$ to 0.95 $mV^2\ Hz^{-1}$ at 5% O-LM–pyramidal cell connectivity and then to 0 power when the connectivity was totally impaired. The gamma power on the other hand increased from a baseline of 2.55 $mV^2\ Hz^{-1}$ to 8.7 $mV^2\ Hz^{-1}$. As seen from Figure 4C, the gamma power remained fairly uniform around 4 $mV^2\ Hz^{-1}$ when the connectivity was between 10 and 40%.

The overall network activity in the form of LFPs showed disappearance of the theta component with reduction in connectivity. Total lack of this connectivity between O-LM–pyramidal cells resulted in high frequency gamma activity with an increase in power.

Scenario 2: effect of increased external inputs received at distal dendrites along with loss of dendritic inhibition

With a successive decrement in dendritic inhibition, a proportional increment in external inputs received through AMPA and NMDA was assumed at the synaptic level. As dendritic inhibition changed from 1× (100%) to 0.8×, 0.6×, 0.4×,

TABLE 2.

Changes in Individual Cell Firing Frequencies, Theta and Gamma Frequencies in the Local Field Potential and the Changes in their Power When Dendritic Inhibition Alone is Reduced

OLM-Pyr Wt	Pyr (Hz)	BC (Hz)	O-LM (Hz)	Theta freq (Hz)	Theta power ($mV^2\ Hz^{-1}$)	Gamma freq (Hz)	Gamma power ($mV^2\ Hz^{-1}$)
1x	2.36 ± 0.024	16.05 ± 0.15	0.96 ± 0.027	6.7	5.35	33.2	2.55
0.8x	2.43 ± 0.026	15.96 ± 0.16	0.98 ± 0.028	6.7	4.6	33.85	1.18
0.6x	2.51 ± 0.027	17.46 ± 0.15	0.95 ± 0.028	6.7	4.2	32.7	1.3
0.4x	2.62 ± 0.03	18.56 ± 0.16	0.95 ± 0.026	6.7	4.1	32	3.7
0.2x	2.76 ± 0.028	19.87 ± 0.15	1.03 ± 0.028	6.7	2.85	32	3.9
0.1x	2.87 ± 0.03	21.62 ± 0.15	1.18 ± 0.03	6.7	1.45	31.5	4.2
0.05x	3.08 ± 0.03	23.17 ± 0.13	1.37 ± 0.034	6.7	0.95	31.1	7.8
0x	4.19 ± 0.04	30.98 ± 0.07	2.7 ± 0.034	0	0	32.4	8.7

As the OLM to pyramidal cell connectivity is reduced, the rate of firing of all the three neuron types increased. The theta frequency has remained constant at 6.7 Hz (except at 0% connectivity), the gamma frequency showed minor variations. With reduction in OLM to pyramidal cell connectivity, the theta power reduced from 5.35 to 0 $mV^2\ Hz^{-1}$ while the gamma power increased from 2.55 to 8.7 $mV^2\ Hz^{-1}$.

0.2×, 0.1×, 0.05×, and 0×, the external inputs received were simultaneously increased from 1× to 1.2×, 1.4×, 1.6×, 1.8×, 1.9×, 1.95×, and 2× (200%), respectively.

All the three types of neurons—pyramidal cells, basket cells, and OLM interneurons showed synchronous activity until the O-LM—pyramidal cell connectivity was reduced to 20%. At 10% connectivity, basket cells had a tighter synchrony among themselves (Fig. 5A). On reducing the connectivity further to 5%, desynchronization was observed among basket cells (Fig. 5B), and at a total lack of O-LM—pyramidal cell connectivity, basket cells became totally desynchronized (Fig. 5C). O-LM cells maintained synchrony with pyramidal cells since the connection from pyramidal cells to OLM cells still existed.

The synchrony between the activities of two arbitrary basket cells (50th and 100th in the network) were analysed when the OLM to pyramidal connectivity was 100, and 0% as described in Scenario 2. Correlation analysis was performed for five seconds and one second of data keeping OLM to pyramidal cell connectivity at 100 and 0%.

When the cross-correlation analysis for five seconds of data was performed, at 100% OLM-Pyramidal cell connectivity, the activity of both basket cells (50th to 100th) had a correlation of 57.7% with a lag time of +0.2 ms, while at 0% connectivity, the correlation was 33.5% with lag time of −0.2 ms. When the cross-correlation analysis for one-second of data was performed, at 100% OLM-pyramidal cell connectivity, the activity of both basket cells had a correlation of 56.5% with a lag time of +0.1 ms and at 0% connectivity, the correlation was 31.3% with lag time of −0.3 ms.

Overall, these data indicate noticeably reduced correlation and hence reduced synchronization in activity between the basket cells at varying connectivities which is around 35% as compared to higher values using different analysis times.

The individual cell firing rates, variations in frequencies and the changes in power of theta and gamma oscillations with changes in connectivity are shown in Figures 6A–C respectively. The individual cell firing frequencies showed a fairly linear increment with decrease in O-LM—pyramidal cell connectivity. The pyramidal cell firing frequency increased from 2.36 ± 0.024 Hz to 6.14 ± 0.054 Hz, the basket cell frequency from 16.05 ± 0.15 Hz to 24.26 ± 0.44 Hz and O-LM frequency from 0.96 ± 0.027 Hz to 4.98 ± 0.035 Hz (Table 3).

The frequency of theta oscillations remained constant at 6.7 Hz due to the strong pacing from MS at this frequency. When the O-LM—pyramidal cell connectivity was 10% and lower the gamma frequency increases from around 33 Hz to 37–38 Hz while the theta power reduces from 5.35 $mV^2\ Hz^{-1}$ to 0. This was due to reduction of dendritic inhibition which reduced the low frequency oscillations. The gamma power on the other hand increases, to a significant level when the O-LM—pyramidal cell connectivity reduced from 20 to 10%. Further, at 5% O-LM—pyramidal cell connectivity, the gamma power drops sharply to 1.6 $mV^2\ Hz^{-1}$ (Fig. 6C).

Because the baseline activity was seen to be significantly altered when the O-LM—pyramidal cell connectivity was reduced to 10%, a special condition was tested whereby the external inputs were increased by eight times over and above the already set increment of 1.9 times. This led to a depolarization block of basket cells, a state where the basket cells are not able to fire action potentials due to excessive drive from the pyramidal cells, and the output local field potentials showed a response characteristic of epileptic activity (Fig. 7). The individual cell firing frequencies before depolarization block of basket cells were 10.45 ± 0.098 Hz for pyramidal cells, 44.2 ± 0.24 Hz for basket cells and 11.52 ± 0.07 Hz for O-LM interneurons. After depolarization block of basket cells, the firing rates were 19.09 ± 0.09 Hz for pyramidal cells and 18.56 ± 0.026 Hz for O-LM interneurons. These simulated epileptic activities are comparable to published experimental results [Cymerblit-Sabba and Schiller, 2012, Fig. 2, p. 1721—Ictal Phase-I); Isaev et al., 2007; Fig. 6B-b (left panel), p. 216)].

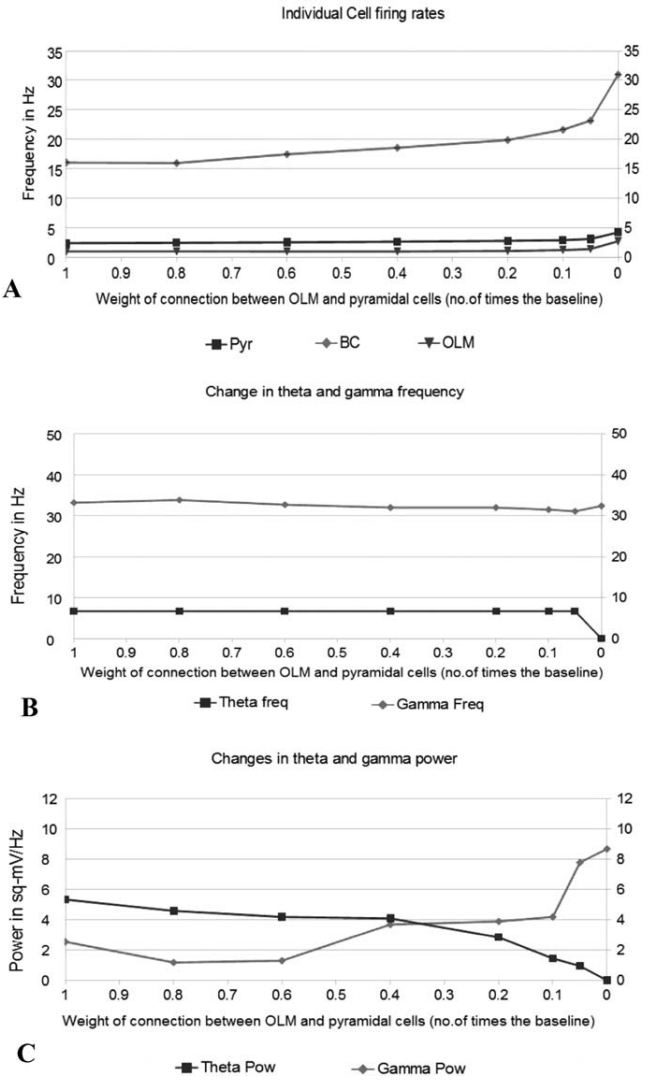

FIGURE 4. (A) Changes in firing rate of individual cell types with decrease in dendritic inhibition. The firing rates of all cells, especially basket cells show marked increase when OLM-Pyr connectivity lowers to 5%. (B) Changes in theta and gamma frequencies with decrease in dendritic inhibition, and (C), changes in theta and gamma power. In all figures *x*-axis shows the weight of connection between OLM and Pyramidal cells (e.g., OLM-Pyr wt 0.4 means 40% of baseline). The error bars are not visible since the range of error is extremely small compared to the values generated.

Scenario 3: effect of changes in connectivity at all synapses in the network

We simulated two conditions in this scenario: O-LM interneuron to pyramidal cell connectivity was first reduced to 50% and then to 30% (70% impairment of dendritic inhibition). The changes in the weights of connectivity between the cells are shown in Figs. 2C,D, respectively.

With reduction in O-LM to pyramidal cell connectivity to 50% of the baseline, the firing rates for pyramidal, basket and O-LM cells changed from baseline values to 1.93 ± 0.022 Hz, 10.58 ± 0.24 Hz, and 3.52 ± 0.034 Hz, respectively. The theta and gamma frequency components were 6.8 and 34.9 Hz, respectively and their powers were 0.4 $mv^2\ Hz^{-1}$ and 0.36 $mv^2\ Hz^{-1}$ respectively. The baseline theta modulated gamma oscillations were disrupted as basket cells lost synchrony with other neurons in the network (Fig. 8).

When the OLM to pyramidal cell connectivity was reduced to 30% (70% impairment of dendritic inhibition), with changes in connectivity between other neurons (see Methods), the basket cells entered depolarization block and the network activity showed a pattern characteristic of epileptic activity (ictal-tonic) as seen from the simulated local field potentials (Fig. 9A). The corresponding raster plot is shown in Figure 9B. This is comparable to published experimental results (Isaev et al., 2007; Cymerblit-Sabba and Schiller, 2012). From Figure 10, it can be noted that there was an increment in the inputs that are received at the distal dendritic compartment of pyramidal cells.

As shown in Table 4, the firing rates for pyramidal, basket and O-LM cells before entering depolarization block of basket cells were 3.14 ± 0.06 Hz, 13.9 ± 0.39 Hz, and 11.6 ± 0.11 Hz, respectively. The theta and gamma frequency components were 10 and 32.65 Hz, respectively and their powers 0.175 and 0.0075 $mv^2\ Hz^{-1}$, respectively. After the depolarization block of basket cells, the firing rates of pyramidal and OLM cells more than doubled to 7.17 ± 0.034 Hz and 23.8 ± 0.054 Hz. The theta frequency remained at 10 Hz while its power increased to 5.4 $mv^2\ Hz^{-1}$. Because the basket cells were inactive, the gamma frequency power components were absent.

The effect of calcium-mediated potassium currents I_{KCa} on the bursting activity were studied since they could play a role in burst termination via contribution to hyperpolarization. To study this, we performed a set of simulations, changing the conductance of calcium-mediated potassium currents, gI_{KCa}. In our model this parameter was applicable to OLM interneurons. When gI_{KCa} of OLM interneruons was reduced from 10 to 5 mS cm^{-2} in scenario 3, while keeping the changes made in the connectivity the same, it resulted in abolishing of the depolarization block of basket cells, but the baseline activity was not restored. Increasing this current conductance to 15 mS cm^{-2} led to depolarization block of basket cells setting in at the beginning of the simulation itself leading to ictal-tonic activity that was observed earlier (which was about 1.3 s after the start of the simulation).

DISCUSSION

We used a computer model to investigate how impairment of dendritic inhibition of pyramidal neurons of the highly vulnerable CA3 subfield of hippocampus leads to hyperexcitability, a characteristic feature of epileptic activity. The baseline activity generated by the network was theta modulated gamma oscillations. The theta oscillations are significant in spatial navigation and motor behaviour and gamma oscillations in learning, memory encoding and retrieval. Though they are generated

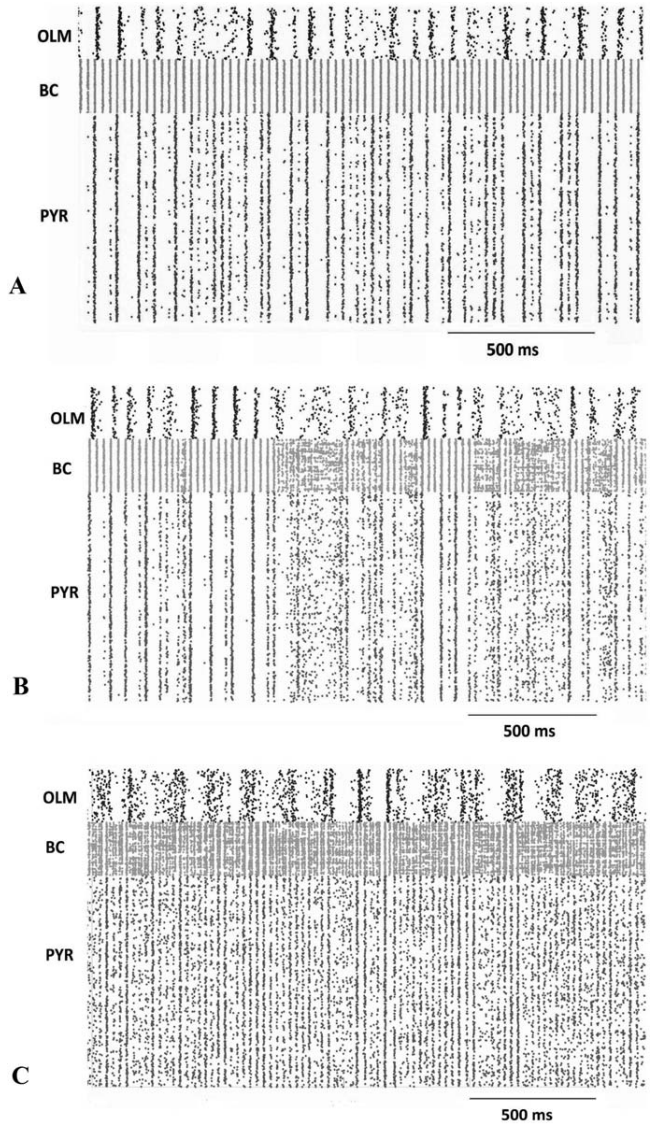

FIGURE 5. Synchrony between the neuron types when strength of OLM—Pyr connectivity is 10% (A), 5% (B), and 0% (C). At 10% connectivity, all the cell types showed synchronous activity; at 5% connectivity, BC starts to undergo desynchrony. At 0%, the basket cells show total lack of synchrony while, OLM and Pyr cells still maintain synchronous activity since the Pyr to OLM connection is unaffected.

independently by different cell assemblies, they are observed to co-occur in a synchronized manner in field potential records (Colgin and Moser, 2010). In our work, impairment of dendritic inhibition was simulated by reducing the strength of connection between O-LM interneurons and pyramidal cells.

Model Assumptions and Observations

Three scenarios were simulated in our model to study impaired dendritic inhibition that could lead to the generation of epileptic activity. First was reducing dendritic inhibition to the pyramidal cells without making any other changes in the network. Second, the external excitatory inputs received at the distal dendrites of pyramidal cells were increased assuming this to be a consequence of reduced dendritic inhibition from the

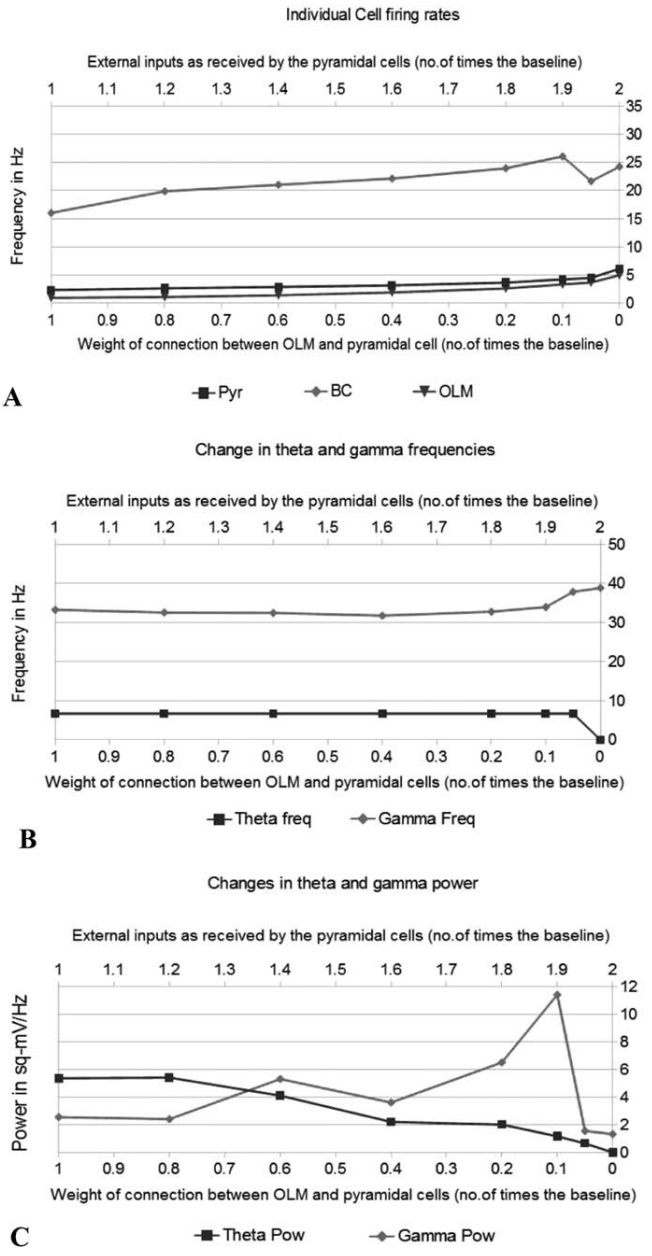

FIGURE 6. Scenario 2, when the external inputs are increased along with decrement in dendritic inhibition. (A), changes in the firing rates of individual cell types. (B) and (C), changes in theta and gamma frequencies and (C), changes in theta and gamma power. The parameters seem to undergo notable change at 10% connectivity between OLM and pyramidal cells. For details refer text. In all figures the bottom line *x*-axis shows the weight of connectivity between OLM and pyramidal cells (e.g., OLM-Pyr wt 0.4 means 40% of baseline) and top line *x*-axis shows the degree of external inputs received by the pyramidal cells (e.g., 1.4 means 40% more than the baseline). The error bars are not visible since the range of error is extremely small compared to the values generated.

TABLE 3.

Changes in Individual Cell Firing Frequencies, Theta and Gamma Frequencies in the Local Field Potential and the Changes in Their Power When Dendritic Inhibition is Reduced and External Inputs Received by the Pyramidal Cells are Increased Simultaneously

OLM-Pyr Wt	External Wt	Pyr (Hz)	BC (Hz)	O-LM (Hz)	Theta freq (Hz)	Theta power ($mV^2\ Hz^{-1}$)	Gamma freq (Hz)	Gamma power ($mV^2\ Hz^{-1}$)
1x	1x	2.36 ± 0.024	16.05 ± 0.15	0.96 ± 0.027	6.7	5.35	33.2	2.55
0.8x	1.2x	2.66 ± 0.029	19.88 ± 0.14	1.11 ± 0.03	6.7	5.4	32.5	2.4
0.6x	1.4x	2.9 ± 0.03	21.04 ± 0.15	1.42 ± 0.03	6.7	4.1	32.4	5.3
0.4x	1.6x	3.19 ± 0.033	22.15 ± 0.15	1.93 ± 0.03	6.7	2.2	31.7	3.6
0.2x	1.8x	3.67 ± 0.036	23.97 ± 0.15	2.64 ± 0.036	6.7	2	32.7	6.5
0.1x	1.9x	4.24 ± 0.038	26.08 ± 0.15	3.35 ± 0.034	6.7	1.16	33.9	11.4
0.05x	1.95x	4.5 ± 0.04	21.68 ± 0.25	3.69 ± 0.033	6.7	0.65	37.8	1.55
0x	2x	6.14 ± 0.054	24.26 ± 0.44	4.98 ± 0.035	0	0	38.8	1.32

As the OLM to pyramidal cell connectivity is reduced along with increase in external inputs received by the pyramidal cells, the rate of firing of pyramidal and OLM cells increased while that of basket cells showed an initial increase and then a decrease. While the theta frequency remained constant at 6.7 Hz (except at 0% connectivity), the gamma frequency varied from 33.2 Hz at 100% connectivity to 38.8 Hz at 0% connectivity. With reduction in OLM to pyramidal cell connectivity, the theta power reduced from 5.35 to 0 $mV^2\ Hz^{-1}$ while the gamma power increased from 2.55 at 100% connectivity to 6.5 $mV^2\ Hz^{-1}$ at 20% connectivity and then dropped to 1.32 $mV^2\ Hz^{-1}$ at 0% connectivity.

OLM neurons. A linear relationship between reduced dendritic inhibition and increased external excitatory inputs was assumed for the purpose of the model since no supporting literature was available as to how these two are related. Third, along with the above changes in the second scenario, strength of connection between the different neuron types was also modified. These scenarios were separately simulated to study the response of the network with step-wise changes in the input and connectivity parameters and to determine to what extent of connectivity as well as input changes, would lead to epileptic activity. Medial Septal inputs were available to OLM interneurons and basket cells in the network at every 150 ms in all the three scenarios. These rhythmic inputs paced the theta oscillations in the baseline network. Our study shows that the theta rhythm is resilient to modifications in the network circuitry, partially due to the strong pacing provided to the interneurons from the medial septal inputs.

In the first scenario, where the dendritic inhibition caused by the O-LM interneurons was reduced without making any other changes in the network, the pyramidal cells were disinhibited and showed increased activity as evident from their increased firing rates. This also resulted in increased activity of basket cells and O-LM cells which receive inputs from pyramidal cells. The increased activity of basket cells increased the gamma power component while the decreased influence of O-LM interneurons reduced the theta component in the LFP. The overall network activity in the form of LFP showed disruption of baseline activity.

In the second scenario, changes were made to the external inputs as received at the distal apical dendritic compartments of the pyramidal cells. These are the excitatory inputs received from extra-hippocampal areas, predominantly from entorhinal cortex. The pyramidal cells showed an increase in their activity as evidenced from their increased firing rates. The basket cells being connected to pyramidal cells, also increased their activity but to a lower extent when compared to the previous situation (first scenario). This could be due to the increased mutual GABAergic inhibition (Cutsuridis et al., 2010) of the basket cells. On the other hand, the O-LM interneurons were much more activated by the enhanced pyramidal cell output in comparison to the first scenario.

The reduction of O-LM to pyramidal cell connectivity to 10% takes on particular significance. This resulted in change in frequency and power of the gamma oscillations. When the connectivity was reduced from 20 to 10% the gamma frequency increased from 33 Hz to ~38 Hz and the power increased from 6.5 to 11.4 $mV^2\ Hz^{-1}$. This could be due to tighter synchrony of the basket cells. When this connectivity was further reduced and external inputs received by pyramidal cells increased, the basket cells lost their synchrony and the gamma power sharply dropped to 1.55 $mV^2\ Hz^{-1}$.

At 10% O-LM-pyramidal cell connectivity, when the external excitatory inputs were increased to 15 times the baseline, the basket cells entered into depolarization block. The overall network response (LFP) showed an ictal-tonic pattern, a characteristic feature of epileptic activity. It shows that at this connectivity, a much higher input from extra-hippocampal regions could trigger abnormal network activity. The main source of external inputs to CA3 subfield of hippocampus is the entorhinal cortex which in turn receives input from different cortical areas (Amaral, 1993; Witter, 2007). Hence, higher inputs such as visual or auditory stimuli could perhaps potentially trigger hyperactivity in the vulnerable hippocampus (Manganotti et al., 1998; Seddig and Vogt, 1999).

In the third scenario additional changes were assumed to occur at synapses in the network. Because of decreased dendritic inhibition, the external inputs received by the pyramidal cells were increased. A recording from the distal apical dendritic compartment of the pyramidal neurons confirms this increase. Occasionally, the inputs received were so enhanced

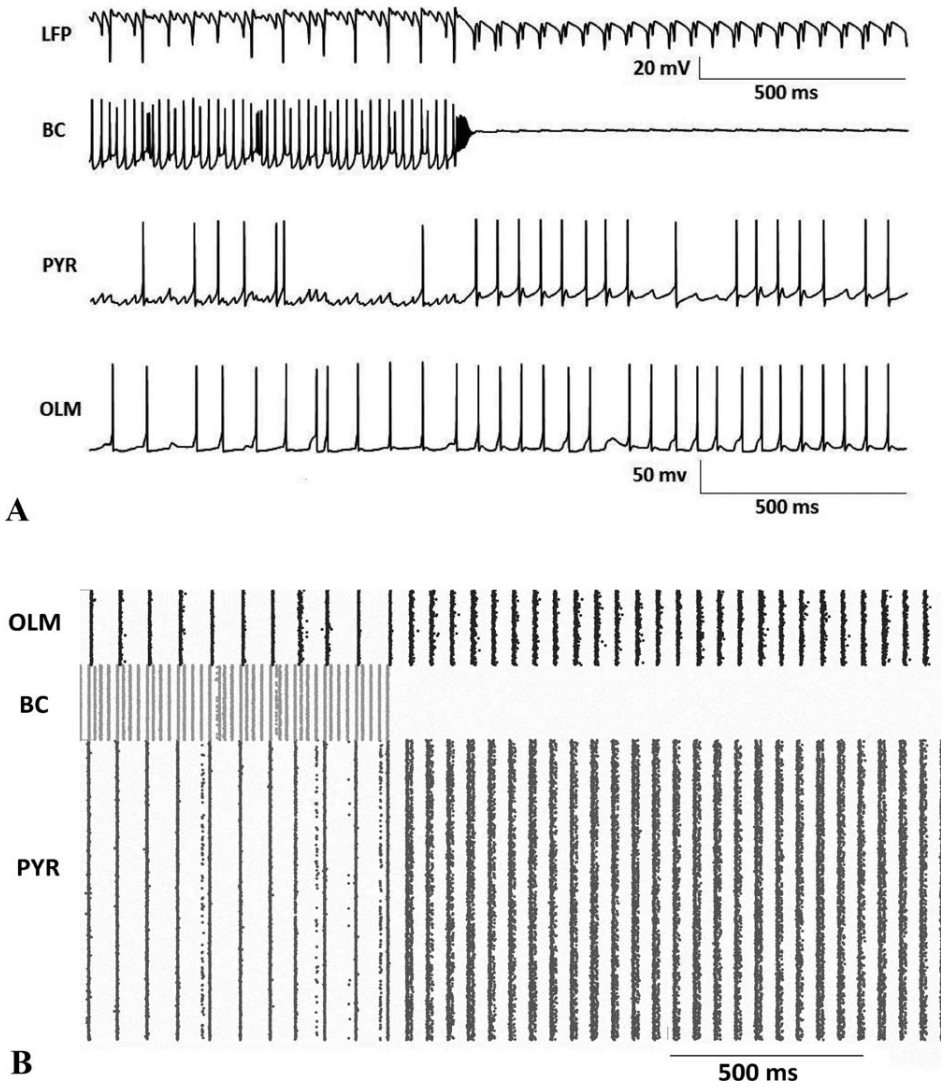

FIGURE 7. (A) Basket Cells (BC) enters depolarization block when the external inputs are significantly increased (about 15 times the basline) at a reduced OLM-Pyr connectivity of 10%. Consequently the LFP shows a characteristic ictal activity. The OLM and Pyramidal cells show synchronous activity during this phase. (B) Raster Plot.

that a short period of tetanic response was observed in these records (Fig. 10). The high degree of mutually recurrent CA3 pyramidal cells drove the connected basket cells and O-LM cells. The inhibitory inputs received by pyramidal neurons from basket cells decreased since there was enhanced mutual inhibition between the basket cells. This led to further disinhibition of pyramidal cells resulting in an overall increase in excitatory activity in the network. The changes in connectivity were such that excitatory responses were much higher than inhibitory responses, effectively creating an excitation-inhibition imbalance.

In this condition, where the O-LM—pyramidal cell connectivity was reduced to 50% and changes made accordingly at other synapses, there was a notable change in the network activity. The basket cells were seen to lose complete synchrony in the network. Presumably, the network activity had entered a stage of transition to characteristic epileptic response. When the O-LM—pyramidal cell connectivity was reduced to 30% (70% impairment of dendritic inhibition), the basket cells entered the state of depolarization block and a pattern characteristic of ictal-tonic activity was observed in the LFP. Compared to the first and second scenarios where only the O-LM—pyramidal connectivity was changed, the third scenario alone generated a characteristic pathological activity at a comparatively earlier stage, i.e., at 30% O-LM-Pyramidal connectivity. The end result is comparable to the ictal activity that has been reported in the literature (Isaev et al., 2007; Cymerblit-Sabba and Schiller, 2012).

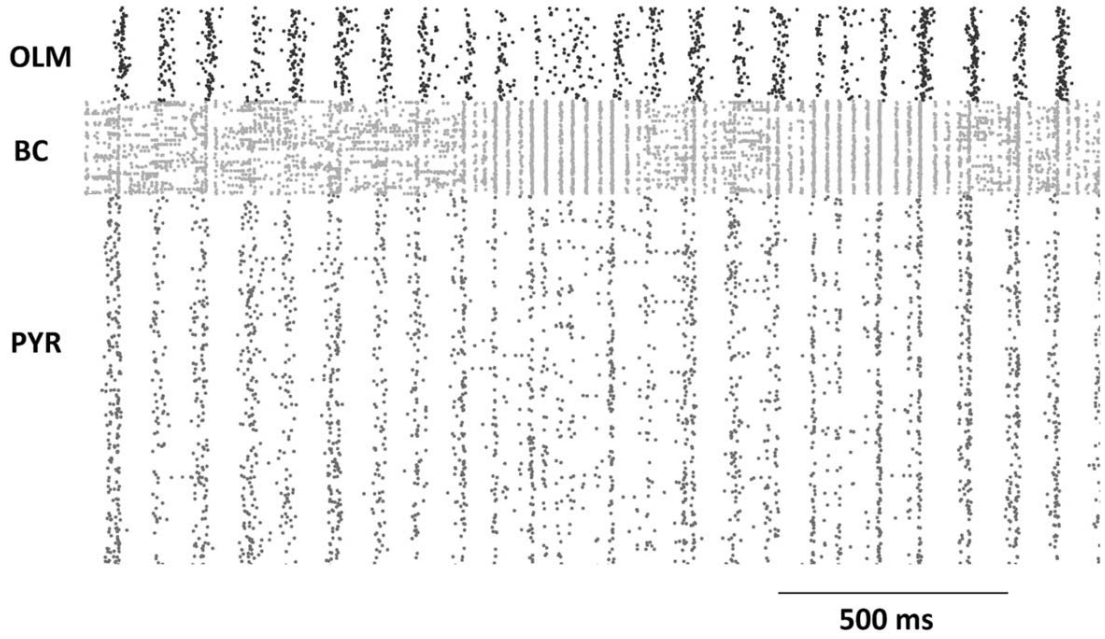

FIGURE 8. Scenario 3 with 50% OLM to Pyramidal connectivity (50% impairment of dendritic inhibition). The basket cells are seen to show intermittent desynchrony with other cell types while OLM and Pyramidal Cells show synchronous activity.

Network Changes Leading to Epileptic Activity Generation

When the dendritic inhibition alone was reduced, and no changes were effected at any other synapse in the network (Scenario 1), there was a change from the theta-modulated gamma pattern at baseline to a full gamma pattern. In addition to this, when we gradually increased the external excitatory inputs received at the distal dendritic compartment of pyramidal cells (Scenario 2), a notable change in the network response was observed at 10% O-LM-Pyramidal cell connectivity. At the point where the external excitatory inputs received by pyramidal cells was increased to about 15 times the baseline, the basket cells entered a state of depolarization block due to the high excitatory drive they received from the pyramidal cells. The residual connectivity between the pyramidal and O-LM cells generated a synchronous ictal activity pattern.

The depolarization block of basket cells was observed to contribute to the ictal-tonic pattern of activity in the final set of simulations where changes were effected across all synapses in the network. The comparison of the firing rates of pyramidal cells before and after depolarization block of basket cells in the second scenario (10.45 ± 0.098 Hz and 19.09 ± 0.09 Hz) and third scenario (3.14 ± 0.06 Hz and 13.9 ± 0.39 Hz) shows an interesting fact. The firing rate of pyramidal cells after the depolarization block of basket cells in the third scenario (where overall network changes by varying the synaptic strengths at all synapses were simulated), is less than the firing rate of pyramidal cells in the second scenario (where only external inputs were increased along with decrement in dendritic inhibition) before the depolarization block of basket cells. The third scenario refers to the plasticity that has occurred at connections between all the neurons in the network. The second scenario refers to the increased external inputs received by the pyramidal cells without any other potentiation of activity between neurons. It is also noted that in the third scenario, the depolarization block of basket cells sets in about 1.3 s after the start of simulation while in the second scenario, it set in about 1.45 s after the start of simulation. Hence, synaptic plasticity which could include axonal and dendritic sprouting, have significant contribution to pathological states like temporal lobe epilepsy. Situations like traumatic brain injury and cerebral ischemia can lead to loss or impairment of neuronal activity. Epileptic activity has been observed to be common in these incidents.

The enhancement of neuronal activity and hence potentiation of network activity is observed in different models of epileptic activity generation. Leite et al. (2005) describes many experimental studies related to enhancement of synaptic strength leading to epileptic activity generation in the temporal lobe including hippocampus. Similarly, McAllistair et al. (2000) describes about the enhancement of activity in neuronal networks due to sprouting at dendrites which have implications in epileptic activity generation. Cook and Bliss (2006) have discussed in their review article as to how enhancement of neuronal connectivity (long-term potentiation) leads to epileptic activity generation in the human central nervous system. Presumably, the network changes in the brain occur at a gross level across various neuronal circuits than at specific connections, leading to faster generation of pathological states like epilepsy.

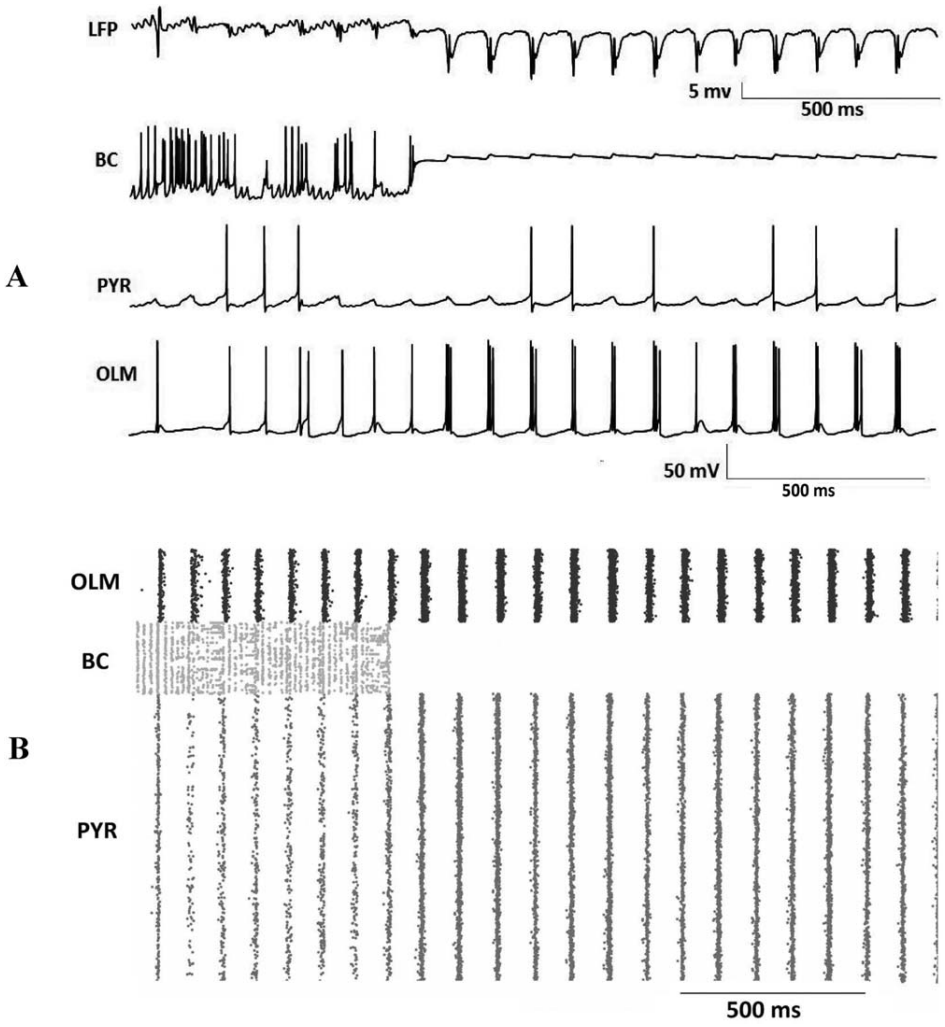

FIGURE 9. Scenario 3 with 30% OLM to Pyramidal connectivity (70% impairment of dendritic inhibition). (A) The basket cells are seen to enter a state of depolarization block and consequently the LFP shows a characteristic ictal activity. The OLM and Pyramidal Cells continue to show synchronous activity. (B) Raster plot.

Depolarization Block of Basket Cells

In our study, depolarization block of basket cells is the main factor that leads to the pathological state in the CA3 network for which a significant contributor is the enhanced activation of pyramidal cells due to dendritic disinhibition. Basket cell inactivation in neuronal networks could also lead to pathological states. The basket cells entering into state of depolarization block could be due to various reasons (Karlocai et al., 2014). One reason is basket cell perisomatic organization which facilitates a much faster activation due to the increased activity of pyramidal cells. Second, they receive a much higher synaptic input from recurrently connected pyramidal cells. Third, K^+ channel mediated hyperpolarizing currents and M-currents are absent in basket cells. In the experimental work by Karlocai et al. (2014), depolarization block of basket cells were observed in three epileptogenic treatments—high extracellular potassium, zero-magnesium, and addition of 4-amino-pyridine in hippocampal CA3 subfield. It was observed that the cell firing of pyramidal cells and interneurons in the network increased during these treatments which eventually led to depolarization block of basket cells due to the high excitation received by them as compared to other neurons in the network. The dendrite-inhibiting interneurons and the pyramidal cells continued to fire after the basket cells entered depolarization block.

Inactivation of basket cells occurring due to mossy cell loss has been reported to lead to epileptic activity in studies on the dentate gyrus network (Sloviter, 1991; Shang and Buckmaster, 2009). Here, the excitations received by basket cells are reduced due to loss of mossy cells causing basket cells to be dormant. However, the correctness of this concept termed the dormant basket cell hypothesis is debated (Sloviter et al.,

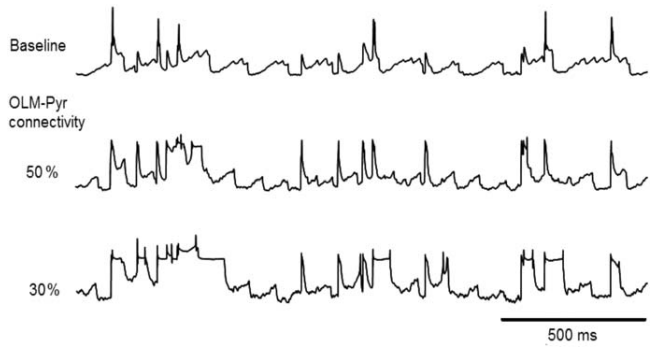

FIGURE 10. Inputs received by the distal dendritic compartment of a representative pyramidal neuron from external sources at baseline connectivity, 50% OLM to pyramidal cell connectivity (50% impairment of dendritic inhibition) and 30% OLM to pyramidal cell connectivity (70% impairment of dendritic inhibition). The increase in the received inputs is clear from the figures, especially at 30% OLM to pyramidal cell connectivity where it is seen to lead to tetanic states intermittently at the distal dendritic compartment.

2003). Basket cell dysfunction and hence reduced inhibition of pyramidal cells due to deficient GABA release has been implicated in psychological disorders like schizophrenia (Curley and Lewis, 2012).

Depolarization block could be caused by various other factors and involvement of other neurons in the network. Studies using 4-aminopyridine combined with low-magnesium model of epilepsy showed that the epileptic activity in the hippocampal CA1 network was caused by the depolarization block of O-LM interneurons. Further inhibitory spike generation in these neurons was suppressed leading to an ictal-like activity in the network (Zyburkus et al., 2006).

High extracellular potassium combined with low extracellular calcium can also lead to depolarization block in neuronal networks since low extracellular calcium enhances persistent sodium currents in neurons (Su et al., 2001). The enhanced activity of neurons leads to higher levels of extracellular potassium (Bikson et al., 2003). This enhances reversal potentials of potassium currents and influences the conductance of hyperpolarization-activated currents and persistent sodium currents further. The study further shows that suppression of activity of pyramidal cells led to the ictal activity pattern in the network. The above mentioned studies show that the suppression of activity of neurons other than basket cells could lead to the same pathological state that we have observed in our simulations.

Comparison With Other Models

Models developed earlier have studied roles of specific currents and conductances in the generation of epileptic activity. Moreover, there have been fewer computational models of CA3, compared to that of CA1 subfield, though CA3 in many experimental studies is the primary area of epileptiform activity generation in the temporal lobe. This relative lack of CA3 models is probably due to the highly heterogeneous patterns of neuronal connectivity within CA3 as well as lack of exact information regarding the biophysical parameters. Usual attempts have been to incorporate the parameter values applicable to CA1 neurons and then modifying them to simulate the patterns observed from CA3 experimentally (e.g., Lazarewicz et al., 2002). Our model generates characteristic theta-modulated gamma oscillations as the baseline activity which is observed to undergo significant changes in activity when changes in network connectivity and input conditions are simulated.

Many studies have attempted to explain how the excitation-inhibition balance in neuronal networks leads to abnormal activity patterns, a characteristic feature of pathological conditions (Wittner et al., 2005; El-Hassar et al., 2007). Our work shows that inhibitory activity is compromised in the network. We have also been able to demonstrate that a particular extent of impairment of inhibition makes the network hyperexcitable. Changes in strength of connection (long term potentiation and depression) are known to occur at synapses between various neurons in networks. Our model shows that this causes hyperactivity in the network at an earlier point in time, as compared to other changes in the network. The strength of our study is that with the proposed set of network changes, we were able to simulate hyperactivity in the network which is comparable with experimental results. We have also been able to demonstrate and propose a threshold of connectivity changes that lead to pathological activity.

Limitations and Future Work

In our study, we have used an accepted computational model of CA3 network which successfully generates theta-modulated

TABLE 4.

Changes in Different Parameters With Changes in the Overall Network

OLM-Pyr connection	Pyr (Hz)	BC (Hz)	OLM (Hz)	Theta-freq (Hz)	Theta power ($mv^2\ Hz^{-1}$)	Gamma freq (Hz)	Gamma power ($mv^2\ Hz^{-1}$)
1x	2.36 ± 0.024	16.05 ± 0.15	0.96 ± 0.027	6.7	5.35	33.2	2.55
0.5 x	1.93 ± 0.022	10.58 ± 0.24	3.52 ± 0.034	6.8	0.4	34.9	0.36
0.3 x (before DB)	3.14 ± 0.06	13.9 ± 0.39	11.6 ± 0.11	10	0.175	32.65	0.0075
0.3 x (after DB)	7.17 ± 0.034	0	23.8 ± 0.054	10	5.4	0	0

When the basket cells enter depolarization block and stop firing, the gamma component reduces to zero.

gamma oscillations as the baseline activity (Neymotin et al., 2011). The individual neuron types in this model contain several biophysical parameters which are comparable to those incorporated in models of other neurons and networks which display normal physiology. A number of such models can be obtained from ModelDB (https://senselab.med.yale.edu/modeldb). Adding more biophysical parameters in these models including ours could help to simulate the neurophysiology of the network in much more detail.

Similar to other computational models, this work also has its limitations. Though there are a number of experimental studies on epileptic activity generation in different areas of the brain, the exact mechanisms of epileptic activity generation or how a network of neurons becomes epileptic is not understood. In this work, we had to make assumptions as to how the external excitatory inputs received by pyramidal neurons undergo changes with stepwise decrement in dendritic inhibition. These along with changes in network connectivity were tested systematically.

Our model takes into consideration two main inhibitory mechanisms—somatic and dendritic through two prominent set of neurons, the basket cells and OLM interneurons respectively. Various other interneurons also are part of this anatomical network in vivo, which have not been included in the model. Although pyramidal to OLM and pyramidal to basket neuron synapses are facilitative and depressive, respectively (e.g., Sylwestrak and Ghosh, 2012), the extra complexity of these types of plasticity was left out in our model so that the effects of modulating synaptic weights could be studied in a more controlled setting.

Because hippocampal CA3 subfield plays a significant role in learning, memory encoding and retrieval, cognitive processes, and spatial navigation, the changes in the network could potentially lead to impairment of these processes in an affected individual. In the future, studies could be performed to quantify the extent of impairment of dendritic inhibition and validate whether and to what extent of impairment could lead to generation of abnormal activity. How the oscillation signals in the network change in relation to network modifications in pathological states could be another interesting area of research. A significant future challenge is to devise methods to control the epileptic activity generation. Our model suggests that therapies designed to restore lost excitatory-inhibitory balance would be particularly promising in reducing pathological dynamics. Hence, the potential of computational studies combined with future experiments is quite promising to advance our present knowledge and develop therapeutic strategies for neurodegenerative disorders.

REFERENCES

Barbarosie M, Avoli M. 2003. CA3-driven hippocampal-entorhinal loop controls rather than sustains in vitro limbic seizures. J Neurosci 17:9308–9314.

Bihi I, Jefferys R, Vreugdenhil JGRM. 2005. The role of extracellular potassium in the epileptogenic transformation of recurrent GABAergic inhibition. Epilepsia 46 (Suppl 5):64–71.

Bikson M, Hahn PJ, Fox JE, Jeffreys JGR. 2003. Depolarization block of neurons during maintenance of electrographic seizures. J Neurophysiol 90:2402–2408.

Borhegyi Z, Varga V, Szilágyi N, Fabo D, Freund TF. 2004. Phase segregation of medial septal GABAergic neurons during hippocampal theta activity. J Neuroscience 24:8470–8479.

Buhl EH, Halasy K, Peter Somogyi P. 1994. Diverse sources of hippocampal unitary inhibitory postsynaptic potentials and the number of synaptic release sites. Nature 368:823–828.

Carnevale NT, Hines ML. 2006. The NEURON Book. Cambridge, UK: Cambridge University Press.

Cobb SR, Halasy K, Vida KI, Nyiri G, Tamas G, Buhl EH, Somogyi P. 1997. Synaptic effects of identified interneuronsv innervating both interneurons and pyramidal cells in the rat hippocampus. Neuroscience 79:629–648.

Colgin LL, Moser EI. 2010. Gamma oscillations in the hippocampus. Physiology 25:319–329.

Cooke SF, Bliss TVP. 2006. Plasticity in the human central nervous system. Brain 129:1659–1673.

Cossart R, Dinocourt C, Hirsch JC, Merchan-Perez A, De Felipe J, Ben-Ari Y, Esclapez M, Bernard C. 2001. Dendritic but not somatic GABAergic inhibition is decreased in experimental epilepsy. Nat Neurosci 4:52–62.

Curley AA, Lewis DA. 2012. Cortical basket cell dysfunction in schizophrenia. J Physiol 590(Pt4):715–724.

Cymerblit-Sabba A, Schiller Y. 2012. Development of hypersynchrony in the cortical network during chemoconvulsant-induced epileptic seizures in vivo. J Neurophysiol 107:1718–1730.

Dinocourt C, Petanjek Z, Freund TF, Ben-Ari Y, Esclapez M. 2003. Loss of interneurons innervating pyramidal cell dendrites and axon initial segments in the ca1 region of the hippocampus following Pilocarpine-induced seizures. J Comp Neurol 459:407–425.

Dragoi G, Carpi D, Recce M, Csicsvari J, Buzsáki G. 1999. Interactions between hippocampus and medial septum during sharp waves and theta oscillation in the behaving rat. J Neurosci 19:6190–6199.

Dzhala VI, Staley KJ. 2003. Transition from interictal to ictal activity in limbic networks in vitro. J Neurosci 23:7873–7880.

Dudek EF, Stanley KJ. 2007. How does the balance of excitation and inhibition shift during epileptogenesis? Epilepsy Curr 7:86–88.

El-Hassar L, Milh M, Wendling F, Ferrand N, Esclapez M, Bernard C. 2007. Cell domain-dependent changes in the glutamatergic and GABAergic drives during epileptogenesis in the rat ca1 region. J Physiol 578:193–211.

Furman M. 2013. Seizure initiation and propagation in the pilocarpine rat model of temporal lobe epilepsy. J Neurosci 33:16409–16411.

Gloveli T, Dugladze T, Rotstein HG, Traub RD, Monyer H, Heinemann U, Whittington MA, Kopell NJ. 2007. Orthogonal arrangement of rhythm-generating microcircuits in the hippocampus. Proc Natl Acad Sci USA 102:13295–13300.

Hines ML, Davison AP, Muller E. 2009. NEURON and python. Front Neuroinform 3:2009.

Jahr CE, Stevens CF. 1990. Voltage dependence of NMDA-activated macroscopic conductances predicted by single-channel kinetics. J Neurosci 10:3178–3182.

Jung S, Warner LN, Pitsch J, Becker AJ, Poolos NP. 2011. Rapid loss of dendritic HCN channel expression in hippocampal pyramidal neurons following status epilepticus. Neuroscience 31:14291–14295.

Karlocai MR, Kohus Z, Kali S, Ulbert I, Mate SG, Freund Z, Gulyas TFAI. 2014. Physiological sharp wave-ripples and interictal events in vitro: What's the difference? Brain 137:463–485.

Kurz JE, Moore BJ, Henderson SC, Campbell JN, Churn SB. 2008. A cellular mechanism for dendritic spine loss in the pilocarpine model of status epilepticus. Epilepsia 49:1696–1710.

Lazarewicz MT, Migliore M, Ascoli GA. 2002. A new bursting model of ca3 pyramidal cell physiology suggests multiple locations for spike initiation. BioSystems 67:129–137.

Leite JP, Neder L, Arisi GA, Carlotti CG Jr, Assirati A, Moreira E. 2005. Plasticity, synaptic strength, and epilepsy: What can we learn from ultrastructural data? Epilepsia 46(Suppl 5):134–141.

Lytton WW. 2008. Computer modelling of epilepsy. Nat Rev Neurosci 9:626–637.

Lytton WW, Orman R, Stewart M. 2005. Computer simulation of epilepsy: Implications for seizure spread and behavioral dysfunction. Epilepsy Behav 7:336–344.

Magloczky Z, Freund TF. 2005. Impaired and repaired inhibitory circuits in the epileptic human hippocampus. Trends Neurosci 28: 334–340.

Manganotti P, Miniussi C, Santorum E, Tinazzi M, Bonato C, Marzi CA, Fiaschi A, Bernardina DB and, Zanette G. 1998. Influence of somatosensory input on paroxysmal activity in benign rolandic epilepsy with "extreme somatosensory evoked potentials." Brain 121:647–658.

McAllistair KA. 2000. Cellular and molecular mechanisms of dendritic growth. Cerebr Cortex 10:963–973.

Middleton S, Jalicsb J, Kisperskyc T, LeBeaua FEN, Roopuna AK, Kopelld NJ, Whittington MA, Cunningham MO. 2008. NMDA receptor-dependent switching between different gamma rhythm-generating microcircuits in entorhinal cortex. Available at: www.pnas.org/cgi/doi/10.1073/pnas.0809302105

Mora GN, Bramanti P, Osculati F, Chakir A, Nicolato E, Marzola P, Sbarbati A, Fabene PF. 2009. Does pilocarpine-induced epilepsy in adult rats require status epilepticus? PlosOne 4:e5759.

Neymotin SA, Lazarewicz MT, Sherif M, Contreras D, Finkel LH, Lytton WW. 2011. Ketamine disrupts theta modulation of gamma in a computer model of hippocampus. J Neurosci 31:11733–11743.

Ren H, Shi Y-J, Lu Q-C, Liang P-J, Zhang P-M. 2014. The role of the entorhinal cortex in epileptiform activities of the hippocampus. Theor Biol Med Model 11:14.

Stoop R, Etienne P. 2000. Functional connections and epileptic spread between hippocampus, entorhinal cortex and amygdala in a modified horizaontal slice preparation of the rat brain. Eur J Neurosci 12:3651–3663.

Rutecki PA, Yang Y. 1998. Ictal epileptiform acitivity in the ca3 region of hippocampal slices produced by pilocarpine. J Neurophysiol 79: 3019–3029.

Seddigh S, Thomke F, Vogt TH. 1999. Complex partial seizures provoked by photic stimulation. J Neurol Neurosurg Psychiatry 66: 801–802.

Sloviter RS, Zappone CA, Harvey BD, Bumanglag AV, Bender RA, Frostscher M. 2003. "Dormant basket cell" hypothesis revisited: Relative vulnerabilities of dentate gyrus mossy cells and inhibitory interneurons after hippocampal status epilepticus in the rat. J Comp Neurol 459:44–76.

Stewart M, Fox SE. 1990. Do septal neurons pace the hippocampal theta rhythm? Trends Neurosci 13:163–168.

Sylwestrak EL, Ghosh A. 2012. Elfn1 regulates target-specific release probability at CA1-interneuron synapses. Science 338:536–540.

Whittington MA, Traub RD, Jefferys JGR. 1995. Erosion of inhibition contributes to the progression of low magnesium bursts in rat hippocampal slices. J Physiol 486:723–734.

Witter MP. 2007. Intrinsic and extrinsic wiring of ca3: Implications for connectional heterogeneity. Learn Mem 14:705–713.

Wittner L, Eross L, Czirjak S, Halász P, Freund TF, Maglóczky ZS. 2005. Surviving ca1 pyramidal cells receive intact perisomatic inhibitory input in the human epileptic hippocampus. Brain 128: 138–152.

Zhang W, Buckmaster PS. 2009. Dysfunction of the dendate basket cell circuit in a rat model of temporal lobe epilepsy. J Neurosci 29: 7846–7856.

Zyburkus J, Cressman JR, Barreto E, Schiff SJ. 2006. Interneuron and pyramidal cell interplay during in vitro Seizure-like events. J Neurophysiol 95:3948–3954.

OFFICE OF RESEARCH
INSTITUTIONAL REVIEW BOARD (IRB)
CHRISTIAN MEDICAL COLLEGE, VELLORE, INDIA.

Dr. B.J. Prashantham, M.A., M.A., Dr. Min (Clinical)
Director, Christian Counseling Center,
Chairperson, Ethics Committee.

Dr. Alfred Job Daniel, D Ortho, MS Ortho, DNB Ortho
Chairperson, Research Committee & Principal

Dr. Nihal Thomas,
MD., MNAMS., DNB (Endo), FRACP (Endo), FRCP (Edin), FRCP (Glasg)
Deputy Chairperson
Secretary, Ethics Committee, IRB
Additional Vice Principal (Research)

November 19, 2014

M. Sanjay
PG Trainee (PhD)
Department of Bioengineering
Christian Medical College,
Vellore 632002

Sub: **Fluid Research Grant Project:**
Computational Network Modelling of Excitatory and Inhibitory Responses in Hippocampal CA3 Neurons.
M. Sanjay, Bioengineering. Dr. K. Srinivasa Babu, Neurosciences, CMC, Vellore

Ref: IRB Min No: 8981 [OTHER] dated 04.08.2014

Dear M. Sanjay,

The Institutional Review Board (Blue, Research and Ethics Committee) of the Christian Medical College, Vellore, reviewed and discussed your project entitled "Computational Network Modelling of Excitatory and Inhibitory Responses in Hippocampal CA3 Neurons." on August 4th 2014.

The Committees reviewed the following documents:

1. IRB Application format
2. Curriculum Vitae' of Drs. M. Sanjay, K. SrinivasaBabu
3. Informed Consent form (English, Tamil, Hindi, Telugu & Bengali)
4. Information Sheet (English, Tamil, Hindi, Telugu & Bengali)
5. Proforma
6. No of documents 1-5

The following Institutional Review Board (Blue, Research & Ethics Committee) members were present at the meeting held on August 4th 2014 in the CREST/SACN Conference Room, Christian Medical College, Bagayam, Vellore 632002.

Ethics Committee Blue, Office of Research, 1st Floor, Carman Block, Christian Medical College, Vellore, Tamil Nadu 632 002.
Tel : 0416 - 2284294, 2284202 Fax : 0416 - 2262788, 2284481 E-mail : research@cmcvellore.ac.in

Dr. B.J. Prashantham, M.A., M.A., Dr. Min (Clinical)
Director, Christian Counseling Center,
Chairperson, Ethics Committee.

Dr. Alfred Job Daniel, D Ortho, MS Ortho, DNB Ortho
Chairperson, Research Committee & Principal

Dr. Nihal Thomas,
MD., MNAMS., DNB (Endo), FRACP (Endo), FRCP (Edin), FRCP (Glasg)
Deputy Chairperson
Secretary, Ethics Committee, IRB
Additional Vice Principal (Research)

Name	Qualification	Designation	Other Affiliations
Dr. Benjamin Perakath	MBBS, MS, FRCS	Professor, Colorectal Surgery, CMC, Vellore	Internal, Clinician
Dr. Rajesh Kannangai	MD, Ph D.	Professor & In-charge Retrovirus Laboratory (NRL under NACO), Department of Clinical Virology, CMC, Vellore	Internal, Clinician
Dr. Anup Ramachandran	Ph. D	The Wellcome Trust Research Laboratory Gastrointestinal Sciences, CMC, Vellore	Internal, Basic Medical Scientist
Dr. Simon Pavamani	MBBS, MD,	Professor, Radiotherapy, CMC, Vellore	Internal, Clinician
Dr. Vivek Mathew	MD (Gen. Med.) D.M (Neuro) Dip. NB (Neuro)	Professor, Neurology, CMC, Vellore	Internal, Clinician
Dr. Mathew Joseph	MBBS, MCH	Professor, Neurosurgery, CMC, Vellore	Internal, Clinician
Dr. Bobby John	MBBS, MD, DM, Ph D, MAMS	Professor, Cardiology, CMC, Vellore	Internal, Clinician
Dr. Chandrasingh	MS, MCH, DMB	Professor, Urology, CMC, Vellore	Internal, Clinician
Dr. Visalakshi. J	MPH, PhD	Lecturer, Dept of Biostatistics.	Internal, Statistician
Dr. Inian Samarasam	MS, FRCS, FRACS	Professor, Surgery, CMC, Vellore	Internal, Clinician

Ethics Committee Blue, Office of Research, 1st Floor, Carman Block, Christian Medical College, Vellore, Tamil Nadu 632 002.
Tel : 0416 - 2284294, 2284202 Fax : 0416 - 2262788, 2284481 E-mail : research@cmcvellore.ac.in

Dr. B.J. Prashantham, M.A., M.A., Dr. Min (Clinical)
Director, Christian Counseling Center,
Chairperson, Ethics Committee.

Dr. Alfred Job Daniel, D Ortho, MS Ortho, DNB Ortho
Chairperson, Research Committee & Principal

Dr. Nihal Thomas,
MD., MNAMS., DNB (Endo), FRACP (Endo), FRCP (Edin), FRCP (Glasg)
Deputy Chairperson
Secretary, Ethics Committee, IRB
Additional Vice Principal (Research)

Dr. B. J. Prashantham	MA(Counseling Psychology), MA(Theology), Dr. Min(Clinical Counselling)	Chairperson, Ethics Committee, IRB. Director, Christian Counseling Centre, Vellore	External, Social Scientist
Mrs. Pattabiraman	B. Sc, DSSA	Social Worker, Vellore	External, Lay Person
Dr. Jayaprakash Muliyil	B. Sc, MBBS, MD, MPH, Dr PH (Epid), DMHC	Retired Professor, CMC, Vellore	External, Scientist &Epidemiologist
Dr. Denise H. Fleming	B. Sc (Hons), PhD	Honorary Professor, Clinical Pharmacology, CMC, Vellore	Internal, Scientist & Pharmacologist
Mrs. Emily Daniel	MSc Nursing	Professor, Medical Surgical Nursing, CMC, Vellore	Internal, Nurse
Mrs. Sheela Durai	MSc Nursing	Professor, Medical Surgical Nursing, CMC, Vellore	Internal, Nurse
Mr. C. Sampath	BSc, BL	Legal Expert, Vellore	External, Legal Expert
Dr. Anuradha Rose	MBBS, MD	Assistant Professor, Community Health, CMC, Vellore	Internal, Clinician
Dr. Nihal Thomas,	MD, MNAMS, DNB(Endo), FRACP(Endo) FRCP(Edin) FRCP (Glasg)	Professor & Head, Endocrinology. Additional Vice Principal (Research), Deputy Chairperson, IRB, Member Secretary (Ethics Committee), IRB	Internal, Clinician

Ethics Committee Blue, Office of Research, 1st Floor, Carman Block, Christian Medical College, Vellore, Tamil Nadu 632 002.
Tel : 0416 - 2284294, 2284202 Fax : 0416 - 2262788, 2284481 E-mail : research@cmcvellore.ac.in

Dr. B.J. Prashantham, M.A., M.A., Dr. Min (Clinical)
Director, Christian Counseling Center,
Chairperson, Ethics Committee.

Dr. Alfred Job Daniel, D Ortho, MS Ortho, DNB Ortho
Chairperson, Research Committee & Principal

Dr. Nihal Thomas,
MD., MNAMS., DNB (Endo), FRACP (Endo), FRCP (Edin), FRCP (Glasg)
Deputy Chairperson
Secretary, Ethics Committee, IRB
Additional Vice Principal (Research)

We approve the project to be conducted as presented.

The Institutional Ethics Committee expects to be informed about the progress of the project, any **adverse events** occurring in the course of the project, any **amendments in the protocol and the patient information / informed consent**. On completion of the study you are expected to submit a copy of the **final report**. Respective forms can be downloaded from the following link: http://172.16.11.136/Research/IRB_Polices.html in the CMC Intranet and in the CMC website link address: http://www.cmch-vellore.edu/static/research/Index.html.

Yours sincerely

Dr. Nihal Thomas
Secretary (Ethics Committee)
Institutional Review Board

Dr. NIHAL THOMAS
MD.,MNAMS.,DNB(Endo),FRACP(Endo),FRCP(Edin),FRCP(Glasg)
SECRETARY - (ETHICS COMMITTEE)
Institutional Review Board,
Christian Medical College, Vellore - 632 002.

NOT TO BE MINISTERED UNTO BUT TO MINISTER
CHRISTIAN MEDICAL COLLEGE
VELLORE
INDIA

Cc: Dr. K. Srinivasa Babu, Neurosciences, CMC, Vellore.

IRB Min No: 8981 [OTHER] dated 04.08.2014

Ethics Committee Blue, Office of Research, 1st Floor, Carman Block, Christian Medical College, Vellore, Tamil Nadu 632 002.
Tel : 0416 - 2284294, 2284202 Fax : 0416 - 2262788, 2284481 E-mail : research@cmcvellore.ac.in